Elsevier Editorial System(tm) for Chemical Engineering Journal

Manuscript Draft

Manuscript Number: CEJ-D-18-11555R1

Title: Prussian blue analogue derived magnetic Cu-Fe oxide as a recyclable photo-Fenton catalyst for the efficient removal of sulfamethazine at near neutral pH values

Article Type: Research Paper

Keywords: Advanced oxidation process; Photo-Fenton; Wastewater; Antibiotics; Metal-organic frameworks; Degradation

Corresponding Author: Professor Guangming Zeng, Ph.D.

Corresponding Author's Institution: Hunan University

First Author: Min Cheng, Ph.D.

Order of Authors: Min Cheng, Ph.D.; Yang Liu, Ph.D.; Danlian Huang, Ph.D.; Cui Lai, Ph.D.; Guangming Zeng, Ph.D.; Jinhui Huang, Ph.D.; Zhifeng Liu, Ph.D.; Chen Zhang, Ph.D.; Chengyun Zhou; Lei Qin; Weiping Xiong; Huan Yi; Yang Yang

Abstract: The presence of antibiotics in aquatic environments has attracted global concern. Heterogeneous photo-Fenton process is an attractive yet challenging method for antibiotics degradation, especially when such a process can be operated at neutral pH values. In this work, a new magnetic Cu-Fe oxide (CuFeO) was developed as the heterogeneous photo-Fenton catalyst through a facile two-step method. The obtained CuFeO particles were found to be more efficient to activate H2O2 into radicals (*OH and *O2-) than Cu-Fe Prussian blue analogue (Cu-Fe PBA, the precursor) at near neutral conditions. The removal rate of sulfamethazine (SMZ) in CuFeO/H2O2/Vis system was much higher than those in CuO/H2O2/Vis and Fe3O4/H2O2/Vis systems. It was observed that nearly complete removal of SMZ from ultrapure water, river water and tap water can be achieved in 30 min in CuFeO/H2O2/Vis system. The influence of different process parameters on the SMZ degradation efficiency was then examined and the catalytic stability of CuFeO was also tested. The SMZ degradation intermediates during the process were analyzed and the degradation pathway was proposed based on LC-MS results. The mechanisms for H2O2 activation were studied by X-ray photoelectron spectrum analysis, radical scavenging and electron spin-trapping experiments. It is suggested that the synergistic effect among photo-induced electrons, Cu and Fe in CuFeO exhibits excellent performance in the catalytic activation of H2O2. This work is expected to provide useful information for the design and synthesis of bimetallic oxide for heterogeneous photo-Fenton reactions

Response to Reviewers: Revisions based on Reviewer #1:
General Comments:
The paper deals about the preparation, characterization and evaluation of a magnetic CuFeO catalyst for sulfamethazine degradation via photo-Fenton. The effects of pH and H2O2 concentration were tested. The pathways and routes of the antibiotic were depicted and the elimination of the antibiotic in several matrices (tap water, river and waste water)

was assessed. The paper is interesting and worthy of publication. However, before publication the following aspects need to clarified or provided:
Response:
The reviewer's comments to our work are highly appreciated. We have revised the manuscript carefully to make it clearer than the previous version. The specific revisions are presented as follows.

Specific comments:
Comment 1: The paper details the identification of only three primary byproducts. However, the fate of them upon the treatment is not provided. Furthermore, mineralization (complete transformation of initial antibiotic in CO2, H2O and inorganic ions) is not considered. In addition, neither the toxicity nor the antimicrobial activity of the treated solutions are evaluated. Therefore, and due to the fact that in many cases the transformation of the pollutants can lead to the formation of more dangerous compounds, the actual applicability of the technology cannot be established. Therefore, and before publication, the authors should provide some insights about the water quality at the final of the treatment.
Response: Thank you for your comment. It is true that for some pollutants, the degradation intermediates can be more toxic than the starting pollutants. Take dichlorodiphenyltrichloroethane (DDT) for example, it was reported that dichlorodiphenyldichloroethylene (4,4'-DDE) and 2,2-bis (4-chlorophenyl)-1- chloroethylene (4,4'-DDMU) generated during DDT degradation by Fenton process are more toxic than DDT [1-3]. In the present work, 3 main degradation intermediates were identified by LC-MS analysis, which included 2-amino-4,6-dimethylpyrimidine (A, m/z 124), 4-aminophenol (B, m/z 110), and 2-amino-4,6-dimethylpyrimidin-5-ol (C, m/z 140) (Fig. S5). These intermediates of SMZ degradation were also found in some other chemical degradation processes [4-12]. According to the literature, these intermediates can be further degraded to carboxylic acids, NH4+ and NO3− ions. It was also reported that the biodegradability of these intermediates was higher than that of SMZ [12-14]. For example, Mansour et al. found the mineralization yield during the biological treatment increased 61.4% after a 0.5 h Fenton pretreatment [12]. According to your comment, the antimicrobial activity of the treated solutions are studied and included in the revised manuscript:
- The toxic effect of SMZ and the degradation intermediates during the process was evaluated by traditional bacterial growth. Escherichia coli (E. coli) was selected as a model bacterium for testing. In a typical test, 0.5 mL of bacterial stock solution (3.0□107 CFU mL-1) was added to 49.5 mL of sterile solution that containing 48.5 mL of ultrapure water and 1 mL of SMZ solution (1 mL of ultrapure water or 1 mL of reaction solution sampled at different time points during the photo-Fenton treatment). The mixed solution was kept in an incubator (37 ℃) for 1 h, then diluted and spread on Eosin Methylene Blue Agar plate. After that, the plate was allowed to incubate at 37 ℃ for 24 h. The viable cell density of each sample was measured by standard plate count method. (See Page 8, line 18 - Page 9, line 5 in the revised manuscript).
- The results show that SMZ in this CuFeO/H2O2/Vis system can be degraded into different intermediates in a very short time (within 30 min). However, this does not guarantee the toxicity abatement of the resulting wastewater since the intermediates can be more toxic than the starting pollutants in some cases [71, 72]. Therefore, the antimicrobial activity of the treated solutions was studied. Preliminary tests suggest that the growth of E. coli can be inhibited by SMZ solution and the intermediates solutions as compared to the blank (sterile water). The E. coli growth

was lower in the photo-Fenton treated samples than in the initial SMZ solution (Fig. S9). The results suggest that the intermediates have higher capacity for inhibiting E. coli growth than that of the parent SMZ. Similar results have been reported elsewhere [18, 73, 74], for example, Perez-Moya et al. [73] reported that the toxicity of an SMZ solution increases during its degradation by means of photo-Fenton reactions. It was suggested that some degradation intermediates, such as cyclic/aromatic compounds and quinone derivatives, are toxic towards the bacteria even at very low concentration [18]. Barhoumi et al. [18] found that the toxicity of the solution can be reduced by prolonging the time of Fenton process. In this work, we also found that the decrease of toxicity at 60 min (Fig. S9). This is probably due to the further degradation of toxic intermediates by •OH. It is well-known that •OH can mineralize most kinds of organic pollutants to carbon dioxide (CO2), water (H2O) and inorganics. On the other hand, there are also reports showing that the biodegradability of SMZ degradation intermediates (produced during the Fenton/Fenton-like process) was higher than that of SMZ [75-77], suggesting a combined Fenton and biological treatment may be suitable for the for depleting toxicity of SMZ solution. Taken together, the results suggest the toxicity of the treated SMZ solution needs to be considered carefully in the practical cases. (See Page 20, line 1 - Page 21, line 3 in the revised manuscript).

In this work, the mineralization of SMZ in the photo-Fenton-like systems was also evaluated by Total Organic Carbon (TOC) analysis. The results showed that the concentration of TOC decreases continuously during the photo-Fenton process in the CuFeO/H2O2/Vis system, and about 50% of TOC can be removed after 30 minutes' treatment. It is suggest that with the prolonging the treatment, a high TOC removal can be obtained. This result is in consist with the general recognition that the •OH generated from Fenton reaction can mineralize most kinds of organic pollutants to carbon dioxide (CO2), water (H2O) and inorganics.

- Besides, these results are consistent with the results of TOC analysis (Fig. S7). The results showed that the concentration of TOC decreases continuously during the photo-Fenton process in the CuFeO/H2O2/Vis system, and about 50% of TOC can be removed after 30 minutes' treatment, suggesting that CuFeO has high potential for the real applications. (See Page 14, line 5-9 in the revised manuscript).

[1] M. Cao, L. Wang, L. Wang, J. Chen, X. Lu, Remediation of DDTs contaminated soil in a novel Fenton-like system with zero-valent iron, Chemosphere 90 (2013) 2303-2308.

[2] Villa, R.D., Nogueira, R.F.P., Oxidation of p, p'-DDT and p, p'-DDE in highly and long-term contaminated soil using Fenton reaction in a slurry system, Sci. Total Environ. 371 (2006), 11–18.

[3] Megharaj, M., Boul, H.L., Thiele, J.H., Effects of DDT and its metabolites on soil algae and enzymatic activity, Biol. Fert. Soils 29 (1999), 130–134.

[4] I. Kim, H. Tanaka, Photodegradation characteristics of PPCPs in water with UV treatment, Environ. Int. 35 (2009) 793–802.

[5] I. Kim, H. Tanaka, Photodegradation characteristics of PPCPs in water with UV treatment, Environ. Int. 35 (2009) 793–802.

[6] Z. Guo, F. Zhou, Y. Zhao, C. Zhang, F. Liu, C. Bao, M. Lin, Gamma irradiationinduced sulfadiazine degradation and its removal mechanisms, Chem. Eng. J. 191 (2012) 256–262.

[7] T. Zhou, X. Wu, J. Mao, Y. Zhang, T. Lim, Rapid degradation of sulfonamides in a novel heterogeneous sonophotochemical magnetite-catalyzed Fenton-like (US/UV/Fe3O4/oxalate) system, Appl. Catal. B 160–161 (2014) 325–334.

[8] A.P.S. Batista, F.C.C. Pires, A.C.S.C. Teixeira, The role of reactive oxygen species in sulfamethazine degradation using UV-based technologies and products identification, J. Photochem. Photobiol. A 290 (2014) 77–85.
[9] S. Fukahori, T. Fujiwara, Photocatalytic decomposition behavior and reaction pathway of sulfamethazine antibiotic using TiO2, J. Environ. Manage. 157 (2015) 103–110.
[10] Y. Fan, Y. Ji, D. Kong, J. Lu, Q. Zhou, Kinetic and mechanistic investigations of the degradation of sulfamethazine in heat-activated persulfate oxidation process, J. Hazard. Mater. 300 (2015) 39–47.
[11] K. Kim, S.K. Kam, Y.S. Mok, Elucidation of the degradation pathways of sulfonamide antibiotics in a dielectric barrier discharge plasma system, Chem. Eng. J. 271 (2015) 31–42.
[12] D. Mansour, F. Fourcade, S. Huguet, I. Soutrel, N. Bellakhal, M. Dachraoui, D. Hauchard, A. Amrane, Improvement of the activated sludge treatment by its combination with electro Fenton for the mineralization of sulfamethazine, Int. Biodeterior. Biodegrad. 88 (2014) 29-36.
[13] A. Ledjeri, I. Yahiaoui, H. Kadji, F. Aissani-Benissad, A. Amrane, F. Fourcade, Combination of the Electro/Fe3+/peroxydisulfate (PDS) process with activated sludge culture for the degradation of sulfamethazine, Environ. Toxicol. Pharmacol. 53 (2017) 34-39.
[14] D. Mansour, F. Fourcade, I. Soutrel, D. Hauchard, N. Bellakhal, A. Amrane, Relevance of a combined process coupling electro-Fenton and biological treatment for the remediation of sulfamethazine solutions – Application to an industrial pharmaceutical effluent, Comptes Rendus Chimie 18 (2015) 39-44.

Comment 2: In section 3.2, concerning the pH effect, the authors indicates that OH radicals have a higher oxidation potential at lower pH. Why is the reason of that behavior of these radicals? In my opinion this is not true, there are not any thermodynamic (or even kinetic) reason to support such affirmation. The same occurs with the affirmation of the higher stability of hydrogen peroxide at lower pH values. Did the authors test the H2O2 stability at the tested pHs to validate this affirmation? In my opinion the better efficiency at lower pH values is probably due to the higher leaching of iron and copper ions as the pH decreases, which facilitates the faster homogeneous photo-Fenton reaction.

Response: Your comments are greatly appreciated. According to your comments, the sentence "Firstly, the higher oxidation potential of •OH can be achieved at the lower pH values, which favored the degradation of SMZ [41]" has been removed, and the sentence "Firstly, better efficiency at lower pH values can be due to the higher leaching of iron and copper ions as the pH decreases, which facilitates the faster homogeneous photo-Fenton reaction." is added in the revised manuscript.
The H2O2 stability at the different pHs (pH > 3) has been studied by many researchers, and it was found that the auto-decomposition of H2O2 (2H2O2 → O2 + 2H2O) is accelerated at higher pH [1-4].
The related text is revised to:
- Two mechanisms can be responsible for this phenomenon. Firstly, better efficiency at lower pH values can be due to the higher leaching of iron and copper ions as the pH decreases, which facilitates the faster homogeneous photo-Fenton reaction [56]. Secondly, H2O2 is less stable at higher pH conditions and tend to decompose into H2O [57]. (See Page 14, line 19 - Page 15, line 1 in the revised manuscript).

[1] L. Szpyrkowicz, C. Juzzolino, S.N. Kaul, A Comparative study on oxidation of disperse dyes by electrochemical process, ozone, hypochlorite and fenton reagent, Water Res. 35 (2001) 2129-2136.

[2] J. Herney-Ramirez, M.A. Vicente, L.M. Madeira, Heterogeneous photo-Fenton oxidation with pillared clay-based catalysts for wastewater treatment: a review, Appl. Catal. B Environ. 98 (2010) 10-26.
[3] A. Babuponnusami, K. Muthukumar, A review on Fenton and improvements to the Fenton process for wastewater treatment, J. Environ. Chem. Eng. 2 (2014) 557-572.
[4] W. Najjar, S. Azabou, S. Sayadi, A. Ghorbel, Catalytic wet peroxide photo-oxidation of phenolic olive oil mill wastewater contaminants: Part I. Reactivity of tyrosol over (Al-Fe)PILC, Appl. Catal. B Environ. 74 (2007) 11-18.

Comment 3: Other minor aspects are:
1) The supplier of polyvinylpyrrolidone should be provided in the experimental part.
Response: In the revised manuscript, the supplier of polyvinylpyrrolidone is provided in the experimental part.
- and polyvinylpyrrolidone (PVP) were obtained from Sinopharm Chemical Reagent Corp (China). (See Page 6, line 11 in the revised manuscript).
2) The protocol for the EDS analysis should be also included in the experimental section.
Response: In the revised manuscript, the protocol for the EDS analysis is included in the experimental section.
- Energy dispersive X-ray spectroscopy (EDS) of the prepared catalyst was obtained using an EDAX Genesis X-ray spectrometer. (See Page 7, line 3-5 in the revised manuscript).
3) In section 3.3, MnFeO is wrong, because not materials containing Mn were considered in this work.
Response: The mentioned mistakes have been corrected. MnFeO is revised to CuFeO (See Page 16, line 7 in the revised manuscript).

Revisions based on Reviewer #2:
General Comments:
This manuscript deals with Magnetic Cu-Fe oxides derived from metal-organic frameworks as a photo-Fenton catalyst for the efficient removal of sulfamethazine. Due to the provided comments, the manuscript needs to be rewritten and major revision to be re-reviewed to make decision on its adequacy toward the publication in CEJ.
Response:
The reviewer’s comments to our work are highly appreciated. We have revised the manuscript carefully to make it clearer than the previous version. The specific revisions are presented as follows.

Specific comments:
Comment 1: Title is not representative.
Response: Thank you for your comment. The title has been revised to “Prussian blue analogue derived magnetic Cu-Fe oxide as a recyclable photo-Fenton catalyst for the efficient removal of sulfamethazine at near neutral pH values”.

Comment 2: "….a synergistic effect between solid-state Cu and Fe was identified in control experiments with CuO and Fe3O4". How authors could

confirm this conclusion? Without experimental confirmation, it would be speculative.
Response: Thank you for your comment. We now realize that without experimental confirmation, it is inappropriate to say that a synergistic effect between solid-state Cu and Fe was identified. In the revised manuscript, this sentence in the Abstract is revised to "The removal rate of SMZ in CuFeO/H2O2/Vis system was much higher than those in CuO/H2O2/Vis and Fe3O4/H2O2/Vis systems." (See Page 2, line 8-10 in the revised manuscript).

Comment 3: "…It is suggested that the synergistic effect among photo-induced electrons, Cu and Fe in CuFeO exhibits excellent performance in the catalytic activation of H2O2". The interaction between Cu and Fe in CuFeO should be given and explain to be able suggesting the synergistic effect.
Response: Thank you for your comment. The interaction between Cu and Fe in CuFeO is discussed in the in the revised manuscript.
- On the other hand, e− can cause an in-situ recycling of copper species (CuII → CuI) and iron species (FeIII → FeII) through eqs. 15 and 16 [68], respectively. In addition, the reduction of FeIII by CuI is thermodynamically favorable (eqs. 17) according to the standard reduction potentials of the Fe and Cu (eqs. 15 and 16) [68].
≡CuII + e− → ≡CuI E0 = 0.16 V (15)
≡FeIII + e− → ≡FeII E0 = 0.77 V
(16)
≡FeIII + CuI → ≡FeII + ≡CuII
(17)
(See Page 18, line 6-11 in the revised manuscript).

Comment 4: A consistent form should be used for hydroxyl radicals (*OH or HO*) throughout the text.
Response: Thank you for your comment. We have checked the manuscript carefully. A consistent form for hydroxyl radicals (•OH) is used throughout the revised manuscript.

Comment 5: The novelty of the study is not clear. The Cu-Fe PBAs were synthesized according to a previously reported method. Only a further calcination step was used to prepare CuFeO.
Response: Thank you for your comment. The bimetallic catalyst, Cu-Fe oxide has gained particular attention in Fenton-like chemistry, not only because of its good catalytic performance but also copper is not regarded as a potential carcinogen [1-4]. The occurrence of metal-organic frameworks (MOFs) brings a great deal of opportunities for the development of new types of Cu-Fe oxide with excellent characteristic features, such as well-defined structure, large pore volume and high specific area.
Prussian blue analogues (PBAs) as a set of the most frequently studied metal-organic frameworks (MOFs), has the common features of MOFs, such as large pore volume and high specific area [5]. Several studies have investigated the catalytic properties of the PBAs in heterogeneous Fenton-like reactions. For example, Li et al. [6] have developed two Fe-Co PBAs, Fe[Co(CN)6]•2H2O and Fe3[Co(CN)6]2•12H2O, as excellent photo-Fenton catalysts. In their study, the removal efficiency of Rhodamine B (RhB, 12 mg L−1) by FeII-Co PBA/H2O2 in 30 min reached 93%. However, to our knowledge no previous study has investigated the preparation of Cu-Fe oxide from Cu-Fe PBAs and its application for Fenton-like reactions. Herein, in this work we report a facile two-step strategy to prepare Cu-Fe oxide. Although Cu-Fe PBAs were synthesized according to a previously

reported method, which is very similar to those for the preparation of Co-Fe PBA and Mn-Fe PBA. However, the catalytic performance of the PBA derived CuFeO together with the mechanism have not been reported. According to your valuable comment, we have revised the Introduction with aim to emphasize the novelty of the study.

- The bimetallic catalyst, Cu-Fe oxide has gained particular attention in the Fenton chemistry, not only because of its good catalytic performance but also copper is not regarded as a potential carcinogen [33]. Recently, some researchers have studied the feasibility of using MOFs to obtain porous nanostructured oxides. The pioneering works showed that the original morphology of the precursor can be almost retained after the thermal treatment, while the catalytic performance can be largely improved [34-36]. To our knowledge, however, no study on the preparation of Cu-Fe oxide from Cu-Fe PBAs and its application for Fenton-like reactions has been reported. Therefore, in this current study, a facile two-step strategy was developed to synthesize porous Cu-Fe oxide (CuFeO) by heating the Cu-Fe PBAs. (See Page 5, line 4-13 in the revised manuscript).

[1] Dorsey, A.; Ingerman, L.; Swarts, S. Toxicological Profile for Copper; Department of Health & Human Services, Public Health Service, Agency for Toxic Substances and Disease Registry, 2004.
[2] Ding, Y.; Zhu, L.; Wang, N.; Tang, H. Sulfate radicals induced degradation of tetrabromobisphenol A with nanoscaled magnetic CuFe2O4 as a heterogeneous catalyst of peroxymonosulfate. Appl. Catal., B 2013, 129, 153-162
[3] Zhang, T.; Zhu, H.; Croue, J. P. Production of sulfate radical from peroxymonosulfate induced by a magnetically separable CuFe2O4 spinel in water: Efficiency, stability, and mechanism. Environ. Sci. Technol. 2013, 47 (6), 2784-2791
[4] Y. Lei, C.-S. Chen, Y.-J. Tu, Y.-H. Huang, H. Zhang, Heterogeneous degradation of organic pollutants by persulfate activated by CuO-Fe3O4: mechanism, stability, and effects of pH and bicarbonate ions, Environ. Sci. Technol. 49 (2015) 6838-6845.
[5] B. Kong, C. Selomulya, G. Zheng, D. Zhao, New faces of porous Prussian blue: interfacial assembly of integrated hetero-structures for sensing applications, Chem. Soc. Rev. 44 (2015) 7997-8018.
[6] X. Li, J. Liu, A.I. Rykov, H. Han, C. Jin, X. Liu, J. Wang, Excellent photo-Fenton catalysts of Fe–Co Prussian blue analogues and their reaction mechanism study. Appl. Catal. B 179 (2015)196.

Comment 6: What about if the catalyst prepared from other precursors (non MOF-based materials)? What is the main feature of the Cu-Fe PBAs that was used for preparation of FeCuO? The Fe2O3/CuO composite has been prepared by different methods. The importance of the selected method is uncleaer.

Response: Thank you for your comment. Several previous studies have reported that the Cu-Fe oxide catalyzed (photo-) Fenton-like process is effective for the destruction of organic contaminants in water [1-5]. Cu-Fe oxide can be obtained by a variety of methods, such as sol–gel combustion method [1, 2], polymeric precursor method [3], co-precipitation method [4], and hydrothermal method [5].

The main feature of the Cu-Fe PBAs that was used for preparation of FeCuO is: Cu-Fe PBA as a kind of MOF, has the advantage features of MOFs, such as large pore volume and high specific area [6]. For example, the BET surface area of CuFeO-Et in Dang and Le' work is 7.5 m2/g [3], the BET surface area and pore volume of CuO-Fe3O4 in Lei et al.'s work is 28.26 m2/g and 0.09728 cm3/g, respectively [5]. However, the BET surface area and pore volume of FeCuO in our present work reach 178.35 m2/g and 0.6993 cm3/g, respectively. The much larger surface area (compared to the

conventional catalysts) is the most interesting property of MOFs [7]. This would lead to unusual chemistry if this large surface could be fully covered by active sites [7]. The high porosity is very useful to expose the active sites completely to reactant(s) and to enhance the reactivity remarkably [8].

According to your valuable comment, we have revised the Introduction with aim to emphasize the importance of the selected method.

- The occurrence of MOFs also brings a great deal of opportunities for the development of new heterogeneous Fenton-like catalysts with excellent characteristic features, such as large surface area and uniform pore sizes [27-29]. This large surface could provide abundant active sites, and the high porosity is very useful to expose the active sites completely to reactant(s) [27]. (See Page 4, line 7-11 in the revised manuscript).

[1] Y. Feng, C. Liao, K. Shih, Copper-promoted circumneutral activation of H2O2 by magnetic CuFe2O4 spinel nanoparticles: Mechanism, stoichiometric efficiency, and pathway of degrading sulfanilamide, Chemosphere 154 (2016) 573-582.
[2] T.T. Dinh, T.Q. Nguyen, G.C. Quan, V.D.N. Nguyen, H.Q. Tran, T.K. Le, Starch-assisted sol-gel synthesis of magnetic CuFe2O4 powder as photo-Fenton catalysts in the presence of oxalic acid, Int. J. Environ. Sci. Technol. 14 (2017) 2613-2622.
[3] H.T. Dang, T.K. Le, Precursor chain length dependence of polymeric precursor method for the preparation of magnetic Fenton-like CuFe2O4-based catalysts, J. Sol-Gel Sci. Technol. 80 (2016) 160-167.
[4] Pereira C, Pereira AM, Fernandes C, Rocha M, Mendes R, Fernandez García MP, Guedes A, Tavares PB, Greneche JM, Araujo JP, Freire C (2012) Superparamagnetic MFe2O4 (M = Fe Co, Mn) nanoparticles: tuning the particle size and magnetic properties through a novel one-step coprecipitation route. Chem Mater 24 1496–1504
[5] Y. Lei, C.-S. Chen, Y.-J. Tu, Y.-H. Huang, H. Zhang, Heterogeneous degradation of organic pollutants by persulfate activated by CuO-Fe3O4: mechanism, stability, and effects of pH and bicarbonate ions, Environ. Sci. Technol. 49 (2015) 6838-6845.
[6] B. Kong, C. Selomulya, G. Zheng, D. Zhao, New faces of porous Prussian blue: interfacial assembly of integrated hetero-structures for sensing applications, Chem. Soc. Rev. 44 (2015) 7997-8018.
[7] Y. Zhang, Y. Zhou, Y. Zhao, C.-j. Liu, Recent progresses in the size and structure control of MOF supported noble metal catalysts, Catal. Today 263 (2016) 61-68.
[8] Q. Yang, Q. Xu, H.L. Jiang, Metal-organic frameworks meet metal nanoparticles: synergistic effect for enhanced catalysis, Chem. Soc. Rev. 46 (2017) 4774.

Comment 7: Since before starting the photo-Fenton reaction the adsorption process was run, a part of SMZ could be adsorbed onto the catalyst and thus the initial concentration for oxidation reactions is something less than 50 mg/L. Authors had better to test the adsorption in a separate experiment and use the results for calculation of synergistic effect.

Response: Thank you for your comment. It is true that "a part of SMZ could be adsorbed onto the catalyst and thus the initial concentration for oxidation reactions is something less than 50 mg/L". Like in many others, in our experiments, the adsorption of SMZ has also been considered. Prior to the catalysis experiments, the SMZ adsorption on the surface of catalysts was carried out to investigate SMZ adsorption capacity of prepared catalysts. The results showed that the adsorption-desorption equilibrium can be reached in 30 min. We also found

that both Cu-Fe PBAs and CuFeO exhibited negligible SMZ adsorption capacity (about 3% of SMZ was removed by adsorption). Since the amount of SMZ removed by adsorption as compared to that removed by degradation is very small, we did not considered the adsorption in the degradation tests. In a typical run, 50 mg of catalyst was added to 100 mL of SMZ solution and stirred for 30 min to establish the adsorption–desorption equilibrium, and then the degradation process was triggered.
The results of adsorption text can be found in Page 13, line 9-13 in the revised manuscript.
- The adsorption of SMZ by Cu-Fe PBAs and CuFeO was studied in the first step. As revealed in Fig. S6, adsorption of SMZ by Cu-Fe PBAs and CuFeO achieved adsorption equilibrium in 30 min. We also found that both Cu-Fe PBAs and CuFeO exhibited similar and negligible SMZ adsorption capacity (about 3% of SMZ was removed by adsorption). (See Page 13, line 9-13 in the revised manuscript).

Comment 8: CuFeO is not a MOF-based catalyst because the organics were incinerated during the calcinations process. In some part of the text it has been expressed that the MOF-based catalyst was prepared as new material for Fenton process. The text should be modified to consider this point.
Response: Thank you for pointing out our mistakes. CuFeO prepared from Cu-Fe PBAs should be a MOF-derived catalyst.
"MOF-based" is revised to "MOF-derived" in the revised manuscript.
- Page 5, line 14 "MOF-based photo-Fenton catalyst" is revised to "MOF-derived photo-Fenton catalyst" (See Page 5, line 19 in the revised manuscript).
- Page 5, line 22 "MOF-based photo-Fenton catalyst" is revised to "MOF-derived photo-Fenton catalyst" (See Page 6, line 5 in the revised manuscript).
- Page 19, line 1 "MOF-based catalyst" is revised to "MOF-derived catalyst" (See Page 21, line 10 in the revised manuscript).

Comment 9: Based on XRD results, the catalyst composed of crystal plane of Fe3O4 and CuO. Why authors say it is FeCuO?
Response: Thank you for your comment. In this article, CuFeO is used as the shortened form of the Cu-Fe PBA-derived Cu-Fe oxide (See Page 5, line 14 in the revised manuscript). This idea is come from some previous published works [1-4].
[1] M. Al-Dossary, A.A. Ismail, J.L.G. Fierro, H. Bouzid, S.A. Al-Sayari, Effect of Mn loading onto MnFeO nanocomposites for the CO2 hydrogenation reaction, Applied Catalysis B: Environmental 165 (2015) 651-660.
[2] T.T. Dinh, T.Q. Nguyen, G.C. Quan, V.D.N. Nguyen, H.Q. Tran, T.K. Le, Starch-assisted sol–gel synthesis of magnetic CuFe2O4 powder as photo-Fenton catalysts in the presence of oxalic acid, Int. J. Environ. Sci. Technol. 14 (2017) 2613-2622.
[3] G.-X. Huang, C.-Y. Wang, C.-W. Yang, P.-C. Guo, H.-Q. Yu, Degradation of Bisphenol A by Peroxymonosulfate Catalytically Activated with Mn1.8Fe1.2O4 Nanospheres: Synergism between Mn and Fe, Environ. Sci. Technol. 51 (2017) 12611-12618.
[4] Y. Wu, L. Zhan, K. Huang, H. Wang, H. Yu, S. Wang, F. Peng, C. Lai, Iron based dual-metal oxides on graphene for lithium-ion batteries anode: Effects of composition and morphology, J. Alloys Compd. 684 (2016) 47-54.

Comment 10: Authors stated that they prepared CuFeO nanospheres. But the SEM image does not show the spherical particles.
Response: Thank you for your comment. According to you comment "CuFeO nanospheres" is revised "CuFeO particles".

- Page 2, line 6 “obtained CuFeO nanospheres” is revised to “obtained CuFeO particles” (See Page 2, line 6 in the revised manuscript).
- Page 9, line 3 “many tiny nanospheres” is revised to “many tiny particles” (See Page 10, line 8 in the revised manuscript).
- Page 9, line 12 “the CuFeO nanospheres” is revised to “the CuFeO particles” (See Page 10, line 16 in the revised manuscript).
- Page 18, line 6 “from CuFeO nanospheres” is revised to “from CuFeO particles” (See Page 21, line 17 in the revised manuscript).

Comment 11: The size distribution of the prepared catalysts should be provided. How much was the average size of particles?
Response: Thank you for your comment. According to you comment, the size distribution of the prepared catalysts was measured with the dynamic light scattering (DLS) method. The measurement was carried out using a DynaPro Dynamic Light Scatterer (Malvern Instruments). The results show that the average size of Cu-Fe PBA and CuFeO was 225.8 and 240.0 nm, respectively.
The tests and results are added in the revised manuscript.
- The size distribution of the prepared catalysts was measured with the dynamic light scattering (DLS) method. The prepared catalysts were fully dispersed in water with the help of ultrasound radiation. The measurement was carried out using a DynaPro Dynamic Light Scatterer (Malvern Instruments). (See Page 7, line 4-8 in the revised manuscript).
- DLS analysis shows that the average size of Cu-Fe PBA and CuFeO (dispersed in water) was 225.8 and 240.0 nm, respectively (Fig. S3). The average size of CuFeO is very closed to that of Cu-Fe PBA, suggesting the thermal treatment did not significantly change the morphology of Cu-Fe PBA, which is in consistent with the results obtained from SEM analysis. (See Page 10, line 21 - Page 11, line 3 in the revised manuscript).

Comment 12: The specific surface area of a catalyst is one the important parameters affecting the catalytic activity. BET and BJH analysis is recommended.
Response: Thank you for your comment. BET and BJH analysis is performed and included in the revised manuscript.
- The Brunauer–Emmett–Teller (BET) specific surface area, the Barrett–Joyner– Halenda (BJH) pore volume and pore size of the catalyst were measured using the Micromeritics ASAP 2010 analyzer. (See Page 7, line 7-10 in the revised manuscript).
- The BET surface area and BJH pore volume of CuFeO nanoparticles are 178.35 m^2/g and 0.6993 cm^3/g, respectively, which are much higher than those of the reported Cu-Fe bimetallic catalysts [33, 39, 40]. As shown in Fig. S4, the BET isotherm of CuFeO nanoparticles belongs to type IV with H3 type hysteresis loops, indicating that CuFeO nanoparticles were mesoporous. The inset of Fig. S4 is the BJH pore size distribution plots of CuFeO nanoparticles. According to the BJH analysis, the pore size of the CuFeO catalyst was determined to be 17.47 nm. The high specific surface area and porous structure of the catalysts may facilitate the catalytic performance. (See Page 11, line 3-10 in the revised manuscript).

Comment 13: The composition of the catalyst is better characterized by the XRF analysis rather than FTIR.
Response: Thank you for your comment. In this work, the prepared catalysts have been systematically characterized by SEM, EDS, TEM, BET, DLS, XRD, XPS, FT-IR, VSM and TG analysis. According to you comment, the XRF analysis will be adopted to study the composition of the prepared materials in our future works. In this work, FTIR analysis was used to

study the changes of chemical groups after the calcination. For example, the absorption band at 2102 cm−1 of PBA spectrum is assignable to the C-N stretching vibration; however, after the calcination, the characteristic peaks of C-N stretching vibration (2102 cm−1) completely disappeared from the spectrum. For another, the strong band emerged at 570 cm−1 in CuFeO pattern suggests the presence of Fe-O in CuFeO sample.

Comment 14: To show and confirm that the prepared catalyst were magnetic, the VSM analysis was conducted. The finding should be better described in the main text.
Response: Thank you for your comment. We have revised the manuscript according to your comment. The description of the results of VSM analysis is revised to:
- Fig. S5 presents the magnetic hysteresis curves for Cu-Fe PBA, CuFeO and the used-CuFeO. These curves display the evolution of magnetization (M) as a function of applied field (H). As indicated in Fig. S5, no magnetism was found in Cu-Fe PBA, while CuFeO exhibited obvious magnetism. Moreover, CuFeO could maintain its original magnetism even after 5 degradation cycles. The saturation magnetization value (Ms) of CuFeO was measured to be 14.18 emu g−1, which is about 25% of that of pure magnetic Fe3O4 under the same conditions. Generally, catalysts with high Ms values means that they can be easily separated from the solution by magnet. In our experiment, CuFeO particles could be collected simply with a magnet in 10 s as shown in the inset picture of Fig. S5. This enhances the technical and economic feasibility because it allows the convenient separation and recycling of catalyst by applying an external magnetic field. (See Page 12, line 19- Page 13, line 7 in the revised manuscript).

Comment 15: The main point in this manuscript is that the authors should explain and confirm why the CuFeO/H2O2/Vis process had drastically greater performance than the CuFeO/Vis and CuFeO/H2O2 processes for the SMZ degradation. Without this confirmation and documentation the statement "the CuFeO/H2O2/Vis system showed a remarkable advantage for the practical applications due to the broader working environment" is misleading. The information provided in section 3.4 is on the mechanism and do not explain why irradiating (by Vis light) the FeCuO/H2O2 could improve the degradation to such a high rate.
Response: Thank you for your comment.
(1) According to the results showed in Fig. 6B, we can found that the •OH and photo-induced e− are highly related to the SMZ degradation efficiency. As indicated in Fig. 6B, the addition of silver nitrate (AgNO3), as a scavenger for photoinduced e− dramatically suppresses the photo-Fenton reaction; and a more distinct inhibition phenomenon was observed when the scavenger of tert-butyl alcohol (TBA) for •OH is added to the reaction system. These results together with eqs. 1-3 can explain why CuFeO/H2O2/Vis system had greater performance than the CuFeO/Vis and CuFeO/H2O2 for the SMZ degradation. For CuFeO/Vis system, because of the absence of H2O2, •OH cannot be efficiently produced via eqs. 1. SMZ degradation is mainly caused by the photo-induced h+, which was proved plays a minor role in SMZ degradation (Fig. 6B). Therefore, SMZ degradation efficiency in this system was low. As for FeCuO/H2O2 system, SMZ degradation is mainly caused by the Fenton-like reactions (eqs. 4-7). Because of the absence of photo-induced e−, •OH cannot be efficiently produced via eqs. 1. Besides, in CuFeO/H2O2/Vis system, a potential in-situ recycling of copper species (CuII → CuI) and iron species (FeIII → FeII) would be easily occur through eqs. 8 and 9. These processes facilitate the continuous cycle of FeIII/FeII and CuII/CuI. Therefore,

SMZ degradation efficiency in CuFeO/H2O2/Vis system was much higher. Similar results were reported by Gao an co-workers [1] who studied the removal of sulfonamide by a CuFe2O4 catalyzed photo-Fenton process.

$H_2O_2 + e^- \rightarrow \bullet OH + OH^-$ (1)

$CuO + h\nu \rightarrow CuO\ (e^- + h^+)$ (2)

$Fe_3O_4 + h\nu \rightarrow Fe_3O_4\ (e^- + h^+)$ (3)

$\equiv Fe^{II} + H_2O_2 \rightarrow \equiv Fe^{III} + \bullet OH + OH^-$ (4)

$\equiv Fe^{III} + H_2O_2 \rightarrow \equiv Fe^{II} + \bullet OOH + H^+$ (5)

$\equiv Cu^{I} + H_2O_2 \rightarrow \equiv Cu^{II} + \bullet OH + OH^-$ (6)

$\equiv Cu^{II} + H_2O_2 \rightarrow \equiv Cu^{I} + \bullet OOH + H^+$ (7)

$\equiv Cu^{II} + e^- \rightarrow \equiv Cu^{I}$ $E_0 = 0.16$ V (8)

$\equiv Fe^{III} + e^- \rightarrow \equiv Fe^{II}$ $E_0 = 0.77$ V (9)

The related content in Section 3.4 has been revised based on the above discussion.

- This can explain the relative low SMZ degradation efficiency in CuFeO/Vis system. As seen from Fig. 6B, the photo-induced e− plays an important role in SMZ degradation. This is because e− could not only react with H2O2 to produce active •OH (eqs. 14), but also can cause an in-situ recycling of copper species (CuII → CuI) and iron species (FeIII → FeII) through eqs. 15 and 16 [68], respectively. In addition, the reduction of FeIII by CuI is thermodynamically favorable (eqs. 17) according to the standard reduction potentials of the Fe and Cu (eqs. 15 and 16) [68]. These processes facilitate the continuous cycle of FeIII/FeII and CuII/CuI in CuFeO/H2O2/Vis system. (See Page 18, line 3-11 in the revised manuscript)

(2) The statement "the CuFeO/H2O2/Vis system showed a remarkable advantage for the practical applications due to the broader working environment" in 3.2. Catalytic performance of CuFeO is based on the pH test results. According to your comment, this part has been revised to:

- From another point of view, at least 80% of SMZ can be degraded in 30 min in the tested pH range (4.0 to 10.0). In particularly, we found that 95.42% of SMZ was removed after 30 minutes' treatment at a near neutral pH (pH=6.0). Traditional homogeneous Fenton process generally needs to be operated at acidic pH conditions, which hinders the industrial application of the technology because the pollutant solutions usually have near neutral pH values [23]. In this regard, the CuFeO/H2O2/Vis system showed a remarkable advantage for the practical applications due to the broader working environment. (See Page 15, line 2-8 in the revised manuscript).

[1] J. Gao, S. Wu, Y. Han, F. Tan, Y. Shi, M. Liu, X. Li, 3D mesoporous CuFe2O4 as a catalyst for photo-Fenton removal of sulfonamide antibiotics at near neutral pH, J. Colloid Interface Sci. 524 (2018) 409-416.

Comment 16: The rate of SMZ degradation in the developed process should be compared with that in the other AOPs based on the degradation rate (r) value.

Response: Thank you for your comment. In the revision, the rate of SMZ degradation in the developed process is compared with that in the other AOPs. In this work, 95.42% of SMZ was removed after 30 minutes' treatment at a near neutral pH (pH=6.0). According to the literature, the rate of SMZ degradation of CuFeO/H2O2/Vis is high than many other AOPs [1-9]. For example, Gao et al reported that about 95% of SMZ (20 mg/L) was removed in 90 min at pH 6.73 in the CuFe2O4 photo-Fenton process [1]; Barhoumi et al reported that about 85% of SMZ (0.2 mM) was removed in 40 min at pH 3.0 in the Pyrite electro-Fenton process [2]; Fan et al reported that about 80% of SMZ (0.03 mM) was removed in 60 min at pH 7.0 in heat-activated persulfate oxidation process [3]; Wang et al reported that

about 50% of SMZ (20 mg/L) was removed in 120 min at pH 6.0 in Bi-doped TiO2 photocatalytic process [4].
The manuscript has been revised accordingly.
- In this work, 95.42% of SMZ was removed after 30 min in CuFeO/H2O2/Vis system. The degradation efficiency of SMZ in this process is higher than those of many reported AOPs, including photo-Fenton process [48], electro-Fenton process [18, 49], photocatalytic processes [50, 51], and peroxymonosulfate/ persulfate-based oxidation [52, 53]. (See Page 14, line 1-5 in the revised manuscript).

[1] J. Gao, S. Wu, Y. Han, F. Tan, Y. Shi, M. Liu, X. Li, 3D mesoporous CuFe2O4 as a catalyst for photo-Fenton removal of sulfonamide antibiotics at near neutral pH, J. Colloid Interface Sci. 524 (2018) 409-416.
[2] N. Barhoumi, N. Oturan, H. Olvera-Vargas, E. Brillas, A. Gadri, S. Ammar, M.A. Oturan, Pyrite as a sustainable catalyst in electro-Fenton process for improving oxidation of sulfamethazine. Kinetics, mechanism and toxicity assessment, Water Res. 94 (2016) 52-61.
[3] Y. Fan, Y. Ji, D. Kong, J. Lu, Q. Zhou, Kinetic and mechanistic investigations of the degradation of sulfamethazine in heat-activated persulfate oxidation process, J. Hazard. Mater. 300 (2015) 39-47.
[4] N. Wang, X. Li, Y. Yang, T. Guo, X. Zhuang, S. Ji, T. Zhang, Y. Shang, Z. Zhou, Enhanced photocatalytic degradation of sulfamethazine by Bi-doped TiO2 nano-composites supported by powdered activated carbon under visible light irradiation, Sep. Purif. Technol. 211 (2018) 673-683.
[5] A. Ledjeri, I. Yahiaoui, H. Kadji, F. Aissani-Benissad, A. Amrane, F. Fourcade, Combination of the Electro/Fe3+/peroxydisulfate (PDS) process with activated sludge culture for the degradation of sulfamethazine, Environ. Toxicol. Pharmacol. 53 (2017) 34-39.
[6] R. Li, Z. Chen, M. Cai, J. Huang, P. Chen, G. Liu, W. Lv, Improvement of Sulfamethazine photodegradation by Fe(III) assisted MIL-53(Fe)/percarbonate system, Appl. Surf. Sci. 457 (2018) 726-734.
[7] Y. Feng, J. Liu, D. Wu, Z. Zhou, Y. Deng, T. Zhang, K. Shih, Efficient degradation of sulfamethazine with CuCo2O4 spinel nanocatalysts for peroxymonosulfate activation, Chem. Eng. J. 280 (2015) 514-524.
[8] M. Cheng, G. Zeng, D. Huang, C. Lai, Y. Liu, C. Zhang, J. Wan, L. Hu, C. Zhou, W. Xiong, Efficient degradation of sulfamethazine in simulated and real wastewater at slightly basic pH values using Co-SAM-SCS /H2O2 Fenton-like system, Water Res. 138 (2018) 7-18.
[9] C. Zhou, C. Lai, D. Huang, G. Zeng, C. Zhang, M. Cheng, L. Hu, J. Wan, W. Xiong, M. Wen, X. Wen, L. Qin, Highly porous carbon nitride by supramolecular preassembly of monomers for photocatalytic removal of sulfamethazine under visible light driven, Appl. Catal. B Environ. 220 (2018) 202-210.

Comment 17: Better performance of Fenton reactions in acidic pHs is well-documented.
Response: Thank you for your comment. It has been well established that pH of the solution plays a critical role in the efficiency of the Fenton/Fenton-like oxidation. Traditional homogeneous Fenton process generally needs to be operated at acidic pH conditions, which hinders the industrial application of the technology because the pollutant solutions usually have near neutral pH values [1-3]. To make these processes can be operated at wider pH range, a lot of attempts have been made on the development of heterogeneous Fenton-like processes in which solid catalysts were used instead of soluble salts. Cu-based solid catalysts are particularly promising when aiming operation at higher pHs because Cu is less sensitive than Fe to changes in this variable, being thus able to hold their activity in a wider pH range [4, 5].

In this work, the effect of solution pH on the removal of SMZ by CuFeO/H2O2/Vis was studied in order to reveal the applicable pH range of CuFeO/H2O2/Vis system. The results indicated that lower pH favored the degradation of SMZ in the CuFeO/H2O2/Vis system. However, the results also showed that at least 70% of SMZ can be degraded in 30 min in the tested pH range (4.0 to 10.0). In particularly, we found that 95.42% of SMZ was removed after 30 minutes' treatment at a near neutral pH (pH=6.0). In this regard, the CuFeO/H2O2/Vis system showed a remarkable advantage to the traditional homogeneous Fenton process for the practical applications due to the broader working environment.

[1] E. Neyens, J. Baeyens, A review of classic Fenton's peroxidation as an advanced oxidation technique, J. Hazard. Mater. 98 (2003) 33-50.
[2] E. Brillas, I. Sirés, M.A. Oturan, Electro-Fenton process and related electrochemical technologies based on Fenton's reaction chemistry, Chem. Rev. 109 (2009) 6570-6631.
[3] N. Barhoumi, N. Oturan, H. Olvera-Vargas, E. Brillas, A. Gadri, S. Ammar, M.A. Oturan, Pyrite as a sustainable catalyst in electro-Fenton process for improving oxidation of sulfamethazine. Kinetics, mechanism and toxicity assessment, Water Res. 94 (2016) 52-61.
[4] J. Herney-Ramirez, M.A. Vicente, L.M. Madeira, Heterogeneous photo-Fenton oxidation with pillared clay-based catalysts for wastewater treatment: A review, Applied Catalysis B: Environmental 98 (2010) 10-26.
[5] A.C.-K. Yip, F.L.-Y. Lam, X. Hu, Chemical-vapor-deposited copper on acid-activated bentonite clay as an applicable heterogeneous catalyst for the photo-Fenton-like oxidation of textile organic pollutants, Ind. Eng. Chem. Res. 44 (2005) 7983-7990.

Comment 18: EPR or ESR?
Response: Thank you for pointing out our mistakes. It should be ESR. In this work, the electron spin resonance (ESR) experiments were performed. "EPR" is revised to "ESR" in the revised manuscript.
- Page 13, line 16, "EPR" is revised to "ESR" (See Page 16, line 2 in the revised manuscript).
- Page 19, line 5, "EPR" is revised to "ESR" (See Page 22, line 17 in the revised manuscript).

Comment 19: Using the scavenging test is a qualitative measure of confirmation the generation of radicals. When authors used ESR/EPR, testing the effect of scavengers is no more need.
Response: Thank you for your comment. According to the literature, ESR experiments and scavenging tests were often used together to studied the radicals involved in the catalysis [1-5]. In this work, ESR experiments were used to identify the radical species involved in the SMZ degradation, and scavenging tests were used to further confirm the contributions of the radicals, electron (e−) and holes (h+).

[1] D. Wen, Z. Wu, Y. Tang, M. Li, Z. Qiang, Accelerated degradation of sulfamethazine in water by VUV/UV photo-Fenton process: Impact of sulfamethazine concentration on reaction mechanism, J. Hazard. Mater. 344 (2018) 1181-1187.
[2] G.-X. Huang, C.-Y. Wang, C.-W. Yang, P.-C. Guo, H.-Q. Yu, Degradation of Bisphenol A by Peroxymonosulfate Catalytically Activated with Mn1.8Fe1.2O4 Nanospheres: Synergism between Mn and Fe, Environ. Sci. Technol. 51 (2017) 12611-12618.
[3] C. Zhou, C. Lai, D. Huang, G. Zeng, C. Zhang, M. Cheng, L. Hu, J. Wan, W. Xiong, M. Wen, X. Wen, L. Qin, Highly porous carbon nitride by supramolecular preassembly of monomers for photocatalytic removal of sulfamethazine under visible light driven, Appl. Catal. B Environ. 220 (2018) 202-210.

[4] N. Wang, Y. Du, W. Ma, P. Xu, X. Han, Rational design and synthesis of SnO2-encapsulated α-Fe2O3 nanocubes as a robust and stable photo-Fenton catalyst, Appl. Catal. B Environ. 210 (2017) 23-33.
[5] H. Zhao, Y. Chen, Q. Peng, Q. Wang, G. Zhao, Catalytic activity of MOF(2Fe/Co)/carbon aerogel for improving H2O2 and OH generation in solar photo-electro-Fenton process, Appl. Catal. B Environ. 203 (2017) 127-137.

Comment 20: How much was the Fe and Cu leached into the solution during the reaction?
Response: Thank you for your comment. The concentration of Fe and Cu leached into the solution during the reaction was measured and provided in the revised manuscript.
- Secondly, the leaching metal ions from CuFeO nanoparticles were studied. In this work, the concentrations of Cu and Fe in the solution increased quickly during the first 10 min, but a slight decrease was observed from 20 min to 30min (Fig. S10). The concentrations of Cu and Fe in the solution at the end of the process were 2.10 and 1.31 mg/L, respectively. The relatively low metal leaching suggests CuFeO could be used as highly active and stable heterogeneous catalysts for the heterogeneous photo-Fenton process [78-82]. (See Page 21, line 15-22 in the revised manuscript).

Comment 21: How authors separated the nanoparticles at the end of each test for testing the reusability? How much was the separation efficiency? It is important because the concentration of catalyst should kept constant at all the reusability tests.
Response: Thank you for your comment. Due to the magnetic property of the catalyst, CuFeO nanoparticles at the end of each test could be separated simply with a magnet. To avoid the loss of catalysts, the catalysts were not taken out from the reaction flask; instead, they were fixed at the bottom of flask by a magnet, and the supernatant liquid was carefully removed by a straw. In a typical procedure, the catalysts were fixed at the bottom of flask by a magnet, and then the solution was carefully drawn out of the reactor. The catalyst was washed with ultrapure water for 3 times. After that, the magnet was removed, and the reactor was put in the oven (60 °C) to remove the residual water. In the experiment, this method was adopted from a previous work [1] because it was very simple and convenient; moreover, the separation efficiency is more than 95%. The description of the separation is included in the revised manuscript: In the recyclability test, the CuFeO catalyst at the end of each run could be separated simply with a magnet. In a typical procedure, the catalysts were fixed at the bottom of flask by a magnet, and then the solution was carefully drawn out of the reactor. The catalyst was washed with ultrapure water for 3 times. After that, the magnet was removed, and the reactor was placed in the oven (60 °C) to remove the residual water. (See Page 8, line 3-7 in the revised manuscript).
[1] J. Zhang, T. Yao, C. Guan, N. Zhang, H. Zhang, X. Zhang, J. Wu, One-pot preparation of ternary reduced graphene oxide nanosheets/Fe2O3/polypyrrole hydrogels as efficient Fenton catalysts, J. Colloid Interface Sci. 505 (2017) 130-138.

Comment 22: How about the toxicity of the degradation intermediates? The bioassay test is recommended.
Response: Thank you for your comment. According to your comment, the toxicity of the degradation intermediates was evaluated by traditional bacterial growth.
The tests and the results are added in the revised manuscript:

- The toxic effect of SMZ and the degradation intermediates during the process was evaluated by traditional bacterial growth. Escherichia coli (E. coli) was selected as a model bacterium for testing. In a typical test, 0.5 mL of bacterial stock solution (3.0□107 CFU mL-1) was added to 49.5 mL of sterile solution that containing 48.5 mL of ultrapure water and 1 mL of SMZ solution (1 mL of ultrapure water or 1 mL of reaction solution sampled at different time points during the photo-Fenton treatment). The mixed solution was kept in an incubator (37 ℃) for 1 h, then diluted and spread on Eosin Methylene Blue Agar plate. After that, the plate was allowed to incubate at 37 ℃ for 24 h. The viable cell density of each sample was measured by standard plate count method. (See Page 8, line 18 - Page 9, line 5 in the revised manuscript).
- The results showed that SMZ in this CuFeO/H2O2/Vis system can be degraded into different intermediates in a very short time (within 30 min). However, this does not guarantee the toxicity abatement of the resulting wastewater since the intermediates can be more toxic than the starting pollutants in some cases [71, 72]. Therefore, the antimicrobial activity of the treated solutions was studied. Preliminary tests suggested that the growth of E. coli can be inhibited by SMZ solution and the intermediates solutions as compared to the blank (sterile water). The E. coli growth was lower in the photo-Fenton treated samples than in the initial SMZ solution (Fig. S9). The results suggested that the intermediates have higher capacity for inhibiting E. coli growth than that of the parent SMZ. Similar results have been reported elsewhere [18, 73, 74], for example, Perez-Moya et al. [73] reported that the toxicity of an SMZ solution increases during its degradation by means of photo-Fenton reactions. It was suggested that some degradation intermediates, such as cyclic/aromatic compounds and quinone derivatives, are toxic towards the bacteria even at very low concentration [18]. Barhoumi et al. [18] found that the toxicity of the solution can be reduced by prolonging the time of Fenton process. In this work, we also found that the decrease of toxicity at 60 min (Fig. S9). This is probably due to the further degradation of toxic intermediates by •OH. It is well-known that •OH can mineralize most kinds of organic pollutants to carbon dioxide (CO2), water (H2O) and inorganics. On the other hand, there are also reports showing that the biodegradability of SMZ degradation intermediates (produced during the Fenton/Fenton-like process) was higher than that of SMZ [75-77], suggesting a combined Fenton and biological treatment may be suitable for the depleting toxicity of SMZ solution. Taken together, the results suggest the toxicity of the treated SMZ solution needs to be considered carefully in the practical cases. (See Page 20, line 1 - Page 21, line 3 in the revised manuscript).
In this work, the mineralization of SMZ in the photo-Fenton-like systems was also evaluated by Total Organic Carbon (TOC) analysis. The results showed that the concentration of TOC decreases continuously during the photo-Fenton process in the CuFeO/H2O2/Vis system, and about 50% of TOC can be removed after 30 minutes' treatment. It is suggest that with the prolonging the treatment, a high TOC removal can be obtained. This result is in consist with the general recognition that the •OH generated from Fenton reaction can mineralize most kinds of organic pollutants to carbon dioxide (CO2), water (H2O) and inorganics.
- Besides, these results are consistent with the results of TOC analysis (Fig. S7). The results showed that the concentration of TOC decreases continuously during the photo-Fenton process in the CuFeO/H2O2/Vis system, and about 50% of TOC can be removed after 30 minutes' treatment, suggesting that CuFeO has high potential for the real applications. (See Page 14, line 5-9 in the revised manuscript).

Dear Prof. Dionysiou and Reviewers,

Thank you for your valuable suggestions and comments on our manuscript entitled '**Magnetic Cu-Fe oxide derived from metal-organic frameworks as a photo-Fenton catalyst for the efficient removal of sulfamethazine**' (Manuscript Number: **CEJ-D-18-11555**). It is very helpful for us to make improvement.

We have read and considered all the comments and suggestions carefully, and tried our best to revise the manuscript according to the comments of reviewers. On behalf of my co-authors, I would like to provide a detailed list (point by point) of responses to each item of the reviewers' comments. We also highlighted our revisions in the manuscript in red so that reviewers/Editors could easily identify them. We hope that the editor and the reviewers will be satisfied with our responses to the 'comments' and the revisions for our original manuscript.

Thanks and best regards.

Yours sincerely,

Guangming Zeng

List of Three Potential Reviewers

I would like to recommend the following three referees to evaluate my manuscript according to their past and present works and achievements in the field of Fenton process or metal-organic frameworks.

1. Professor Mehmet A. Oturan
Laboratoire Géomatériaux et Environnement, Université Paris-Est
Email: Mehmet.Oturan@univ-paris-est.fr

2. Dr Mark H Wang
School of Chemical & Biomedical Engineering, Nanyang Technological University
Email: wanghou@ntu.edu.sg

3. Dr Wendy Z Wei
Department of Chemistry, University of Warwick
Email: Z.Wei.4@warwick.ac.uk

Revisions based on Reviewer #1:

General Comments:

The paper deals about the preparation, characterization and evaluation of a magnetic CuFeO catalyst for sulfamethazine degradation via photo-Fenton. The effects of pH and H_2O_2 concentration were tested. The pathways and routes of the antibiotic were depicted and the elimination of the antibiotic in several matrices (tap water, river and waste water) was assessed. The paper is interesting and worthy of publication. However, before publication the following aspects need to clarified or provided:

Response:

The reviewer's comments to our work are highly appreciated. We have revised the manuscript carefully to make it clearer than the previous version. The specific revisions are presented as follows.

Specific comments:

Comment 1: The paper details the identification of only three primary byproducts. However, the fate of them upon the treatment is not provided. Furthermore, mineralization (complete transformation of initial antibiotic in CO_2, H_2O and inorganic ions) is not considered. In addition, neither the toxicity nor the antimicrobial activity of the treated solutions are evaluated. Therefore, and due to the fact that in many cases the transformation of the pollutants can lead to the formation of more dangerous compounds, the actual applicability of the technology cannot be established. Therefore, and before publication, the authors should provide some insights about the water quality at the final of the treatment.

Response: Thank you for your comment. It is true that for some pollutants, the degradation intermediates can be more toxic than the starting pollutants. Take dichlorodiphenyltrichloroethane (DDT) for example, it was reported that dichlorodiphenyldichloroethylene (4,4'-DDE) and 2,2-bis (4-chlorophenyl)-1-chloroethylene (4,4'-DDMU) generated during DDT degradation by Fenton process are more toxic than DDT [1-3]. In the present work, 3 main degradation intermediates

were identified by LC-MS analysis, which included 2-amino-4,6-dimethylpyrimidine (A, *m/z* 124), 4-aminophenol (B, *m/z* 110), and 2-amino-4,6-dimethylpyrimidin-5-ol (C, *m/z* 140) (Fig. S5). These intermediates of SMZ degradation were also found in some other chemical degradation processes [4-12]. According to the literature, these intermediates can be further degraded to carboxylic acids, NH_4^+ and NO_3^- ions. It was also reported that the biodegradability of these intermediates was higher than that of SMZ [12-14]. For example, Mansour et al. found the mineralization yield during the biological treatment increased 61.4% after a 0.5 h Fenton pretreatment [12].

According to your comment, the antimicrobial activity of the treated solutions are studied and included in the revised manuscript:

- The toxic effect of SMZ and the degradation intermediates during the process was evaluated by traditional bacterial growth. *Escherichia coli* (*E. coli*) was selected as a model bacterium for testing. In a typical test, 0.5 mL of bacterial stock solution (3.0×10^7 CFU mL^{-1}) was added to 49.5 mL of sterile solution that containing 48.5 mL of ultrapure water and 1 mL of SMZ solution (1 mL of ultrapure water or 1 mL of reaction solution sampled at different time points during the photo-Fenton treatment). The mixed solution was kept in an incubator (37 ℃) for 1 h, then diluted and spread on Eosin Methylene Blue Agar plate. After that, the plate was allowed to incubate at 37 ℃ for 24 h. The viable cell density of each sample was measured by standard plate count method. (See Page 8, line 18 - Page 9, line 5 in the revised manuscript).

- The results show that SMZ in this CuFeO/H_2O_2/Vis system can be degraded into different intermediates in a very short time (within 30 min). However, this does not guarantee the toxicity abatement of the resulting wastewater since the intermediates can be more toxic than the starting pollutants in some cases [71, 72]. Therefore, the antimicrobial activity of the treated solutions was studied. Preliminary tests suggest that the growth of *E. coli* can be inhibited by SMZ solution and the intermediates solutions as compared to the blank (sterile water). The E. coli growth was lower in the photo-Fenton treated samples than in the initial SMZ solution (Fig. S9). The results suggest that the intermediates have higher capacity for inhibiting *E. coli* growth than that of the parent SMZ. Similar results have been reported elsewhere [18, 73, 74], for

example, Perez-Moya et al. [73] reported that the toxicity of an SMZ solution increases during its degradation by means of photo-Fenton reactions. It was suggested that some degradation intermediates, such as cyclic/aromatic compounds and quinone derivatives, are toxic towards the bacteria even at very low concentration [18]. Barhoumi et al. [18] found that the toxicity of the solution can be reduced by prolonging the time of Fenton process. In this work, we also found that the decrease of toxicity at 60 min (Fig. S9). This is probably due to the further degradation of toxic intermediates by •OH. It is well-known that •OH can mineralize most kinds of organic pollutants to carbon dioxide (CO_2), water (H_2O) and inorganics. On the other hand, there are also reports showing that the biodegradability of SMZ degradation intermediates (produced during the Fenton/Fenton-like process) was higher than that of SMZ [75-77], suggesting a combined Fenton and biological treatment may be suitable for the for depleting toxicity of SMZ solution. Taken together, the results suggest the toxicity of the treated SMZ solution needs to be considered carefully in the practical cases. (See Page 20, line 1 - Page 21, line 3 in the revised manuscript).

In this work, the mineralization of SMZ in the photo-Fenton-like systems was also evaluated by Total Organic Carbon (TOC) analysis. The results showed that the concentration of TOC decreases continuously during the photo-Fenton process in the CuFeO/H_2O_2/Vis system, and about 50% of TOC can be removed after 30 minutes' treatment. It is suggest that with the prolonging the treatment, a high TOC removal can be obtained. This result is in consist with the general recognition that the •OH generated from Fenton reaction can mineralize most kinds of organic pollutants to carbon dioxide (CO_2), water (H_2O) and inorganics.

- Besides, these results are consistent with the results of TOC analysis (Fig. S7). The results showed that the concentration of TOC decreases continuously during the photo-Fenton process in the CuFeO/H_2O_2/Vis system, and about 50% of TOC can be removed after 30 minutes' treatment, suggesting that CuFeO has high potential for the real applications. (See Page 14, line 5-9 in the revised manuscript).

[1] M. Cao, L. Wang, L. Wang, J. Chen, X. Lu, Remediation of DDTs contaminated soil in a novel Fenton-like system with zero-valent iron, Chemosphere 90 (2013) 2303-2308.

[2] Villa, R.D., Nogueira, R.F.P., Oxidation of p, p′ -DDT and p, p′ -DDE in highly and long-term contaminated soil using Fenton reaction in a slurry system, Sci. Total Environ. 371 (2006), 11–18.
[3] Megharaj, M., Boul, H.L., Thiele, J.H., Effects of DDT and its metabolites on soil algae and enzymatic activity, Biol. Fert. Soils 29 (1999), 130–134.
[4] I. Kim, H. Tanaka, Photodegradation characteristics of PPCPs in water with UV treatment, Environ. Int. 35 (2009) 793–802.
[5] I. Kim, H. Tanaka, Photodegradation characteristics of PPCPs in water with UV treatment, Environ. Int. 35 (2009) 793–802.
[6] Z. Guo, F. Zhou, Y. Zhao, C. Zhang, F. Liu, C. Bao, M. Lin, Gamma irradiationinduced sulfadiazine degradation and its removal mechanisms, Chem. Eng. J. 191 (2012) 256–262.
[7] T. Zhou, X. Wu, J. Mao, Y. Zhang, T. Lim, Rapid degradation of sulfonamides in a novel heterogeneous sonophotochemical magnetite-catalyzed Fenton-like (US/UV/Fe3O4/oxalate) system, Appl. Catal. B 160–161 (2014) 325–334.
[8] A.P.S. Batista, F.C.C. Pires, A.C.S.C. Teixeira, The role of reactive oxygen species in sulfamethazine degradation using UV-based technologies and products identification, J. Photochem. Photobiol. A 290 (2014) 77–85.
[9] S. Fukahori, T. Fujiwara, Photocatalytic decomposition behavior and reaction pathway of sulfamethazine antibiotic using TiO2, J. Environ. Manage. 157 (2015) 103–110.
[10] Y. Fan, Y. Ji, D. Kong, J. Lu, Q. Zhou, Kinetic and mechanistic investigations of the degradation of sulfamethazine in heat-activated persulfate oxidation process, J. Hazard. Mater. 300 (2015) 39–47.
[11] K. Kim, S.B. Kam, Y.S. Mok, Elucidation of the degradation pathways of sulfonamide antibiotics in a dielectric barrier discharge plasma system, Chem. Eng. J. 271 (2015) 31–42.
[12] D. Mansour, F. Fourcade, S. Huguet, I. Soutrel, N. Bellakhal, M. Dachraoui, D. Hauchard, A. Amrane, Improvement of the activated sludge treatment by its combination with electro Fenton for the mineralization of sulfamethazine, Int. Biodeterior. Biodegrad. 88 (2014) 29-36.
[13] A. Ledjeri, I. Yahiaoui, H. Kadji, F. Aissani-Benissad, A. Amrane, F. Fourcade, Combination of the Electro/Fe3+/peroxydisulfate (PDS) process with activated sludge culture for the degradation of sulfamethazine, Environ. Toxicol. Pharmacol. 53 (2017) 34-39.
[14] D. Mansour, F. Fourcade, I. Soutrel, D. Hauchard, N. Bellakhal, A. Amrane, Relevance of a combined process coupling electro-Fenton and biological treatment for the remediation of sulfamethazine solutions – Application to an industrial pharmaceutical effluent, Comptes Rendus Chimie 18 (2015) 39-44.

Comment 2: In section 3.2, concerning the pH effect, the authors indicates that OH radicals have a higher oxidation potential at lower pH. Why is the reason of that behavior of these radicals? In my opinion this is not true, there are not any thermodynamic (or even kinetic) reason to support such affirmation. The same occurs with the affirmation of the higher stability of hydrogen peroxide at lower pH values. Did the authors test the H_2O_2 stability at the tested pHs to validate this affirmation?

In my opinion the better efficiency at lower pH values is probably due to the higher leaching of iron and copper ions as the pH decreases, which facilitates the faster homogeneous photo-Fenton reaction.

Response: Your comments are greatly appreciated. According to your comments, the sentence "Firstly, the higher oxidation potential of •OH can be achieved at the lower pH values, which favored the degradation of SMZ [41]" has been removed, and the sentence "Firstly, better efficiency at lower pH values can be due to the higher leaching of iron and copper ions as the pH decreases, which facilitates the faster homogeneous photo-Fenton reaction." is added in the revised manuscript.

The H_2O_2 stability at the different pHs (pH > 3) has been studied by many researchers, and it was found that the auto-decomposition of H_2O_2 ($2H_2O_2 \rightarrow O_2 + 2H_2O$) is accelerated at higher pH [1-4].

The related text is revised to:

- Two mechanisms can be responsible for this phenomenon. Firstly, better efficiency at lower pH values can be due to the higher leaching of iron and copper ions as the pH decreases, which facilitates the faster homogeneous photo-Fenton reaction [56]. Secondly, H_2O_2 is less stable at higher pH conditions and tend to decompose into H_2O [57]. (See Page 14, line 19 - Page 15, line 1 in the revised manuscript).

[1] L. Szpyrkowicz, C. Juzzolino, S.N. Kaul, A Comparative study on oxidation of disperse dyes by electrochemical process, ozone, hypochlorite and fenton reagent, Water Res. 35 (2001) 2129-2136.
[2] J. Herney-Ramirez, M.A. Vicente, L.M. Madeira, Heterogeneous photo-Fenton oxidation with pillared clay-based catalysts for wastewater treatment: a review, Appl. Catal. B Environ. 98 (2010) 10-26.
[3] A. Babuponnusami, K. Muthukumar, A review on Fenton and improvements to the Fenton process for wastewater treatment, J. Environ. Chem. Eng. 2 (2014) 557-572.
[4] W. Najjar, S. Azabou, S. Sayadi, A. Ghorbel, Catalytic wet peroxide photo-oxidation of phenolic olive oil mill wastewater contaminants: Part I. Reactivity of tyrosol over (Al–Fe)PILC, Appl. Catal. B Environ. 74 (2007) 11-18.

Comment 3: Other minor aspects are:

1) The supplier of polyvinylpyrrolidone should be provided in the experimental part.

Response: In the revised manuscript, the supplier of polyvinylpyrrolidone is provided

in the experimental part.

- and polyvinylpyrrolidone (PVP) were obtained from Sinopharm Chemical Reagent Corp (China). (See Page 6, line 11 in the revised manuscript).

2) The protocol for the EDS analysis should be also included in the experimental section.

Response: In the revised manuscript, the protocol for the EDS analysis is included in the experimental section.

- Energy dispersive X-ray spectroscopy (EDS) of the prepared catalyst was obtained using an EDAX Genesis X-ray spectrometer. (See Page 7, line 3-5 in the revised manuscript).

3) In section 3.3, MnFeO is wrong, because not materials containing Mn were considered in this work.

Response: The mentioned mistakes have been corrected. MnFeO is revised to CuFeO (See Page 16, line 7 in the revised manuscript).

Revisions based on Reviewer #2:

General Comments:

This manuscript deals with Magnetic Cu-Fe oxides derived from metal-organic frameworks as a photo-Fenton catalyst for the efficient removal of sulfamethazine. Due to the provided comments, the manuscript needs to be rewritten and major revision to be re-reviewed to make decision on its adequacy toward the publication in CEJ.

Response:

The reviewer's comments to our work are highly appreciated. We have revised the manuscript carefully to make it clearer than the previous version. The specific revisions are presented as follows.

Specific comments:

Comment 1: Title is not representative.

Response: Thank you for your comment. The title has been revised to "Prussian blue analogue derived magnetic Cu-Fe oxide as a recyclable photo-Fenton catalyst for the efficient removal of sulfamethazine at near neutral pH values".

Comment 2: "….a synergistic effect between solid-state Cu and Fe was identified in control experiments with CuO and Fe_3O_4". How authors could confirm this conclusion? Without experimental confirmation, it would be speculative.

Response: Thank you for your comment. We now realize that without experimental confirmation, it is inappropriate to say that a synergistic effect between solid-state Cu and Fe was identified. In the revised manuscript, this sentence in the Abstract is revised to "The removal rate of SMZ in $CuFeO/H_2O_2$/Vis system was much higher than those in CuO/H_2O_2/Vis and Fe_3O_4/H_2O_2/Vis systems." (See Page 2, line 8-10 in the revised manuscript).

Comment 3: "…It is suggested that the synergistic effect among photo-induced electrons, Cu and Fe in CuFeO exhibits excellent performance in the catalytic activation of H_2O_2". The interaction between Cu and Fe in CuFeO should be given and explain to be able suggesting the synergistic effect.

Response: Thank you for your comment. The interaction between Cu and Fe in CuFeO is discussed in the in the revised manuscript.

- On the other hand, e^- can cause an in–situ recycling of copper species ($Cu^{II} \rightarrow Cu^{I}$) and iron species ($Fe^{III} \rightarrow Fe^{II}$) through eqs. 15 and 16 [68], respectively. In addition, the reduction of Fe^{III} by Cu^{I} is thermodynamically favorable (eqs. 17) according to the standard reduction potentials of the Fe and Cu (eqs. 15 and 16) [68].

$$\equiv Cu^{II} + e^- \rightarrow \equiv Cu^{I} \qquad E_0 = 0.16\ V \tag{15}$$

$$\equiv Fe^{III} + e^- \rightarrow \equiv Fe^{II} \qquad E_0 = 0.77\ V \tag{16}$$

$$\equiv Fe^{III} + Cu^{I} \rightarrow \equiv Fe^{II} + \equiv Cu^{II} \tag{17}$$

(See Page 18, line 6-11 in the revised manuscript).

Comment 4: A consistent form should be used for hydroxyl radicals (*OH or HO*) throughout the text.

Response: Thank you for your comment. We have checked the manuscript carefully. A consistent form for hydroxyl radicals (•OH) is used throughout the revised manuscript.

Comment 5: The novelty of the study is not clear. The Cu-Fe PBAs were synthesized according to a previously reported method. Only a further calcination step was used to prepare CuFeO.

Response: Thank you for your comment. The bimetallic catalyst, Cu-Fe oxide has gained particular attention in Fenton-like chemistry, not only because of its good catalytic performance but also copper is not regarded as a potential carcinogen [1-4]. The occurrence of metal–organic frameworks (MOFs) brings a great deal of opportunities for the development of new types of Cu-Fe oxide with excellent characteristic features, such as well-defined structure, large pore volume and high

specific area.

Prussian blue analogues (PBAs) as a set of the most frequently studied metal–organic frameworks (MOFs), has the common features of MOFs, such as large pore volume and high specific area [5]. Several studies have investigated the catalytic properties of the PBAs in heterogeneous Fenton-like reactions. For example, Li et al. [6] have developed two Fe-Co PBAs, $Fe[Co(CN)_6]\bullet 2H_2O$ and $Fe_3[Co(CN)_6]_2\bullet 12H_2O$, as excellent photo-Fenton catalysts. In their study, the removal efficiency of Rhodamine B (RhB, 12 mg L^{-1}) by Fe^{II}-Co PBA/H_2O_2 in 30 min reached 93%. However, to our knowledge no previous study has investigated the preparation of Cu-Fe oxide from Cu-Fe PBAs and its application for Fenton-like reactions. Herein, in this work we report a facile two-step strategy to prepare Cu-Fe oxide. Although Cu-Fe PBAs were synthesized according to a previously reported method, which is very similar to those for the preparation of Co-Fe PBA and Mn-Fe PBA. However, the catalytic performance of the PBA derived CuFeO together with the mechanism have not been reported.

According to your valuable comment, we have revised the Introduction with aim to emphasize the novelty of the study.

- The bimetallic catalyst, Cu-Fe oxide has gained particular attention in the Fenton chemistry, not only because of its good catalytic performance but also copper is not regarded as a potential carcinogen [33]. Recently, some researchers have studied the feasibility of using MOFs to obtain porous nanostructured oxides. The pioneering works showed that the original morphology of the precursor can be almost retained after the thermal treatment, while the catalytic performance can be largely improved [34-36]. To our knowledge, however, no study on the preparation of Cu-Fe oxide from Cu-Fe PBAs and its application for Fenton-like reactions has been reported. Therefore, in this current study, a facile two-step strategy was developed to synthesize porous Cu-Fe oxide (CuFeO) by heating the Cu-Fe PBAs. (See Page 5, line 4-13 in the revised manuscript).

[1] Dorsey, A.; Ingerman, L.; Swarts, S. Toxicological Profile for Copper; Department of Health & Human Services, Public Health Service, Agency for Toxic Substances and Disease Registry, 2004.

[2] Ding, Y.; Zhu, L.; Wang, N.; Tang, H. Sulfate radicals induced degradation of tetrabromobisphenol A with nanoscaled magnetic CuFe2O4 as a heterogeneous catalyst of peroxymonosulfate. Appl. Catal., B 2013, 129, 153-162
[3] Zhang, T.; Zhu, H.; Croue, J. P. Production of sulfate radical from peroxymonosulfate induced by a magnetically separable CuFe2O4 spinel in water: Efficiency, stability, and mechanism. Environ. Sci. Technol. 2013, 47 (6), 2784-2791
[4] Y. Lei, C.-S. Chen, Y.-J. Tu, Y.-H. Huang, H. Zhang, Heterogeneous degradation of organic pollutants by persulfate activated by CuO-Fe_3O_4: mechanism, stability, and effects of pH and bicarbonate ions, Environ. Sci. Technol. 49 (2015) 6838-6845.
[5] B. Kong, C. Selomulya, G. Zheng, D. Zhao, New faces of porous Prussian blue: interfacial assembly of integrated hetero-structures for sensing applications, Chem. Soc. Rev. 44 (2015) 7997-8018.
[6] X. Li, J. Liu, A.I. Rykov, H. Han, C. Jin, X. Liu, J. Wang, Excellent photo-Fenton catalysts of Fe–Co Prussian blue analogues and their reaction mechanism study. Appl. Catal. B 179 (2015)196.

Comment 6: What about if the catalyst prepared from other precursors (non MOF-based materials)? What is the main feature of the Cu-Fe PBAs that was used for preparation of FeCuO? The Fe_2O_3/CuO composite has been prepared by different methods. The importance of the selected method is unclear.

Response: Thank you for your comment. Several previous studies have reported that the Cu-Fe oxide catalyzed (photo-) Fenton-like process is effective for the destruction of organic contaminants in water [1-5]. Cu-Fe oxide can be obtained by a variety of methods, such as sol–gel combustion method [1, 2], polymeric precursor method [3], co-precipitation method [4], and hydrothermal method [5].

The main feature of the Cu-Fe PBAs that was used for preparation of FeCuO is: Cu-Fe PBA as a kind of MOF, has the advantage features of MOFs, such as large pore volume and high specific area [6]. For example, the BET surface area of CuFeO-Et in Dang and Le' work is **7.5 m^2/g** [3], the BET surface area and pore volume of CuO-Fe3O4 in Lei et al.'s work is **28.26 m^2/g** and **0.09728 cm^3/g**, respectively [5]. However, the BET surface area and pore volume of FeCuO in our present work reach **178.35 m^2/g** and **0.6993 cm^3/g**, respectively. The much larger surface area (compared to the conventional catalysts) is the most interesting property of MOFs [7]. This would lead to unusual chemistry if this large surface could be fully covered by active sites [7]. The high porosity is very useful to expose the active sites completely to

reactant(s) and to enhance the reactivity remarkably [8].

According to your valuable comment, we have revised the Introduction with aim to emphasize the importance of the selected method.

- The occurrence of MOFs also brings a great deal of opportunities for the development of new heterogeneous Fenton-like catalysts with excellent characteristic features, such as large surface area and uniform pore sizes [27-29]. This large surface could provide abundant active sites, and the high porosity is very useful to expose the active sites completely to reactant(s) [27]. (See Page 4, line 7-11 in the revised manuscript).

[1] Y. Feng, C. Liao, K. Shih, Copper-promoted circumneutral activation of H_2O_2 by magnetic $CuFe_2O_4$ spinel nanoparticles: Mechanism, stoichiometric efficiency, and pathway of degrading sulfanilamide, Chemosphere 154 (2016) 573-582.

[2] T.T. Dinh, T.Q. Nguyen, G.C. Quan, V.D.N. Nguyen, H.Q. Tran, T.K. Le, Starch-assisted sol–gel synthesis of magnetic $CuFe_2O_4$ powder as photo-Fenton catalysts in the presence of oxalic acid, Int. J. Environ. Sci. Technol. 14 (2017) 2613-2622.

[3] H.T. Dang, T.K. Le, Precursor chain length dependence of polymeric precursor method for the preparation of magnetic Fenton-like $CuFe_2O_4$-based catalysts, J. Sol-Gel Sci. Technol. 80 (2016) 160-167.

[4] Pereira C, Pereira AM, Fernandes C, Rocha M, Mendes R, Fernandez García MP, Guedes A, Tavares PB, Greneche JM, Araujo JP, Freire C (2012) Superparamagnetic MFe_2O_4 (M = Fe Co, Mn) nanoparticles: tuning the particle size and magnetic properties through a novel one-step coprecipitation route. Chem Mater 24:1496–1504

[5] Y. Lei, C.-S. Chen, Y.-J. Tu, Y.-H. Huang, H. Zhang, Heterogeneous degradation of organic pollutants by persulfate activated by $CuO-Fe_3O_4$: mechanism, stability, and effects of pH and bicarbonate ions, Environ. Sci. Technol. 49 (2015) 6838-6845.

[6] B. Kong, C. Selomulya, G. Zheng, D. Zhao, New faces of porous Prussian blue: interfacial assembly of integrated hetero-structures for sensing applications, Chem. Soc. Rev. 44 (2015) 7997-8018.

[7] Y. Zhang, Y. Zhou, Y. Zhao, C.-j. Liu, Recent progresses in the size and structure control of MOF supported noble metal catalysts, Catal. Today 263 (2016) 61-68.

[8] Q. Yang, Q. Xu, H.L. Jiang, Metal-organic frameworks meet metal nanoparticles: synergistic effect for enhanced catalysis, Chem. Soc. Rev. 46 (2017) 4774.

Comment 7: Since before starting the photo-Fenton reaction the adsorption process was run, a part of SMZ could be adsorbed onto the catalyst and thus the initial concentration for oxidation reactions is something less than 50 mg/L. Authors had better to test the adsorption in a separate experiment and use the results for calculation

of synergistic effect.

Response: Thank you for your comment. It is true that "a part of SMZ could be adsorbed onto the catalyst and thus the initial concentration for oxidation reactions is something less than 50 mg/L". Like in many others, in our experiments, the adsorption of SMZ has also been considered. Prior to the catalysis experiments, the SMZ adsorption on the surface of catalysts was carried out to investigate SMZ adsorption capacity of prepared catalysts. The results showed that the adsorption−desorption equilibrium can be reached in 30 min. We also found that both Cu-Fe PBAs and CuFeO exhibited negligible SMZ adsorption capacity (about 3% of SMZ was removed by adsorption). Since the amount of SMZ removed by adsorption as compared to that removed by degradation is very small, we did not considered the adsorption in the degradation tests. In a typical run, 50 mg of catalyst was added to 100 mL of SMZ solution and stirred for 30 min to establish the adsorption−desorption equilibrium, and then the degradation process was triggered.

The results of adsorption text can be found in Page 13, line 9-13 in the revised manuscript.

- The adsorption of SMZ by Cu-Fe PBAs and CuFeO was studied in the first step. As revealed in Fig. S6, adsorption of SMZ by Cu-Fe PBAs and CuFeO achieved adsorption equilibrium in 30 min. We also found that both Cu-Fe PBAs and CuFeO exhibited similar and negligible SMZ adsorption capacity (about 3% of SMZ was removed by adsorption). (See Page 13, line 9-13 in the revised manuscript).

Comment 8: CuFeO is not a MOF-based catalyst because the organics were incinerated during the calcinations process. In some part of the text it has been expressed that the MOF-based catalyst was prepared as new material for Fenton process. The text should be modified to consider this point.

Response: Thank you for pointing out our mistakes. CuFeO prepared from Cu-Fe PBAs should be a MOF-derived catalyst.

"MOF-based" is revised to "MOF-derived" in the revised manuscript.

- Page 5, line 14 "MOF-based photo-Fenton catalyst" is revised to "MOF-derived

photo-Fenton catalyst" (See Page 5, line 19 in the revised manuscript).

- Page 5, line 22 "MOF-based photo-Fenton catalyst" is revised to "MOF-derived photo-Fenton catalyst" (See Page 6, line 5 in the revised manuscript).

- Page 19, line 1 "MOF-based catalyst" is revised to "MOF-derived catalyst" (See Page 21, line 10 in the revised manuscript).

Comment 9: Based on XRD results, the catalyst composed of crystal plane of Fe_3O_4 and CuO. Why authors say it is FeCuO?

Response: Thank you for your comment. In this article, CuFeO is used as the shortened form of the Cu-Fe PBA-derived Cu-Fe oxide (See Page 5, line 14 in the revised manuscript). This idea is come from some previous published works [1-4].

[1] M. Al-Dossary, A.A. Ismail, J.L.G. Fierro, H. Bouzid, S.A. Al-Sayari, Effect of Mn loading onto MnFeO nanocomposites for the CO_2 hydrogenation reaction, Applied Catalysis B: Environmental 165 (2015) 651-660.

[2] T.T. Dinh, T.Q. Nguyen, G.C. Quan, V.D.N. Nguyen, H.Q. Tran, T.K. Le, Starch-assisted sol–gel synthesis of magnetic CuFe2O4 powder as photo-Fenton catalysts in the presence of oxalic acid, Int. J. Environ. Sci. Technol. 14 (2017) 2613-2622.

[3] G.-X. Huang, C.-Y. Wang, C.-W. Yang, P.-C. Guo, H.-Q. Yu, Degradation of Bisphenol A by Peroxymonosulfate Catalytically Activated with Mn1.8Fe1.2O4 Nanospheres: Synergism between Mn and Fe, Environ. Sci. Technol. 51 (2017) 12611-12618.

[4] Y. Wu, L. Zhan, K. Huang, H. Wang, H. Yu, S. Wang, F. Peng, C. Lai, Iron based dual-metal oxides on graphene for lithium-ion batteries anode: Effects of composition and morphology, J. Alloys Compd. 684 (2016) 47-54.

Comment 10: Authors stated that they prepared CuFeO nanospheres. But the SEM image does not show the spherical particles.

Response: Thank you for your comment. According to you comment "CuFeO nanospheres" is revised "CuFeO particles".

- Page 2, line 6 "obtained CuFeO nanospheres" is revised to "obtained CuFeO particles" (See Page 2, line 6 in the revised manuscript).

- Page 9, line 3 "many tiny nanospheres" is revised to "many tiny particles" (See Page 10, line 8 in the revised manuscript).

- Page 9, line 12 "the CuFeO nanospheres" is revised to "the CuFeO particles" (See Page 10, line 16 in the revised manuscript).

- Page 18, line 6 “from CuFeO nanospheres” is revised to “from CuFeO particles” (See Page 21, line 17 in the revised manuscript).

Comment 11: The size distribution of the prepared catalysts should be provided. How much was the average size of particles?

Response: Thank you for your comment. According to you comment, the size distribution of the prepared catalysts was measured with the dynamic light scattering (DLS) method. The measurement was carried out using a DynaPro Dynamic Light Scatterer (Malvern Instruments). The results show that the average size of Cu-Fe PBA and CuFeO was 225.8 and 240.0 nm, respectively.

The tests and results are added in the revised manuscript.

- The size distribution of the prepared catalysts was measured with the dynamic light scattering (DLS) method. The prepared catalysts were fully dispersed in water with the help of ultrasound radiation. The measurement was carried out using a DynaPro Dynamic Light Scatterer (Malvern Instruments). (See Page 7, line 4-8 in the revised manuscript).

- DLS analysis shows that the average size of Cu-Fe PBA and CuFeO (dispersed in water) was 225.8 and 240.0 nm, respectively (Fig. S3). The average size of CuFeO is very closed to that of Cu-Fe PBA, suggesting the thermal treatment did not significantly change the morphology of Cu-Fe PBA, which is in consistent with the results obtained from SEM analysis. (See Page 10, line 21 - Page 11, line 3 in the revised manuscript).

Comment 12: The specific surface area of a catalyst is one the important parameters affecting the catalytic activity. BET and BJH analysis is recommended.

Response: Thank you for your comment. BET and BJH analysis is performed and included in the revised manuscript.

- The Brunauer–Emmett–Teller (BET) specific surface area, the Barrett–Joyner–Halenda (BJH) pore volume and pore size of the catalyst were measured using the Micromeritics ASAP 2010 analyzer. (See Page 7, line 7-10 in the revised manuscript).

- The BET surface area and BJH pore volume of CuFeO nanoparticles are 178.35 m^2/g and 0.6993 cm^3/g, respectively, which are much higher than those of the reported Cu-Fe bimetallic catalysts [33, 39, 40]. As shown in Fig. S4, the BET isotherm of CuFeO nanoparticles belongs to type IV with H3 type hysteresis loops, indicating that CuFeO nanoparticles were mesoporous. The inset of Fig. S4 is the BJH pore size distribution plots of CuFeO nanoparticles. According to the BJH analysis, the pore size of the CuFeO catalyst was determined to be 17.47 nm. The high specific surface area and porous structure of the catalysts may facilitate the catalytic performance. (See Page 11, line 3-10 in the revised manuscript).

Comment 13: The composition of the catalyst is better characterized by the XRF analysis rather than FTIR.

Response: Thank you for your comment. In this work, the prepared catalysts have been systematically characterized by SEM, EDS, TEM, BET, DLS, XRD, XPS, FT-IR, VSM and TG analysis. According to you comment, the XRF analysis will be adopted to study the composition of the prepared materials in our future works. In this work, FTIR analysis was used to study the changes of chemical groups after the calcination. For example, the absorption band at 2102 cm^{-1} of PBA spectrum is assignable to the C-N stretching vibration; however, after the calcination, the characteristic peaks of C-N stretching vibration (2102 cm^{-1}) completely disappeared from the spectrum. For another, the strong band emerged at 570 cm^{-1} in CuFeO pattern suggests the presence of Fe-O in CuFeO sample.

Comment 14: To show and confirm that the prepared catalyst were magnetic, the VSM analysis was conducted. The finding should be better described in the main text.

Response: Thank you for your comment. We have revised the manuscript according to your comment. The description of the results of VSM analysis is revised to:

- Fig. S5 presents the magnetic hysteresis curves for Cu-Fe PBA, CuFeO and the used-CuFeO. These curves display the evolution of magnetization (M) as a function of applied field (H). As indicated in Fig. S5, no magnetism was found in Cu-Fe PBA,

while CuFeO exhibited obvious magnetism. Moreover, CuFeO could maintain its original magnetism even after 5 degradation cycles. The saturation magnetization value (*M*s) of CuFeO was measured to be 14.18 emu g^{-1}, which is about 25% of that of pure magnetic Fe_3O_4 under the same conditions. Generally, catalysts with high *M*s values means that they can be easily separated from the solution by magnet. In our experiment, CuFeO particles could be collected simply with a magnet in 10 s as shown in the inset picture of Fig. S5. This enhances the technical and economic feasibility because it allows the convenient separation and recycling of catalyst by applying an external magnetic field. (See Page 12, line 19- Page 13, line 7 in the revised manuscript).

Comment 15: The main point in this manuscript is that the authors should explain and confirm why the CuFeO/H_2O_2/Vis process had drastically greater performance than the CuFeO/Vis and CuFeO/H_2O_2 processes for the SMZ degradation. Without this confirmation and documentation the statement "the CuFeO/H_2O_2/Vis system showed a remarkable advantage for the practical applications due to the broader working environment" is misleading. The information provided in section 3.4 is on the mechanism and do not explain why irradiating (by Vis light) the FeCuO/H_2O_2 could improve the degradation to such a high rate.

Response: Thank you for your comment.

(1) According to the results showed in Fig. 6B, we can found that the •OH and photo-induced e^- are highly related to the SMZ degradation efficiency. As indicated in Fig. 6B, the addition of silver nitrate ($AgNO_3$), as a scavenger for photoinduced e^- dramatically suppresses the photo-Fenton reaction; and a more distinct inhibition phenomenon was observed when the scavenger of tert-butyl alcohol (TBA) for •OH is added to the reaction system. These results together with eqs. 1-3 can explain why CuFeO/H_2O_2/Vis system had greater performance than the CuFeO/Vis and CuFeO/H_2O_2 for the SMZ degradation. For CuFeO/Vis system, because of the absence of H_2O_2, •OH cannot be efficiently produced via eqs. 1. SMZ degradation is mainly caused by the photo-induced h^+, which was proved plays a minor role in SMZ

degradation (Fig. 6B). Therefore, SMZ degradation efficiency in this system was low. As for FeCuO/H_2O_2 system, SMZ degradation is mainly caused by the Fenton-like reactions (eqs. 4-7). Because of the absence of photo-induced e^-, •OH cannot be efficiently produced via eqs. 1. Besides, in CuFeO/H_2O_2/Vis system, a potential in–situ recycling of copper species ($Cu^{II} \rightarrow Cu^{I}$) and iron species ($Fe^{III} \rightarrow Fe^{II}$) would be easily occur through eqs. 8 and 9. These processes facilitate the continuous cycle of Fe^{III}/Fe^{II} and Cu^{II}/Cu^{I}. Therefore, SMZ degradation efficiency in CuFeO/H_2O_2/Vis system was much higher. Similar results were reported by Gao an co-workers [1] who studied the removal of sulfonamide by a $CuFe_2O_4$ catalyzed photo-Fenton process.

$$H_2O_2 + e^- \rightarrow \bullet OH + OH^- \quad (1)$$

$$CuO + h\nu \rightarrow CuO\ (e^- + h^+) \quad (2)$$

$$Fe_3O_4 + h\nu \rightarrow Fe_3O_4\ (e^- + h^+) \quad (3)$$

$$\equiv Fe^{II} + H_2O_2 \rightarrow \equiv Fe^{III} + \bullet OH + OH^- \quad (4)$$

$$\equiv Fe^{III} + H_2O_2 \rightarrow \equiv Fe^{II} + \bullet OOH + H^+ \quad (5)$$

$$\equiv Cu^{I} + H_2O_2 \rightarrow \equiv Cu^{II} + \bullet OH + OH^- \quad (6)$$

$$\equiv Cu^{II} + H_2O_2 \rightarrow \equiv Cu^{I} + \bullet OOH + H^+ \quad (7)$$

$$\equiv Cu^{II} + e^- \rightarrow \equiv Cu^{I} \qquad E_0 = 0.16\ V \quad (8)$$

$$\equiv Fe^{III} + e^- \rightarrow \equiv Fe^{II} \qquad E_0 = 0.77\ V \quad (9)$$

The related content in Section 3.4 has been revised based on the above discussion.

- This can explain the relative low SMZ degradation efficiency in CuFeO/Vis system. As seen from Fig. 6B, the photo-induced e^- plays an important role in SMZ degradation. This is because e^- could not only react with H_2O_2 to produce active •OH (eqs. 14), but also can cause an in–situ recycling of copper species ($Cu^{II} \rightarrow Cu^{I}$) and iron species ($Fe^{III} \rightarrow Fe^{II}$) through eqs. 15 and 16 [68], respectively. In addition, the reduction of Fe^{III} by Cu^{I} is thermodynamically favorable (eqs. 17) according to the standard reduction potentials of the Fe and Cu (eqs. 15 and 16) [68]. These processes facilitate the continuous cycle of Fe^{III}/Fe^{II} and Cu^{II}/Cu^{I} in CuFeO/H_2O_2/Vis system.

(See Page 18, line 3-11 in the revised manuscript)

(2) The statement "the CuFeO/H_2O_2/Vis system showed a remarkable advantage for the practical applications due to the broader working environment" in *3.2. Catalytic performance of CuFeO* is based on the pH test results. According to you comment, this part has been revised to:

- From another point of view, at least 70% of SMZ can be degraded in 30 min in the tested pH range (4.0 to 10.0). In particularly, we found that 95.42% of SMZ was removed after 30 minutes' treatment at a near neutral pH (pH=6.0). Traditional homogeneous Fenton process generally needs to be operated at acidic pH conditions, which hinders the industrial application of the technology because the pollutant solutions usually have near neutral pH values [23]. In this regard, the CuFeO/H_2O_2/Vis system showed a remarkable advantage for the practical applications due to the broader working environment. (See Page 15, line 2-8 in the revised manuscript).

[1] J. Gao, S. Wu, Y. Han, F. Tan, Y. Shi, M. Liu, X. Li, 3D mesoporous $CuFe_2O_4$ as a catalyst for photo-Fenton removal of sulfonamide antibiotic at near neutral pH, J. Colloid Interface Sci. 524 (2018) 409-416.

Comment 16: The rate of SMZ degradation in the developed process should be compared with that in the other AOPs based on the degradation rate (r) value.

Response: Thank you for your comment. In the revision, the rate of SMZ degradation in the developed process is compared with that in the other AOPs. In this work, 95.42% of SMZ was removed after 30 minutes' treatment at a near neutral pH (pH=6.0). According to the literature, the rate of SMZ degradation of CuFeO/H_2O_2/Vis is high than many other AOPs [1-9]. For example, Gao et al reported that about 95% of SMZ (20 mg/L) was removed in 90 min at pH 6.73 in the CuFe2O4 photo-Fenton process [1]; Barhoumi et al reported that about 85% of SMZ (0.2 mM) was removed in 40 min at pH 3.0 in the Pyrite electro-Fenton process [2]; Fan et al reported that about 80% of SMZ (0.03 mM) was removed in 60 min at pH 7.0 in heat-activated persulfate oxidation process [3]; Wang et al reported that about 50% of SMZ (20 mg/L) was removed in 120 min at pH 6.0 in Bi-doped TiO_2

photocatalytic process [4].

The manuscript has been revised accordingly.

- In this work, 95.42% of SMZ was removed after 30 min in CuFeO/H_2O_2/Vis system. The degradation efficiency of SMZ in this process is higher than those of many reported AOPs, including photo-Fenton process [48], electro-Fenton process [18, 49], photocatalytic processes [50, 51], and peroxymonosulfate/ persulfate-based oxidation [52, 53]. (See Page 14, line 1-5 in the revised manuscript).

[1] J. Gao, S. Wu, Y. Han, F. Tan, Y. Shi, M. Liu, X. Li, 3D mesoporous CuFe2O4 as a catalyst for photo-Fenton removal of sulfonamide antibiotics at near neutral pH, J. Colloid Interface Sci. 524 (2018) 409-416.

[2] N. Barhoumi, N. Oturan, H. Olvera-Vargas, E. Brillas, A. Gadri, S. Ammar, M.A. Oturan, Pyrite as a sustainable catalyst in electro-Fenton process for improving oxidation of sulfamethazine. Kinetics, mechanism and toxicity assessment, Water Res. 94 (2016) 52-61.

[3] Y. Fan, Y. Ji, D. Kong, J. Lu, Q. Zhou, Kinetic and mechanistic investigations of the degradation of sulfamethazine in heat-activated persulfate oxidation process, J. Hazard. Mater. 300 (2015) 39-47.

[4] N. Wang, X. Li, Y. Yang, T. Guo, X. Zhuang, S. Ji, T. Zhang, Y. Shang, Z. Zhou, Enhanced photocatalytic degradation of sulfamethazine by Bi-doped TiO2 nano-composites supported by powdered activated carbon under visible light irradiation, Sep. Purif. Technol. 211 (2018) 673-683.

[5] A. Ledjeri, I. Yahiaoui, H. Kadji, F. Aissani-Benissad, A. Amrane, F. Fourcade, Combination of the Electro/Fe^{3+}/peroxydisulfate (PDS) process with activated sludge culture for the degradation of sulfamethazine, Environ. Toxicol. Pharmacol. 53 (2017) 34-39.

[6] R. Li, Z. Chen, M. Cai, J. Huang, P. Chen, G. Liu, W. Lv, Improvement of Sulfamethazine photodegradation by Fe(III) assisted MIL-53(Fe)/percarbonate system, Appl. Surf. Sci. 457 (2018) 726-734.

[7] Y. Feng, J. Liu, D. Wu, Z. Zhou, Y. Deng, T. Zhang, K. Shih, Efficient degradation of sulfamethazine with $CuCo_2O_4$ spinel nanocatalysts for peroxymonosulfate activation, Chem. Eng. J. 280 (2015) 514-524.

[8] M. Cheng, G. Zeng, D. Huang, C. Lai, Y. Liu, C. Zhang, J. Wan, L. Hu, C. Zhou, W. Xiong, Efficient degradation of sulfamethazine in simulated and real wastewater at slightly basic pH values using Co-SAM-SCS /H_2O_2 Fenton-like system, Water Res. 138 (2018) 7-18.

[9] C. Zhou, C. Lai, D. Huang, G. Zeng, C. Zhang, M. Cheng, L. Hu, J. Wan, W. Xiong, M. Wen, X. Wen, L. Qin, Highly porous carbon nitride by supramolecular preassembly of monomers for photocatalytic removal of sulfamethazine under visible light driven, Appl. Catal. B Environ. 220 (2018) 202-210.

Comment 17: Better performance of Fenton reactions in acidic pHs is well-documented.

Response: Thank you for your comment. It has been well established that pH of the solution plays a critical role in the efficiency of the Fenton/Fenton-like oxidation. Traditional homogeneous Fenton process generally needs to be operated at acidic pH conditions, which hinders the industrial application of the technology because the pollutant solutions usually have near neutral pH values [1-3]. To make these processes can be operated at wider pH range, a lot of attempts have been made on the development of heterogeneous Fenton-like processes in which solid catalysts were used instead of soluble salts. Cu-based solid catalysts are particularly promising when aiming operation at higher pHs because Cu is less sensitive than Fe to changes in this variable, being thus able to hold their activity in a wider pH range [4, 5].

In this work, the effect of solution pH on the removal of SMZ by CuFeO/H_2O_2/Vis was studied in order to reveal the applicable pH range of CuFeO/H_2O_2/Vis system. The results indicated that lower pH favored the degradation of SMZ in the CuFeO/H_2O_2/Vis system. However, the results also showed that at least 70% of SMZ can be degraded in 30 min in the tested pH range (4.0 to 10.0). In particularly, we found that 95.42% of SMZ was removed after 30 minutes' treatment at a near neutral pH (pH=6.0). In this regard, the CuFeO/H_2O_2/Vis system showed a remarkable advantage to the traditional homogeneous Fenton process for the practical applications due to the broader working environment.

[1] E. Neyens, J. Baeyens, A review of classic Fenton's peroxidation as an advanced oxidation technique, J. Hazard. Mater. 98 (2003) 33-50.

[2] E. Brillas, I. Sirés, M.A. Oturan, Electro-Fenton process and related electrochemical technologies based on Fenton's reaction chemistry, Chem. Rev. 109 (2009) 6570-6631.

[3] N. Barhoumi, N. Oturan, H. Olvera-Vargas, E. Brillas, A. Gadri, S. Ammar, M.A. Oturan, Pyrite as a sustainable catalyst in electro-Fenton process for improving oxidation of sulfamethazine. Kinetics, mechanism and toxicity assessment, Water Res. 94 (2016) 52-61.

[4] J. Herney-Ramirez, M.A. Vicente, L.M. Madeira, Heterogeneous photo-Fenton oxidation with pillared clay-based catalysts for wastewater treatment: A review, Applied Catalysis B: Environmental 98 (2010) 10-26.

[5] A.C.-K. Yip, F.L.-Y. Lam, X. Hu, Chemical-vapor-deposited copper on acid-activated bentonite clay as an applicable heterogeneous catalyst for the photo-Fenton-like oxidation of textile organic pollutants, Ind. Eng. Chem. Res. 44 (2005) 7983-7990.

Comment 18: EPR or ESR?

Response: Thank you for pointing out our mistakes. It should be ESR. In this work, the electron spin resonance (ESR) experiments were performed. "EPR" is revised to "ESR" in the revised manuscript.

- Page 13, line 16, "EPR" is revised to "ESR" (See Page 16, line 2 in the revised manuscript).
- Page 19, line 5, "EPR" is revised to "ESR" (See Page 22, line 17 in the revised manuscript).

Comment 19: Using the scavenging test is a qualitative measure of confirmation the generation of radicals. When authors used ESR/EPR, testing the effect of scavengers is no more need.

Response: Thank you for your comment. According to the literature, ESR experiments and scavenging tests were often used together to studied the radicals involved in the catalysis [1-5]. In this work, ESR experiments were used to identify the radical species involved in the SMZ degradation, and scavenging tests were used to further confirm the contributions of the radicals, electron (e^-) and holes (h^+).

[1] D. Wen, Z. Wu, Y. Tang, M. Li, Z. Qiang, Accelerated degradation of sulfamethazine in water by VUV/UV photo-Fenton process: Impact of sulfamethazine concentration on reaction mechanism, J. Hazard. Mater. 344 (2018) 1181-1187.

[2] G.-X. Huang, C.-Y. Wang, C.-W. Yang, P.-C. Guo, H.-Q. Yu, Degradation of Bisphenol A by Peroxymonosulfate Catalytically Activated with Mn1.8Fe1.2O4 Nanospheres: Synergism between Mn and Fe, Environ. Sci. Technol. 51 (2017) 12611-12618.

[3] C. Zhou, C. Lai, D. Huang, G. Zeng, C. Zhang, M. Cheng, L. Hu, J. Wan, W. Xiong, M. Wen, X. Wen, L. Qin, Highly porous carbon nitride by supramolecular preassembly of monomers for photocatalytic removal of sulfamethazine under visible light driven, Appl. Catal. B Environ. 220 (2018) 202-210.

[4] N. Wang, Y. Du, W. Ma, P. Xu, X. Han, Rational design and synthesis of SnO_2-encapsulated α-Fe2O3 nanocubes as a robust and stable photo-Fenton catalyst, Appl. Catal. B Environ. 210 (2017) 23-33.

[5] H. Zhao, Y. Chen, Q. Peng, Q. Wang, G. Zhao, Catalytic activity of MOF(2Fe/Co)/carbon aerogel for improving H_2O_2 and OH generation in solar photo–electro–Fenton process, Appl. Catal. B Environ. 203 (2017) 127-137.

Comment 20: How much was the Fe and Cu leached into the solution during the reaction?

Response: Thank you for your comment. The concentration of Fe and Cu leached into the solution during the reaction was measured and provided in the revised manuscript.

- Secondly, the leaching metal ions from CuFeO nanoparticles were studied. In this work, the concentrations of Cu and Fe in the solution increased quickly during the first 10 min, but a slight decrease was observed from 20 min to 30min (Fig. S10). The concentrations of Cu and Fe in the solution at the end of the process were 2.10 and 1.31 mg/L, respectively. The relatively low metal leaching suggests CuFeO could be used as highly active and stable heterogeneous catalysts for the heterogeneous photo-Fenton process [78-82]. (See Page 21, line 15-22 in the revised manuscript).

Comment 21: How authors separated the nanoparticles at the end of each test for testing the reusability? How much was the separation efficiency? It is important because the concentration of catalyst should kept constant at all the reusability tests.

Response: Thank you for your comment. Due to the magnetic property of the catalyst, CuFeO nanoparticles at the end of each test could be separated simply with a magnet. To avoid the loss of catalysts, the catalysts were not taken out from the reaction flask; instead, they were fixed at the bottom of flask by a magnet, and the supernatant liquid was carefully removed by a straw. In a typical procedure, the catalysts were fixed at the bottom of flask by a magnet, and then the solution was carefully drawn out of the reactor. The catalyst was washed with ultrapure water for 3 times. After that, the magnet was removed, and the reactor was put in the oven (60 °C) to remove the residual water. In the experiment, this method was adopted from a previous work [1] because it was very simple and convenient; moreover, the separation efficiency is more than 95%.

The description of the separation is included in the revised manuscript:

In the recyclability test, the CuFeO catalyst at the end of each run could be separated simply with a magnet. In a typical procedure, the catalysts were fixed at the bottom of flask by a magnet, and then the solution was carefully drawn out of the reactor. The catalyst was washed with ultrapure water for 3 times. After that, the magnet was

removed, and the reactor was placed in the oven (60 °C) to remove the residual water. (See Page 8, line 3-7 in the revised manuscript).

[1] J. Zhang, T. Yao, C. Guan, N. Zhang, H. Zhang, X. Zhang, J. Wu, One-pot preparation of ternary reduced graphene oxide nanosheets/Fe_2O_3/polypyrrole hydrogels as efficient Fenton catalysts, J. Colloid Interface Sci. 505 (2017) 130-138.

Comment 22: How about the toxicity of the degradation intermediates? The bioassay test is recommended.

Response: Thank you for your comment. According to your comment, the toxicity of the degradation intermediates was evaluated by traditional bacterial growth.

The tests and the results are added in the revised manuscript:

- The toxic effect of SMZ and the degradation intermediates during the process was evaluated by traditional bacterial growth. *Escherichia coli* (*E. coli*) was selected as a model bacterium for testing. In a typical test, 0.5 mL of bacterial stock solution (3.0×10^7 CFU mL^{-1}) was added to 49.5 mL of sterile solution that containing 48.5 mL of ultrapure water and 1 mL of SMZ solution (1 mL of ultrapure water or 1 mL of reaction solution sampled at different time points during the photo-Fenton treatment). The mixed solution was kept in an incubator (37 ℃) for 1 h, then diluted and spread on Eosin Methylene Blue Agar plate. After that, the plate was allowed to incubate at 37 ℃ for 24 h. The viable cell density of each sample was measured by standard plate count method. (See Page 8, line 18 - Page 9, line 5 in the revised manuscript).

- The results showed that SMZ in this CuFeO/H_2O_2/Vis system can be degraded into different intermediates in a very short time (within 30 min). However, this does not guarantee the toxicity abatement of the resulting wastewater since the intermediates can be more toxic than the starting pollutants in some cases [71, 72]. Therefore, the antimicrobial activity of the treated solutions was studied. Preliminary tests suggested that the growth of *E. coli* can be inhibited by SMZ solution and the intermediates solutions as compared to the blank (sterile water). The E. coli growth was lower in the photo-Fenton treated samples than in the initial SMZ solution (Fig. S9). The results suggested that the intermediates have higher capacity for inhibiting *E. coli* growth

than that of the parent SMZ. Similar results have been reported elsewhere [18, 73, 74], for example, Perez-Moya et al. [73] reported that the toxicity of an SMZ solution increases during its degradation by means of photo-Fenton reactions. It was suggested that some degradation intermediates, such as cyclic/aromatic compounds and quinone derivatives, are toxic towards the bacteria even at very low concentration [18]. Barhoumi et al. [18] found that the toxicity of the solution can be reduced by prolonging the time of Fenton process. In this work, we also found that the decrease of toxicity at 60 min (Fig. S9). This is probably due to the further degradation of toxic intermediates by •OH. It is well-known that •OH can mineralize most kinds of organic pollutants to carbon dioxide (CO_2), water (H_2O) and inorganics. On the other hand, there are also reports showing that the biodegradability of SMZ degradation intermediates (produced during the Fenton/Fenton-like process) was higher than that of SMZ [75-77], suggesting a combined Fenton and biological treatment may be suitable for the depleting toxicity of SMZ solution. Taken together, the results suggest the toxicity of the treated SMZ solution needs to be considered carefully in the practical cases. (See Page 20, line 1 - Page 21, line 3 in the revised manuscript).

In this work, the mineralization of SMZ in the photo-Fenton-like systems was also evaluated by Total Organic Carbon (TOC) analysis. The results showed that the concentration of TOC decreases continuously during the photo-Fenton process in the CuFeO/H_2O_2/Vis system, and about 50% of TOC can be removed after 30 minutes' treatment. It is suggest that with the prolonging the treatment, a high TOC removal can be obtained. This result is in consist with the general recognition that the •OH generated from Fenton reaction can mineralize most kinds of organic pollutants to carbon dioxide (CO_2), water (H_2O) and inorganics.

- Besides, these results are consistent with the results of TOC analysis (Fig. S7). The results showed that the concentration of TOC decreases continuously during the photo-Fenton process in the CuFeO/H_2O_2/Vis system, and about 50% of TOC can be removed after 30 minutes' treatment, suggesting that CuFeO has high potential for the real applications. (See Page 14, line 5-9 in the revised manuscript).

Accepted MS

Graphical Abstract

Graphical abstract

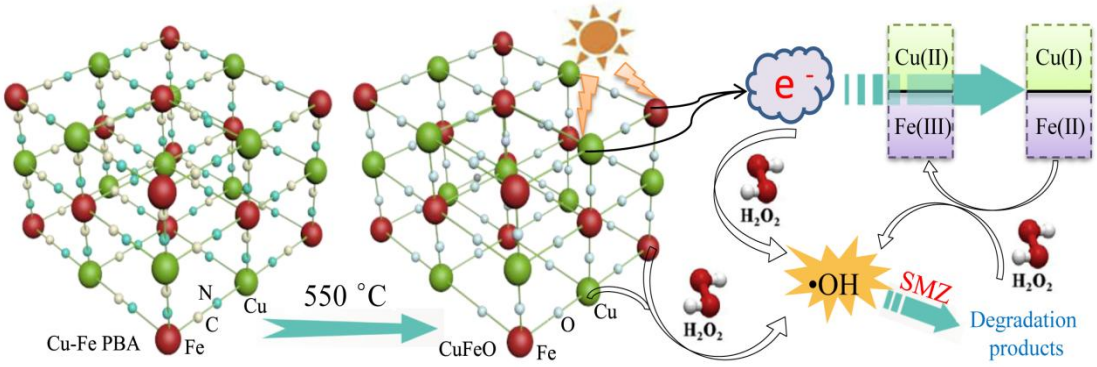

Accepted MS

Highlights

A new magnetic Cu-Fe oxide (CuFeO) was developed as the photo-Fenton catalyst.

CuFeO/H_2O_2/Vis system can work efficiently at slightly basic pH conditions.

The completely removal of 50 mg L^{-1} of SMZ has been achieved in 30 min.

HO• and photoinduced e^- are mainly responsible for the degradation of SMZ.

Prussian blue analogue derived magnetic Cu-Fe oxide as a recyclable photo-Fenton catalyst for the efficient removal of sulfamethazine at near neutral pH values

Min Cheng [a,b,1], Yang Liu [a,b,1], Danlian Huang [a,b,1], Cui Lai [a,b,1], Guangming Zeng [a,b,*], Jinhui Huang [a,b,*], Zhifeng Liu [a,b], Chen Zhang [a,b], Chengyun Zhou [a,b], Lei Qin [a,b], Weiping Xiong [a,b], Huan Yi [a,b], Yang Yang [a,b]

a. College of Environmental Science and Engineering, Hunan University, Changsha, Hunan 410082, China

b. Key Laboratory of Environmental Biology and Pollution Control (Hunan University), Ministry of Education, Changsha, Hunan 410082, China

1 These authors contribute equally to this article.

* Corresponding author at: College of Environmental Science and Engineering, Hunan University, Changsha, Hunan 410082, China.
Tel.: +86–731– 88822754; fax: +86–731–88823701.
E-mail address: zgming@hnu.edu.cn (G.M. Zeng), huangjinhui@hnu.edu.cn (J.H.Huang).

Abstract

The presence of antibiotics in aquatic environments has attracted global concern. Heterogeneous photo-Fenton process is an attractive yet challenging method for antibiotics degradation, especially when such a process can be operated at neutral pH values. In this work, a new magnetic Cu-Fe oxide (CuFeO) was developed as the heterogeneous photo-Fenton catalyst through a facile two-step method. The obtained CuFeO particles were found to be more efficient to activate H_2O_2 into radicals (•OH and •O_2^-) than Cu-Fe Prussian blue analogue (Cu-Fe PBA, the precursor) at near neutral conditions. The removal rate of sulfamethazine (SMZ) in CuFeO/H_2O_2/Vis system was much higher than those in CuO/H_2O_2/Vis and Fe_3O_4/H_2O_2/Vis systems. It was observed that nearly complete removal of SMZ from ultrapure water, river water and tap water can be achieved in 30 min in CuFeO/H_2O_2/Vis system. The influence of different process parameters on the SMZ degradation efficiency was then examined and the catalytic stability of CuFeO was also tested. The SMZ degradation intermediates during the process were analyzed and the degradation pathway was proposed based on LC–MS results. The mechanisms for H_2O_2 activation were studied by X-ray photoelectron spectrum analysis, radical scavenging and electron spin-trapping experiments. It is suggested that the synergistic effect among photo-induced electrons, Cu and Fe in CuFeO exhibits excellent performance in the catalytic activation of H_2O_2. This work is expected to provide useful information for the design and synthesis of bimetallic oxide for heterogeneous photo-Fenton reactions.

Keywords: Advanced oxidation process; Photo-Fenton; Wastewater; Antibiotics; Metal−organic frameworks; Degradation

1. Introduction

Water pollution is one of the most serious environmental problems in the world. Huge amounts of organic pollutants, such as dyes, pesticides and antibiotics, are released daily into natural water channels [1-3]. Many of these contaminants are able to cause damages to living organisms including human being, which has gained increasing concerns in recent years [4-7]. This problem has been exacerbated by the fact that the vast majority of organic contaminants are resistance to microbial attack and show high stability under sunlight irradiation [8-11]. As a result, some persistent organic contaminants have been frequently detected in lakes, rivers and groundwater all over the world [12-14]. Therefore, searching for effective approaches for the removal of organic contaminants from the polluted water is important and necessary.

As a typical advanced oxidation process (AOP), Fenton process has gained wide spread acceptance for efficient degradation of recalcitrant organic contaminants [15-19]. As shown in eqs. 1, Fenton reaction causes the decomposition of hydrogen peroxide (H_2O_2) and the generation of highly reactive hydroxyl radicals (•OH) [20], which are able to degrade most organic contaminants. More importantly, Fe^{3+} can be reduced to Fe^{2+} by H_2O_2 via Fenton-like reaction (eqs. 2) [21], which enables the continuous generation of •OH. However, the traditional Fenton process generally requires to be operated under acidic pH conditions and may also suffer from the loss of catalyst, which limit its practical applications. The heterogeneous Fenton-like processes using solid catalyst can overcome these drawbacks [22-24], but many of them still suffer from the problem of low utilization rate of H_2O_2 and long reaction time. Therefore, the development of new types of Fenton-like catalysts is still urgently needed.

$$Fe^{2+} + H_2O_2 \rightarrow Fe^{3+} + HO^- + \bullet OH \quad (1)$$

$$Fe^{3+} + H_2O_2 \leftrightarrows Fe^{2+} + H^+ + \bullet OOH \quad (2)$$

Metal−organic frameworks (MOFs) are an emerging class of porous materials assembled from organic ligands and metal ions (or clusters) [25]. The synthesis of MOFs has attracted tremendous attention in the recent years due to the possibility to obtain various numbers of porous materials that could be of great interest for applications in a number of fields such as separation [26], catalysis [27], storage [28], and sensing [29]. The occurrence of MOFs also brings a great deal of opportunities for the development of new heterogeneous Fenton-like catalysts with excellent characteristic features, such as large surface area and uniform pore sizes [27-29]. This large surface could provide abundant active sites, and the high porosity is very useful to expose the active sites completely to reactant(s) [27]. Several iron-containing MOFs, for example, MIL-53(Fe), MIL-68(Fe), MIL-100(Fe) and Prussian blue analogues (PBAs), were found to be effective for the activation of H_2O_2 [1, 30].

The combination of photo-energies (ultraviolet light/visible light) can largely enhance the efficiency of MOFs catalyzed Fenton-like process, which is current active area of interest for this technology [1]. In 2015, Li et al. [31] have developed two Fe-Co PBAs, $Fe[Co(CN)_6]\bullet 2H_2O$ and $Fe_3[Co(CN)_6]_2\bullet 12H_2O$, as excellent photo-Fenton catalysts. In this report, the removal efficiency of Rhodamine B (RhB, 12 mg/L) by Fe^{II}-Co PBA/H_2O_2 in 30 min reached 93%. In a recent study, the MIL-53(Fe)/H_2O_2/Vis system exhibited significantly higher efficiency for the degradation of organic contaminants than TiO_2/Vis, Fe(II)/H_2O_2 or MIL-53 (Fe)/H_2O_2 system [32]. It was suggested that two mechanisms could be responsible for the excellent catalytic performance of MOFs catalysts in the photo-Fenton system. Firstly,

iron sites on the surface of catalyst can catalyze the decomposition of H_2O_2 to generate •OH through Fenton-like reaction. Secondly, H_2O_2 as an efficient scavenger could capture the photo-induced electrons (e^-) in the catalyst to form •OH [1].

The bimetallic catalyst, Cu-Fe oxide has gained particular attention in the Fenton chemistry, not only because of its good catalytic performance but also copper is not regarded as a potential carcinogen [33]. Recently, some researchers have studied the feasibility of using MOFs to obtain porous nanostructured oxides. The pioneering works showed that the original morphology of the precursor can be almost retained after the thermal treatment, while the catalytic performance can be largely improved [34-36]. To our knowledge, however, no study on the preparation of Cu-Fe oxide from Cu-Fe PBAs and its application for Fenton-like reactions has been reported. Therefore, in this current study, a facile two-step strategy was developed to synthesize porous Cu-Fe oxide (CuFeO) by heating the Cu-Fe PBAs. The morphology and chemicals structures of the prepared catalysts before and after the Fenton process were thoroughly characterized by various techniques. Sulfamethazine (SMZ), one of the most commonly used antibiotics, was used as the model organic pollutant due to its adverse effects on living being and frequent occurrence in natural water environment [37, 38]. The catalytic properties of the prepared catalysts was evaluated by activation of H_2O_2 under the visible light irradiation ($\lambda > 420$ nm).

The main objective of this study was to construct a new MOFs-derived photo-Fenton catalyst for the efficient removal of organic pollutants. The catalytic performance of the CuFeO was studied in details and the involved reactive species were also investigated. More importantly, the synergistic effect among photo-induced e^-, Cu and Fe in CuFeO was

explored in order to understand the catalytic mechanism. Additionally, the possible degradation pathways of SMZ in this photo-Fenton system were proposed based on the identified intermediates during the degradation process and the stability and reusability of the catalyst were also evaluated. This work is expected to help to develop new types of MOFs derived photo-Fenton catalyst and give a deeper insight into the mechanisms of heterogeneous photo-Fenton process.

2. Experimental section

2.1. Chemicals and Reagents.

Sulfamethazine ($C_{14}H_{20}ClNO_2$, standard grade) was purchased from Sigma-Aldrich Company (Missouri, USA). The analytical grade cupric chloride tetrahydrate ($CuCl_2 \cdot 4H_2O$, analytical grade), potassium hexacyanoferrate (III) ($K_3[Fe(CN)_6]$, and polyvinylpyrrolidone (PVP) were obtained from Sinopharm Chemical Reagent Corp (China).

2.2. Synthesis of Cu-Fe PBAs and CuFeO

The Cu-Fe PBAs were synthesized according to a reported method with some modification [31]. In brief, 2 g of PVP was first dissolved in 100 mL $CuCl_2 \cdot 4H_2O$ (50 mM) solution. A certain amount (50 mL, 100 mL or 200 mL) of $K_3[Fe(CN)_6]$ (50 mM) solution was then dropwise added into the aforementioned solution. The mixed solution was then stirred for 30 min, the obtained precipitate was collected via centrifugation, and finally the Cu-Fe PBAs can be obtained by the subsequent washing and drying procedures. To prepare the CuFeO, the obtained Cu-Fe PBAs was heated to 550 °C with a temperate ramp of 3.6 °C min^{-1} and kept at the same temperature for 2 h in air.

2.3. Characterization

The morphology of Cu-Fe PBA and CuFeO was examined by scanning electron microscopy (FEI Quanta 400) and FEI Tecnai G2F20 transmission electron microscopy (TEM). Energy dispersive X-ray spectroscopy (EDS) of the prepared catalysts was obtained using an EDAX Genesis X-ray spectrometer. The size distribution of the prepared catalysts was measured with the dynamic light scattering (DLS) method. The prepared catalysts were fully dispersed in water with the help of ultrasound radiation. The measurement was carried out using a DynaPro Dynamic Light Scatterer (Malvern Instruments). The Brunauer–Emmett–Teller (BET) specific surface area, the Barrett–Joyner–Halenda (BJH) pore volume and pore size of the catalyst were measured using the Micromeritics ASAP 2010 analyzer. The crystal structure of the Cu-Fe PBAs and CuFeO was studied using a D/max-2500 X-ray diffractometer. X-ray photoelectron spectrum (XPS) recorded on the Axis Ultra spectrometer were fitted using XPSPEAK41 software. Fourier transform infrared spectroscopy (FT-IR) spectra were obtained by BIO RAD FTS-600 spectrometer. The thermogravimetric (TG) analysis was conducted on a Setaram Setsys 16/18 thermo-analyzer. The magnetic properties of the prepared catalysts were investigated with a MPMS (SQUID) XL vibration sample magnetometer (VSM) at room temperature. The electron spin resonance (ESR) measurement carried out with a Bruker ER200-SRC spectrometer.

2.4. Photo-Fenton reaction

The photo-Fenton reaction was performed in 250 mL reactors containing 100 mL of 50 mg L^{-1} SMZ solution under the visible-light (λ > 420 nm) irradiation with a 300 W Xe lamp. All the experiments were performed in triplicate. In a typical test, 50 mg of catalyst was added to 100 mL of SMZ solution (50 mg/L) and stirred for 30 min to establish the

adsorption−desorption equilibrium. After that, a certain amount of H_2O_2 solution (30 %, w/w) was then added to trigger the Fenton-like reaction. At the same time, the reactor was exposed to the 300 W Xe lamp. In the recyclability test, the CuFeO catalyst at the end of each run could be separated simply with a magnet. In a typical procedure, the catalysts were fixed at the bottom of flask by a magnet, and then the solution was carefully drawn out of the reactor. The catalyst was washed with ultrapure water for 3 times. After that, the magnet was removed, and the reactor was placed in the oven (60 °C) to remove the residual water.

2.5. Analytical methods

The concentration of SMZ during the process was determined by high performance liquid chromatography (HPLC, Agilent 1200 series) according to a published method [37]. The SMZ degradation kinetic was fitted by the pseudo first-order model (eqs. 3).

$$\mathrm{Ln}\,(C_t / C_0) = -kt \quad (3)$$

Where C_t is the SMZ concentration at a certain reaction time (t) and C_0 is the initial SMZ concentration.

In addition, the mineralization of SMZ in the photo-Fenton-like system was evaluated with a TOC-5000A model analyzer. The degradation intermediates were determined by the Agilent 1290/6460 high-performance liquid chromatography mass spectrometry (LC-MS) system. The detailed description of the operation condition of LC-MS was provided in Supplementary Material. The toxic effect of SMZ and the degradation intermediates during the process was evaluated by traditional bacterial growth. *Escherichia coli* (*E. coli*) was selected as a model bacterium for testing. In a typical test, 0.5 mL of bacterial stock solution (3.0×10^7 CFU mL^{-1}) was added to 49.5 mL of sterile solution that containing 48.5 mL of

ultrapure water and 1 mL of SMZ solution (1 mL of ultrapure water or 1 mL of reaction solution sampled at different time points during the photo-Fenton treatment). The mixed solution was kept in an incubator (37 ℃) for 1 h, then diluted and spread on Eosin Methylene Blue Agar plate. After that, the plate was allowed to incubate at 37 ℃ for 24 h. The viable cell density of each sample was measured by standard plate count method. The concentration of leached metals in the solution was determined by a DR 2800 spectrophotometer (Hach, USA) using the standard methods.

3. Results and discussion

3.1. Characterization of Cu-Fe PBA and CuFeO

Fig. 1 shows the XRD patterns of the 3 obtained Cu-Fe PBAs with different initial ratios of Cu/Fe. The results revealed that Cu/Fe(1:2) PBA, Cu/Fe(1:1) PBA and Cu/Fe(2:1) PBA have almost the same XRD patterns. That is to say, the ratio of Fe/Cu had no obvious influence on the final product. All the characteristic diffraction peaks (2θ; 17.61º, 24.91º, 35.62º, 39.96º, 43.93º, 51.24º, 54.47º and 57.91º) could be assigned to $Cu_3[Fe(CN)_6]_2$ (JCPDS No. 86-0514). No other impurity diffraction peaks were detected in these samples, indicating the high purity of the products. The as-prepared Cu-Fe PBA could be transformed into CuFeO after heating in air at 550 ºC. As indicated in TG analysis (Fig. S1), the weight loss of Cu-Fe PBA took place in 3 different stages, and the total weight loss rate was about 26%, 3% or 30%, respectively. The weight loss in the first stage (below 150 ºC) and second stage (150-280 ºC) were due to the removal of the crystalline and coordinated water, respectively. The weight loss over 280 ºC was caused by the decomposition of C-N ligands [35]. In this stage, the organic ligands can be oxidized into gases (CO_2, NO_x, etc.) and the

Cu-Fe PBAs were decomposed into CuFeO. Consequently, the thermal treatment led to a significant change in the XRD patterns. In XRD patterns of CuFeO (derived from Cu/Fe(2:1) PBA), two distinct diffraction peaks at 2θ values of 35.56º and 38.75º (Fig. 1) were assigned to the (311) and (111) crystal plane of Fe_3O_4 (JCPDS No. 88-0315) and CuO (JCPDS No. 48-1548), respectively.

The morphology and microstructure of Cu-Fe PBA and CuFeO were investigated by SEM and TEM technologies. As shown in Fig. 2A, Cu-Fe PBA was comprised of many tiny particles, which is likely due to the formation of compactly arranged $Cu_3[Fe(CN)_6]_2 \cdot nH_2O$. It can be observed that SEM image of CuFeO (Fig. 2B) is very similar to that of Cu-Fe PBAs, indicating no significant change occurred in the morphology of Cu-Fe PBAs during the heat treatment. EDS analysis indicated that Cu-Fe PBA mainly consists of N, C, Fe, Cu and O (Fig. S2B). After the thermal treatment, these elements are still detected (Fig. S2D), but the signal strength of N and C decreased very obviously. This is in consisted with the elemental mapping images, which show C and N were almost completely removed from Cu-Fe PBA. In addition, the element mapping clearly illustrates the homogeneous distribution of Fe, Cu and O species in the CuFeO particles (Fig. 2C-2H). TEM images (Fig. 2I and J) confirmed the uniform structures of CuFeO. Fig. 2K and 2L show the HR-TEM image and FFT-filtered TEM pattern images of CuFeO, the lattice spacings of 0.29 nm and 0.25 nm were correspond well to the (2 2 0) plane Fe_3O_4 (JCPDS No. 88-0315) and (1 1 -1) plane of CuO (JCPDS No. 48-1548), respectively.

DLS analysis showed that the average size of Cu-Fe PBA and CuFeO (dispersed in water) was 225.8 and 240.0 nm, respectively (Fig. S3). The average size of CuFeO is very

closed to that of Cu-Fe PBA, suggesting the thermal treatment did not significantly change the morphology of Cu-Fe PBA, which is in consistent with the results obtained from SEM analysis. The BET surface area and BJH pore volume of CuFeO particles are 178.35 m^2/g and 0.6993 cm^3/g, respectively, which are much higher than those of the reported Cu-Fe bimetallic catalysts [33, 39, 40]. As shown in Fig. S4, the BET isotherm of CuFeO particles belongs to type IV with H3 type hysteresis loops, indicating that CuFeO particles were mesoporous. The inset of Fig. S4 is the BJH pore size distribution plots of CuFeO particles. According to the BJH analysis, the pore size of the CuFeO catalyst was determined to be 17.47 nm. The high specific surface area and porous structure of the catalysts may facilitate the catalytic performance.

The FTIR spectra of the as-synthesized Cu-Fe PBA and CuFeO were shown in Fig. 3A. As can be seen in Fig. 3A, the two peaks detected at 1651 cm^{-1} (H-O-H bending mode) and 3440 cm^{-1} (O-H stretching mode) demonstrated the presence of water molecules in the structure of Cu-Fe PBA [31], which is in good agreement with the TG analysis (Fig. S1). The absorption band at 2102 cm^{-1} is assignable to the C-N stretching vibration of PBA [41]. As compared with Cu-Fe PBA, the number of characteristic peaks in CuFeO is much less. Noticeably, the characteristic peaks of C-N stretching vibration (2102 cm^{-1}) completely disappeared from the spectrum of Cu-Fe PBA after the heating treatment. The strong band emerged at 570 cm^{-1} in CuFeO pattern is the characteristic peak of the Fe-O stretching vibration from Fe_3O_4 [42].

The surface chemical composition and electronic state of Cu-Fe PBA and CuFeO were determined by the XPS. As revealed in Fig. 3B, five elements: Cu, Fe, O, N, and C were

detected in the XPS survey spectrum of Cu-Fe PBA. For CuFeO, the enhanced signal of Cu, Fe and O were observed in the survey spectrum, while no significant signal of N and C were detected. The changes observed in the high resolution XPS of Cu 2p (Fig. 4A and 4B) confirmed that the CuO was truly produced in CuFeO. The two peaks located at 933.6 eV and 953.4 eV are belonging to Cu $2p_{3/2}$ and Cu $2p_{1/2}$ of CuO, respectively. CuO is also known to possess characteristic high-intensity shake-up satellites [43]. Previous studies have demonstrated the satellites are usually located at a higher binding energy than the main Cu $2p_{3/2}$ and Cu $2p_{1/2}$ peaks by about 9 eV [44], which are in good agreement with our result. The observed peak located at 962.1 eV is the satellite peak for the Cu $2p_{1/2}$, and the peaks at 943.5 eV and 941.1 eV are the signals for the presence of satellite peaks of Cu $2p_{3/2}$. In the high resolution XPS of Fe $2p_{3/2}$ of Cu-Fe PBA (Fig. 4C), the binding energy of Fe $2p_{3/2}$ at 708.3 eV could be corresponded to Fe(III). The high resolution XPS of Fe in CuFeO (Fig. 4D) is quite similar to that of Fe_3O_4 [45]. The Fe $2p_{3/2}$ spectrum (Fig. 4D) of CuFeO can be split into three peaks with binding energies at 712.6 eV, 711.0 and 709.9, which could be assigned to tetrahedral Fe(III), octahedral Fe(III) and octahedral Fe(II), respectively [46, 47]. Overall the XPS results coincided well with the XRD, SEM, TEM and FT-IR analysis.

According to the above analysis, we speculated that the synthesized CuFeO should be a kind of magnetic material due to the existence of Fe_3O_4. To verify this speculation, the magnetic property of the prepared catalysts was thus studied. Fig. S5 presents the magnetic hysteresis curves for Cu-Fe PBA, CuFeO and the used-CuFeO. These curves display the evolution of magnetization (*M*) as a function of applied field (*H*). As indicated in Fig. S5, no magnetism was found in Cu-Fe PBA, while CuFeO exhibited obvious magnetism. Moreover,

CuFeO could maintain its original magnetism even after 5 degradation cycles. The saturation magnetization value (*M*s) of CuFeO was measured to be 14.18 emu g^{-1}, which is about 25% of that of pure magnetic Fe_3O_4 under the same conditions. Generally, catalysts with high *M*s values means that they can be easily separated from the solution by magnet. In this work, CuFeO particles could be collected simply with a magnet in 10 s as shown in the inset picture of Fig. S5. This enhances the technical and economic feasibility because it allows the convenient separation and recycling of catalyst by applying an external magnetic field.

3.2. Catalytic performance of CuFeO

The adsorption of SMZ by Cu-Fe PBAs and CuFeO was studied in the first step. As revealed in Fig. S6, adsorption of SMZ by Cu-Fe PBAs and CuFeO achieved adsorption equilibrium in 30 min. We also found that both Cu-Fe PBAs and CuFeO exhibited similar and negligible SMZ adsorption capacity (about 3% of SMZ was removed by adsorption). Then, the degradation behaviors of SMZ were studied by different Fenton-like processes to evaluate the catalytic performance of CuFeO (Fig. 5A). On the one side, the photo-Fenton performance of CuFeO was investigated under different reaction conditions. It was found that neither CuFeO/Vis nor CuFeO/H_2O_2 could effectively degrade SMZ, while CuFeO/H_2O_2/Vis can almost completely remove SMZ in 30 min, suggesting both H_2O_2 and light irradiation are essential for the efficient catalytic reaction. On the other side, the photo-Fenton performance of CuFeO/H_2O_2/Vis was compared with those of other photo-Fenton system. As displayed in Fig. 5A, H_2O_2/Vis could hardly degrade any SMZ, which is in well accordance with the previous studies [31, 35]. The SMZ degradation efficacy of CuFeO/H_2O_2/Vis was significantly higher than that of Cu-Fe PBA/H_2O_2/Vis, and much higher than the sum of

CuO/H_2O_2/Vis and Fe_3O_4/H_2O_2/Vis. In this work, 95.42% of SMZ was removed after 30 min in $CuFeO/H_2O_2$/Vis system. The degradation efficiency of SMZ in this process is higher than those of many reported AOPs, including photo-Fenton process [48], electro-Fenton process [18, 49], photocatalytic processes [50, 51], and peroxymonosulfate/ persulfate-based oxidation [52, 53]. Besides, these results are consistent with the results of TOC analysis (Fig. S7). The results showed that the concentration of TOC decreased continuously during the photo-Fenton process in the $CuFeO/H_2O_2$/Vis system, and about 50% of TOC can be removed after 30 minutes' treatment, suggesting that CuFeO has high potential for the real applications. This excellent photo-Fenton activity of CuFeO is likely because CuFeO has porous structure with abundant metals (Fe and Cu) sites. In this study, the SMZ degradation kinetics can be well described by the first order kinetics as displayed in Fig. 5B. The apparent rate constant (k) of CuFeO system was 0.09961 min^{-1}, which is much higher than that of CuO (0.01332 min^{-1}), Fe_3O_4 (0.00534 min^{-1}), or CuO-Fe PBA (0.04328 min^{-1}) system for the SMZ degradation under the same conditions.

It is well known that pH of the solution plays an important role in the Fenton/Fenton-like reactions [8, 54, 55]. Therefore, the effect of solution pH on the removal of SMZ by $CuFeO/H_2O_2$/Vis was examined. As shown in Fig. 5C, the removal efficiency of SMZ increased markedly from 71.3% to 98.1% in 30 min as pH decreased from 10.0 to 4.0, which indicated that lower pH favored the degradation of SMZ in the $CuFeO/H_2O_2$/Vis system. Two mechanisms can be responsible for this phenomenon. Firstly, better efficiency at lower pH values can be due to the higher leaching of iron and copper ions as the pH decreases, which facilitates the faster homogeneous photo-Fenton reaction [56]. Secondly,

H_2O_2 is less stable at higher pH conditions and tend to decompose into H_2O [57]. From another point of view, at least 70% of SMZ can be degraded in 30 min in the tested pH range (4.0 to 10.0). In particularly, we found that 95.42% of SMZ was removed after 30 minutes' treatment at a near neutral pH (pH=6.0). Traditional homogeneous Fenton process generally needs to be operated at acidic pH conditions, which hinder the industrial application of the technology because the pollutant solutions usually have near neutral pH values [23]. In this regard, the CuFeO/H_2O_2/Vis system showed a remarkable advantage for the practical applications due to the broader working environment.

In addition, the degradation of SMZ at different H_2O_2 concentrations (20 to 100 mM) was studied. The experimental results (Fig. 5D) showed the removal efficiency of SMZ increased significantly along with the increase of H_2O_2 concentration from 20 to 60 mM, indicating that H_2O_2 concentrations were significantly related to the degradation of SMZ. The important roles that H_2O_2 plays in this photo-Fenton process were discussed later in the mechanism section. However, the increase in degradation rate of SMZ became insignificant when H_2O_2 concentration increased from 60 to 80 mM, and even started to decline when H_2O_2 concentration further increased to 100 mM. This may possibly result from the scavenging of •OH by excessive H_2O_2 (eqs. 4 and 5). For an excessive H_2O_2 loading, H_2O_2 can react with •OH to generate hydroperoxyl radicals (•OOH) and superoxide anions ($•O_2^-$) [58]. Compared with •OH, $•O_2^-$ and •OOH have much lower oxidation potentials, and thus led to lower SMZ degradation efficiency [48, 59, 60].

$$•OH + H_2O_2 \rightarrow H_2O + •OOH \quad (4)$$

$$•OOH \leftrightarrow •O_2^- + H^+ \quad (5)$$

3.3. Identification of the dominant radicals

To identify the radical generation, the ESR/DMPO experiments were performed. As seen from Fig. 6A, no signal of DMPO-•O_2^- was detected in the dark, while the light was on, the characteristic signals of DMPO-•O_2^- with an intensity ratio of 1:1:1:1 could be observed, indicating the generation of •O_2^- during the photo-Fenton process. In the dark, a weak ESR signal assigned to DMPO-•OH (with an intensity ratio of 1:2:2:1) was obtained, confirming the low catalytic performance of CuFeO for decomposing H_2O_2. In the photo-Fenton process, much stronger signal of DMPO-•OH could be detected (Fig. 6A). And the peaks intensity of •OH enhanced with the irradiation from 5 min to 10 min, suggesting •OH played an important role in the enhancement of photocatalytic performance.

In order to elucidate the activation mechanism in depth, the involved active species during the photo-Fenton process were identified by the photoinduced electron (e^-) and holes (h^+) and free radicals trapping experiments. As indicated in Fig. 6B, the addition of silver nitrate ($AgNO_3$) [61], as a scavenger for photoinduced e^- dramatically suppressed the photo-Fenton reaction. A more distinct inhibition phenomenon was observed when the scavenger of tert-butyl alcohol (TBA) for •OH was added to the reaction system [62]. The removal rate of SMZ decreased from 96.72% to 17.13% in the presence of 20 mM of TBA, which suggested that •OH played a crucial role in the catalytic degradation processes. When 1.4-benzoquinone (BQ) for superoxide radical (•O_2^-) is added [63], the degradation rate of SMZ displayed a slight decrease, indicating that •O_2^- played a minor role in SMZ degradation. The introduction of ethylenediamintetraacetic acid disodium (EDTA-2Na) as a

scavenger for h^+ has small influence on the degradation of SMZ [64], suggesting that photoinduced h^+ is not involved in SMZ degradation.

3.4. Mechanisms study

The XPS spectra of the CuFeO before and after the degradation process were also used to explore the H_2O_2 activation mechanism. As can be seen, Cu 2p spectrum of fresh CuFeO (Fig. 7A) displayed a single peak with binding energy at 933.6 eV, which is assigned to Cu (II) [44]. After the catalytic reaction, a new peak belongs to Cu (I) appeared at 735.2 eV in the deconvoluted Cu $2p_{3/2}$ spectrum (Fig. 7B), suggesting that Cu_2O was generated on the surface of CuFeO [65]. As for Fe, three peaks at 709.9, 711.0, and 712.6 eV [46] can be found in the deconvoluted Fe $2p_{3/2}$ spectra before and after the catalytic reaction, however, about 13% of the total Fe was transformed from octahedral Fe(II) (709.9 eV) to octahedral Fe(III) (711.0 eV) (Fig. 7C and 7D). The collective results indicated that both Cu species and Fe species take part in the catalytic reaction.

Fe_3O_4 and CuO are two widely studied heterogeneous Fenton-like catalyst, they can activate H_2O_2 to produce active radicals via eqs. 6-9 [42, 44]. Specifically, Fe^{II} (or Cu^{I}) can catalyze H_2O_2 decomposition to produce •OH, and then Cu and Fe at higher valence states were reduced by H_2O_2 to complete the redox cycle (eqs. 6-9), which ensure the catalytic reactions work continuously. However, the reaction rate of Cu^{II} and H_2O_2 (eqs. 9), Fe^{III} and H_2O_2 (eqs. 6) are both very slow and would thus slow the regeneration of Cu^{I} and Fe^{II}, which is mainly responsible for the relatively low SMZ degradation rate in CuO/H_2O_2 and Fe_3O_4/H_2O_2 system. Under the light radiation, the Fe_3O_4 and CuO can be excited and produce the holes (h^+) and electron (e^-) (eqs. 10 and 11) [66]. It was known that the h^+ could react

with H_2O to generate •OH (eqs. 12) or directly oxidize pollutants (eqs. 13) [67]. However, based on the results obtained from trapping experiments (Fig. 6B), the above reactions must play a minor role in the degradation of SMZ. This can explain the relative low SMZ degradation efficiency in CuFeO/Vis system. As seen from Fig. 6B, the photo-induced e^- plays an important role in SMZ degradation. This is because e^- could not only react with H_2O_2 to produce active •OH (eqs. 14), but also can cause an in–situ recycling of copper species ($Cu^{II} \rightarrow Cu^{I}$) and iron species ($Fe^{III} \rightarrow Fe^{II}$) through eqs. 15 and 16 [68], respectively. In addition, the reduction of Fe^{III} by Cu^{I} is thermodynamically favorable (eqs. 17) according to the standard reduction potentials of the Fe and Cu (eqs. 15 and 16) [68]. These processes facilitate the continuous cycle of Fe^{III}/Fe^{II} and Cu^{II}/Cu^{I} in CuFeO/H_2O_2/Vis system. Overall, the collective results indicated that the photo-induced e^- did significantly contribute to the improvement of •OH generation. On the basis of the above discussion, a reasonable schematic mechanism for enhancing •OH generation in CuFeO/H_2O_2 photo-Fenton process was illustrated in Fig. 8. In this system, high yield of •OH can be continuously generated by photo-induced e^- and surface copper species and iron species. And then the formed radicals (•OH mainly) reacted with SMZ, leading to the degradation intermediates and final mineralization products.

$$\equiv Fe^{II} + H_2O_2 \rightarrow \equiv Fe^{III} + \bullet OH + OH^- \quad (6)$$

$$\equiv Fe^{III} + H_2O_2 \rightarrow \equiv Fe^{II} + \bullet OOH + H^+ \quad (7)$$

$$\equiv Cu^{I} + H_2O_2 \rightarrow \equiv Cu^{II} + \bullet OH + OH^- \quad (8)$$

$$\equiv Cu^{II} + H_2O_2 \rightarrow \equiv Cu^{I} + \bullet OOH + H^+ \quad (9)$$

$$CuO + h\nu \rightarrow CuO\ (e^- + h^+) \quad (10)$$

$$Fe_3O_4 + h\nu \rightarrow Fe_3O_4\ (e^- + h^+) \quad (11)$$

$$H_2O + h^+ \rightarrow \bullet OH + H^+ \quad (12)$$

$$h^+ + \text{pollutant} \rightarrow \text{degradation products} \quad (13)$$

$$H_2O_2 + e^- \rightarrow \bullet OH + OH^- \quad (14)$$

$$\equiv Cu^{II} + e^- \rightarrow \equiv Cu^{I} \qquad E_0 = 0.16\ V \quad (15)$$

$$\equiv Fe^{III} + e^- \rightarrow \equiv Fe^{II} \qquad E_0 = 0.77\ V \quad (16)$$

$$\equiv Fe^{III} + Cu^{I} \rightarrow \equiv Fe^{II} + \equiv Cu^{II} \quad (17)$$

3.5. Degradation intermediates of SMZ and the toxicity assessment

To fully understand the degradation process of SMZ in CuFeO/H_2O_2/Vis system, LC-MS analysis was further performed to identify the degradation intermediates of SMZ. The LC patterns displayed in Fig. 9A showed the intensity of SMZ peaks (3.48 min) decreased quickly during the photo-Fenton process. Meanwhile, another distinct peak emerged at 0.756 min, indicating that SMZ was decomposed into intermediates gradually. In this work, 3 main degradation intermediates were identified by LC-MS analysis, which included 2-amino-4,6-dimethylpyrimidine (A, *m/z* 124), 4-aminophenol (B, *m/z* 110), and 2-amino-4,6-dimethylpyrimidin-5-ol (C, *m/z* 140) (Fig. S8). Further, it was found that A and B were the dominant products during the degradation process. On the basis of the above results and the results published previously [23, 69], a possible degradation pathway of SMZ in the CuFeO/H_2O_2/Vis system was proposed in Fig. 9B. First, the attack of active species resulted in the cleavage of S-N bond in SMZ, forming two aromatic intermediates respectively with aniline ring and pyrimidine, which was also observed in an electrochemical degradation system [70]. Then, C-N bond on the aniline residue of SMZ was cleaved to form

B, and meanwhile, the hydroxylation of the pyrimidine residue of SMZ led to the formation of C. Finally, B and C could be further decomposed to inorganic species (H_2O, CO_2, etc.).

The results showed that SMZ in this CuFeO/H_2O_2/Vis system can be degraded into different intermediates in a very short time (within 30 min). However, this does not guarantee the toxicity abatement of the resulting wastewater since the intermediates can be more toxic than the starting pollutants in some cases [71, 72]. Therefore, the antimicrobial activity of the treated solutions was studied. Preliminary tests suggested that the growth of *E. coli* can be inhibited by SMZ solution and the intermediates solutions as compared to the blank (sterile water). The E. coli growth was lower in the photo-Fenton treated samples than in the initial SMZ solution (Fig. S9). The results suggested that the intermediates have higher capacity for inhibiting *E. coli* growth than that of the parent SMZ. Similar results have been reported elsewhere [18, 73, 74], for example, Perez-Moya et al. [73] reported that the toxicity of an SMZ solution increases during its degradation by means of photo-Fenton reactions. It was suggested that some degradation intermediates, such as cyclic/aromatic compounds and quinone derivatives, are toxic towards the bacteria even at very low concentration [18]. Barhoumi et al. [18] found that the toxicity of the solution can be reduced by prolonging the time of Fenton process. In this work, we also found that the decrease of toxicity at 60 min (Fig. S9). This is probably due to the further degradation of toxic intermediates by •OH. It is well-known that •OH can mineralize most kinds of organic pollutants to carbon dioxide (CO_2), water (H_2O) and inorganics. On the other hand, there are also reports showing that the biodegradability of SMZ degradation intermediates (produced during the Fenton/Fenton-like process) was higher than that of SMZ [75-77], suggesting a combined Fenton and biological

treatment may be suitable for the depleting toxicity of SMZ solution. Taken together, the results suggest the toxicity of the treated SMZ solution needs to be considered carefully in the practical cases.

3.6. The recyclability and chemical stability of CuFeO

From the view of long-term practical applications, the recyclability of the synthesized catalysts is an important issue that should be considered. The result displayed in Fig. 10A demonstrates the as-synthetized CuFeO exhibited good recyclability. The slight decline in catalytic activity after five-cycle runs is likely due to the blockage of active sites by degradation intermediates [31, 35].

The stability of the MOFs-derived catalysts is another key issue to be considered. Firstly, it is important to know whether the CuFeO catalyst could maintain its initial structures during the oxidation process. In the experiment, we studied the XRD patterns, FTIR spectra and XPS patterns of CuFeO before and after the reaction. Results showed both the XRD patterns (Fig. 10B), FTIR spectra (Fig. 10C), and full XPS spectra (Fig. 10D) of CuFeO before and after photo-Fenton process were almost the same, suggesting that the crystal structure of CuFeO was very stable during the oxidation process. Secondly, the leaching metal ions from CuFeO particles were studied. In this work, the concentrations of Cu and Fe in the solution increased quickly during the first 10 min, but a slight decrease was observed from 20 min to 30min (Fig. S10). The concentrations of Cu and Fe in the solution at the end of the process were 2.10 and 1.31 mg/L, respectively. The relatively low metal leaching suggests CuFeO could be used as highly active and stable heterogeneous catalysts for the heterogeneous photo-Fenton process [78-83].

The removal efficiency of SMZ by CuFeO/H_2O_2/Vis system was also investigated using different types of water, which include ultrapure water, tap water (supplied by Changsha Running-water Company), municipal wastewater (obtained from Changsha GuoZhen sewage treatment plant, China) and river water (taken from Xiangjiang River). The results showed near complete removal of SMZ can be obtained in ultrapure water, river water and tap water, while about 84% of SMZ was removed in municipal wastewater (Fig. S11). The relatively lower removal of SMZ for wastewater is likely due to the blockage of light and competition of •OH by the abundant organic matters in municipal wastewater. Over all, it can be concluded that CuFeO is a promising photo-Fenton catalyst for the practical application. Besides, the versatility of this CuFeO/H_2O_2/Vis system is also enhanced by the fact the catalyst can be easily separated from the solution by a magnetic field, which enables the reuse of the catalyst.

4. Conclusions

In this study, the magnetic Cu-Fe oxide (CuFeO) was synthesized via a facile strategy by heating Cu-Fe PBA. The as-synthesized CuFeO exhibited high catalytic activity at a wide pH range. 95.42% of SMZ was removed after 30 minutes' photo-Fenton treatment at a near neutral pH (pH=6.0). Through ESR/DMPO and radical scavenger experiments, both •OH and •O_2^- were proved to be involved and the former played a more critical role in the degradation of SMZ. Based on the LC–MS analysis, the SMZ degradation intermediates were identified and the possible degradation pathway was proposed. CuFeO was shown to be stable and reusable even after a five-cycle test. In addition to the relatively low metal leaching and magnetic properties of CuFeO, the synthesized catalyst has a promising potential for the

treatment of organic wastewater. Furthermore, our findings may expand the further development of other Cu-Fe bimetallic heterogeneous Fenton-like catalysts for the degradation of organic pollutants by activation of H_2O_2.

Acknowledgements

This study was financially supported by the Program for the National Natural Science Foundation of China (51879101, 51579098, 51779090, 51709101, 51521006, 51809090, 51278176, 51378190), the National Program for Support of Top-Notch Young Professionals of China (2014), the Program for Changjiang Scholars and Innovative Research Team in University (IRT-13R17), the Program for New Century Excellent Talents in University (NCET-13-0186), Hunan Provincial Science and Technology Plan Project (2016RS3026, 2017SK2243), and the Fundamental Research Funds for the Central Universities (531109200027, 531107051080, 531107050978, 531107051205).

References

[1] M. Cheng, C. Lai, Y. Liu, G. Zeng, D. Huang, C. Zhang, L. Qin, L. Hu, C. Zhou, W. Xiong, Metal-organic frameworks for highly efficient heterogeneous Fenton-like catalysis, Coord. Chem. Rev. 368 (2018) 80-92.

[2] M. Cheng, G. Zeng, D. Huang, C. Lai, Y. Liu, C. Zhang, R. Wang, L. Qin, W. Xue, B. Song, S. Ye, H. Yi, High adsorption of methylene blue by salicylic acid–methanol modified steel converter slag and evaluation of its mechanism, J. Colloid Interface Sci. 515 (2018) 232-239.

[3] M. Cheng, G. Zeng, D. Huang, C. Lai, Z. Wei, N. Li, P. Xu, C. Zhang, Y. Zhu, X. He, Combined biological removal of methylene blue from aqueous solutions using rice straw

and Phanerochaete chrysosporium, Appl. Microbiol. Biotechnol. 99 (2015) 5247-5256.

[4] M. Cheng, G. Zeng, D. Huang, C. Yang, C. Lai, C. Zhang, Y. Liu, Advantages and challenges of Tween 80 surfactant-enhanced technologies for the remediation of soils contaminated with hydrophobic organic compounds, Chem. Eng. J. 314 (2017) 98-113.

[5] M. Cheng, G. Zeng, D. Huang, C. Yang, C. Lai, C. Zhang, Y. Liu, Tween 80 surfactant-enhanced bioremediation: toward a solution to the soil contamination by hydrophobic organic compounds, Crit. Rev. Biotechnol. 38 (2018) 17-30.

[6] Y. Liu, G. Zeng, H. Zhong, Z. Wang, Z. Liu, M. Cheng, G. Liu, X. Yang, S. Liu, Effect of rhamnolipid solubilization on hexadecane bioavailability: enhancement or reduction?, J. Hazard. Mater. 322 (2017) 394-401.

[7] O. Sacco, V. Vaiano, C. Han, D. Sannino, D.D. Dionysiou, Photocatalytic removal of atrazine using N-doped TiO2 supported on phosphors, Appl. Catal. B Environ. 164 (2015) 462-474.

[8] E. Brillas, I. Sirés, M.A. Oturan, Electro-Fenton process and related electrochemical technologies based on Fenton's reaction chemistry, Chem. Rev. 109 (2009) 6570-6631.

[9] H. Yi, D. Huang, L. Qin, G. Zeng, C. Lai, M. Cheng, S. Ye, B. Song, X. Ren, X. Guo, Selective prepared carbon nanomaterials for advanced photocatalytic application in environmental pollutant treatment and hydrogen production, Appl. Catal. B Environ. 239 (2018) 408-424.

[10] S. Wacławek, H.V. Lutze, K. Grübel, V.V. Padil, M. Černík, D.D. Dionysiou, Chemistry of persulfates in water and wastewater treatment: A review, Chem. Eng. J. 330 (2017) 44-62.

[11] J. Lalley, C. Han, X. Li, D.D. Dionysiou, M.N. Nadagouda, Phosphate adsorption using modified iron oxide-based sorbents in lake water: Kinetics, equilibrium, and column tests, Chem. Eng. J. 284 (2016) 1386-1396.

[12] X. Zhou, C. Lai, D. Huang, G. Zeng, L. Chen, L. Qin, P. Xu, M. Cheng, C. Huang, C. Zhang, Preparation of water-compatible molecularly imprinted thiol-functionalized activated titanium dioxide: Selective adsorption and efficient photodegradation of 2, 4-dinitrophenol in aqueous solution, J. Hazard. Mater. 346 (2018) 113.

[13] C. Lai, M.M. Wang, G.M. Zeng, Y.G. Liu, D.L. Huang, C. Zhang, R.Z. Wang, P. Xu, M. Cheng, C. Huang, Synthesis of surface molecular imprinted TiO_2/graphene photocatalyst and its highly efficient photocatalytic degradation of target pollutant under visible light irradiation, Appl. Surf. Sci. 390 (2016) 368-376.

[14] L. Qin, G. Zeng, C. Lai, D. Huang, P. Xu, C. Zhang, M. Cheng, X. Liu, S. Liu, B. Li, H. Yi, “Gold rush” in modern science: Fabrication strategies and typical advanced applications of gold nanoparticles in sensing, Coord. Chem. Rev. 359 (2018) 1-31.

[15] D. Huang, C. Hu, G. Zeng, M. Cheng, P. Xu, X. Gong, R. Wang, W. Xue, Combination of Fenton processes and biotreatment for wastewater treatment and soil remediation, Sci. Total Environ. 574 (2017) 1599-1610.

[16] C. Hu, D. Huang, G. Zeng, M. Cheng, X. Gong, R. Wang, W. Xue, Z. Hu, Y. Liu, The combination of Fenton process and Phanerochaete chrysosporium for the removal of bisphenol A in river sediments: Mechanism related to extracellular enzyme, organic acid and iron, Chem. Eng. J. 338 (2018) 432-439.

[17] B. Li, C. Lai, G. Zeng, L. Qin, H. Yi, D. Huang, C. Zhou, X. Liu, M. Cheng, P. Xu, C.

Zhang, F. Huang, S. Liu, Facile Hydrothermal Synthesis of Z-Scheme $Bi_2Fe_4O_9/Bi_2WO_6$ Heterojunction Photocatalyst with Enhanced Visible Light Photocatalytic Activity, ACS Appl. Mater. Interfaces 10 (2018) 18824-18836.

[18] N. Barhoumi, N. Oturan, H. Olvera-Vargas, E. Brillas, A. Gadri, S. Ammar, M.A. Oturan, Pyrite as a sustainable catalyst in electro-Fenton process for improving oxidation of sulfamethazine. Kinetics, mechanism and toxicity assessment, Water Res. 94 (2016) 52-61.

[19] S. Ammar, M.A. Oturan, L. Labiadh, A. Guersalli, R. Abdelhedi, N. Oturan, E. Brillas, Degradation of tyrosol by a novel electro-Fenton process using pyrite as heterogeneous source of iron catalyst, Water Res. 74 (2015) 77-87.

[20] F. Haber, J. Weiss, The catalytic decomposition of hydrogen peroxide by iron salts, in: Proceedings of the Royal Society of London A: Mathematical, Physical and Engineering Sciences, The Royal Society, 1934, pp. 332-351.

[21] C. Walling, A. Goosen, Mechanism of the ferric ion catalyzed decomposition of hydrogen peroxide. Effect of organic substrates, JACS 95 (1973) 2987-2991.

[22] M. Cheng, G. Zeng, D. Huang, C. Lai, Y. Liu, P. Xu, C. Zhang, J. Wan, L. Hu, W. Xiong, C. Zhou, Salicylic acid–methanol modified steel converter slag as heterogeneous Fenton-like catalyst for enhanced degradation of alachlor, Chem. Eng. J. 327 (2017) 686-693.

[23] M. Cheng, G. Zeng, D. Huang, C. Lai, Y. Liu, C. Zhang, J. Wan, L. Hu, C. Zhou, W. Xiong, Efficient degradation of sulfamethazine in simulated and real wastewater at slightly basic pH values using Co-SAM-SCS/H_2O_2 Fenton-like system, Water Res. 138

(2018) 7-18.

[24] M. Cheng, G. Zeng, D. Huang, C. Lai, P. Xu, C. Zhang, Y. Liu, J. Wan, X. Gong, Y. Zhu, Degradation of atrazine by a novel Fenton-like process and assessment the influence on the treated soil, J. Hazard. Mater. 312 (2016) 184-191.

[25] S.S. Han, J.L. Mendoza-Cortes, W.A. Goddard, III, Recent advances on simulation and theory of hydrogen storage in metal-organic frameworks and covalent organic frameworks, Chem. Soc. Rev. 38 (2009) 1460-1476.

[26] W. Xiong, G. Zeng, Z. Yang, Y. Zhou, C. Zhang, M. Cheng, Y. Liu, L. Hu, J. Wan, C. Zhou, R. Xu, X. Li, Adsorption of tetracycline antibiotics from aqueous solutions on nanocomposite multi-walled carbon nanotube functionalized MIL-53(Fe) as new adsorbent, Sci. Total Environ. 627 (2018) 235-244.

[27] Q. Yang, Q. Xu, H.L. Jiang, Metal-organic frameworks meet metal nanoparticles: synergistic effect for enhanced catalysis, Chem. Soc. Rev. 46 (2017) 4774.

[28] L.J. Murray, M. Dinca, J.R. Long, Hydrogen storage in metal-organic frameworks, Chem. Soc. Rev. 38 (2009) 1294-1314.

[29] Y. Bai, Y. Dou, L.-H. Xie, W. Rutledge, J.-R. Li, H.-C. Zhou, Zr-based metal–organic frameworks: design, synthesis, structure, and applications, Chem. Soc. Rev. 45 (2016) 2327-2367.

[30] C. Zhou, C. Lai, D. Huang, G. Zeng, C. Zhang, M. Cheng, L. Hu, J. Wan, W. Xiong, M. Wen, X. Wen, L. Qin, Highly porous carbon nitride by supramolecular preassembly of monomers for photocatalytic removal of sulfamethazine under visible light driven, Appl. Catal. B Environ. 220 (2018) 202-210.

[31] X. Li, J. Liu, A.I. Rykov, H. Han, C. Jin, X. Liu, J. Wang, Excellent photo-Fenton catalysts of Fe–Co Prussian blue analogues and their reaction mechanism study, Appl. Catal. B Environ. 179 (2015) 196-205.

[32] Y. Gao, G. Yu, K. Liu, S. Deng, B. Wang, J. Huang, Y. Wang, Integrated adsorption and visible-light photodegradation of aqueous clofibric acid and carbamazepine by a Fe-based metal-organic framework, Chem. Eng. J. 330 (2017) 157-165.

[33] Y. Lei, C.-S. Chen, Y.-J. Tu, Y.-H. Huang, H. Zhang, Heterogeneous degradation of organic pollutants by persulfate activated by CuO-Fe_3O_4: mechanism, stability, and effects of pH and bicarbonate ions, Environ. Sci. Technol. 49 (2015) 6838-6845.

[34] L. Hu, Q. Chen, Hollow/porous nanostructures derived from nanoscale metal-organic frameworks towards high performance anodes for lithium-ion batteries, Nanoscale 6 (2014) 1236-1251.

[35] X. Li, Z. Wang, B. Zhang, A.I. Rykov, M.A. Ahmed, J. Wang, $FexCo_{3-x}O_4$ nanocages derived from nanoscale metal–organic frameworks for removal of bisphenol A by activation of peroxymonosulfate, Appl. Catal. B Environ. 181 (2016) 788-799.

[36] G.X. Huang, C.Y. Wang, C.W. Yang, P.C. Guo, H.Q. Yu, Degradation of Bisphenol A by Peroxymonosulfate Catalytically Activated with $Mn_{1.8}Fe_{1.2}O_4$ Nanospheres: Synergism between Mn and Fe, Environ. Sci. Technol. (2017) 12611-12618.

[37] C. Zhang, C. Lai, G. Zeng, D. Huang, C. Yang, Y. Wang, Y. Zhou, M. Cheng, Efficacy of carbonaceous nanocomposites for sorbing ionizable antibiotic sulfamethazine from aqueous solution, Water Res. 95 (2016) 103-112.

[38] W. Xue, D. Huang, G. Zeng, J. Wan, C. Zhang, R. Xu, M. Cheng, R. Deng, Nanoscale

zero-valent iron coated with rhamnolipid as an effective stabilizer for immobilization of Cd and Pb in river sediments, J. Hazard. Mater. 341 (2017) 381.

[39] H.T. Dang, T.K. Le, Precursor chain length dependence of polymeric precursor method for the preparation of magnetic Fenton-like $CuFe_2O_4$-based catalysts, J. Sol-Gel Sci. Technol. 80 (2016) 160-167.

[40] F. Qi, W. Chu, B. Xu, Comparison of phenacetin degradation in aqueous solutions by catalytic ozonation with $CuFe_2O_4$ and its precursor: Surface properties, intermediates and reaction mechanisms, Chem. Eng. J. 284 (2016) 28-36.

[41] J.B. Ayers, W.H. Waggoner, Synthesis and properties of two series of heavy metal hexacyanoferrates, J. lnorg. Nucl. Chem. 33 (1971) 721-733.

[42] M. Wang, G. Fang, P. Liu, D. Zhou, C. Ma, D. Zhang, J. Zhan, Fe_3O_4@β-CD nanocomposite as heterogeneous Fenton-like catalyst for enhanced degradation of 4-chlorophenol (4-CP), Appl. Catal. B Environ. 188 (2016) 113-122.

[43] M. Okada, L. Vattuone, K. Moritani, L. Savio, Y. Teraoka, T. Kasai, M. Rocca, X-ray photoemission study of the temperature-dependent CuO formation on Cu(410) using an energetic O_2 molecular beam, PhRvB 75 (2007) 233413.

[44] S. Dolai, R. Dey, S. Das, S. Hussain, R. Bhar, A.K. Pal, Cupric oxide (CuO) thin films prepared by reactive d.c. magnetron sputtering technique for photovoltaic application, J. Alloys Compd. 724 (2017) 456-464.

[45] G.-X. Huang, C.-Y. Wang, C.-W. Yang, P.-C. Guo, H.-Q. Yu, Degradation of Bisphenol A by Peroxymonosulfate Catalytically Activated with Mn1.8Fe1.2O4 Nanospheres: Synergism between Mn and Fe, Environ. Sci. Technol. 51 (2017) 12611-12618.

[46] D. Wilson, M.A. Langell, XPS analysis of oleylamine/oleic acid capped Fe_3O_4 nanoparticles as a function of temperature, Appl. Surf. Sci. 303 (2014) 6-13.

[47] A. Petran, T. Radu, B. Culic, R. Turcu, Tailoring the properties of magnetite nanoparticles clusters by coating with double inorganic layers, Appl. Surf. Sci. 390 (2016) 1-6.

[48] J. Gao, S. Wu, Y. Han, F. Tan, Y. Shi, M. Liu, X. Li, 3D mesoporous $CuFe_2O_4$ as a catalyst for photo-Fenton removal of sulfonamide antibiotics at near neutral pH, J. Colloid Interface Sci. 524 (2018) 409-416.

[49] A. Ledjeri, I. Yahiaoui, H. Kadji, F. Aissani-Benissad, A. Amrane, F. Fourcade, Combination of the Electro/Fe^{3+}/peroxydisulfate (PDS) process with activated sludge culture for the degradation of sulfamethazine, Environ. Toxicol. Pharmacol. 53 (2017) 34-39.

[50] C. Zhou, C. Lai, P. Xu, G. Zeng, D. Huang, C. Zhang, M. Cheng, L. Hu, J. Wan, Y. Liu, W. Xiong, Y. Deng, M. Wen, In Situ Grown Agl/$Bi_{12}O_{17}C_{l2}$ Heterojunction Photocatalysts for Visible Light Degradation of Sulfamethazine: Efficiency, Pathway, and Mechanism, ACS Sustain. Chem. Eng. 6 (2018) 4174-4184.

[51] N. Wang, X. Li, Y. Yang, T. Guo, X. Zhuang, S. Ji, T. Zhang, Y. Shang, Z. Zhou, Enhanced photocatalytic degradation of sulfamethazine by Bi-doped TiO_2 nano-composites supported by powdered activated carbon under visible light irradiation, Sep. Purif. Technol. 211 (2018) 673-683.

[52] Y. Feng, J. Liu, D. Wu, Z. Zhou, Y. Deng, T. Zhang, K. Shih, Efficient degradation of sulfamethazine with $CuCo_2O_4$ spinel nanocatalysts for peroxymonosulfate activation,

Chem. Eng. J. 280 (2015) 514-524.

[53] Y. Fan, Y. Ji, D. Kong, J. Lu, Q. Zhou, Kinetic and mechanistic investigations of the degradation of sulfamethazine in heat-activated persulfate oxidation process, J. Hazard. Mater. 300 (2015) 39-47.

[54] B. Shao, Z. Liu, G. Zeng, Z. Wu, Y. Liu, M. Cheng, M. Chen, Y. Liu, W. Zhang, H. Feng, Nitrogen-Doped Hollow Mesoporous Carbon Spheres Modified g-C_3N_4/Bi_2O_3 Direct Dual Semiconductor Photocatalytic System with Enhanced Antibiotics Degradation under Visible Light, ACS Sustain. Chem. Eng. 6 (2018) 16424–16436.

[55] B. Shao, Z. Liu, G. Zeng, Y. Liu, X. Yang, C. Zhou, M. Chen, Y. Liu, Y. Jiang, M. Yan, Immobilization of laccase on hollow mesoporous carbon nanospheres: Noteworthy immobilization, excellent stability and efficacious for antibiotic contaminants removal, J. Hazard. Mater. 362 (2019) 318-326.

[56] M. Cheng, G. Zeng, D. Huang, C. Lai, P. Xu, C. Zhang, Y. Liu, Hydroxyl radicals based advanced oxidation processes (AOPs) for remediation of soils contaminated with organic compounds: A review, Chem. Eng. J. 284 (2016) 582-598.

[57] L. Szpyrkowicz, C. Juzzolino, S.N. Kaul, A Comparative study on oxidation of disperse dyes by electrochemical process, ozone, hypochlorite and fenton reagent, Water Res. 35 (2001) 2129-2136.

[58] W. Li, Y. Wang, A. Irini, Effect of pH and H_2O_2 dosage on catechol oxidation in nano-Fe_3O_4 catalyzing UV–Fenton and identification of reactive oxygen species, Chem. Eng. J. 244 (2014) 1-8.

[59] M. Cheng, G. Zeng, D. Huang, L. Liu, M. Zhao, C. Lai, C. Huang, Z. Wei, N. Li, P. Xu,

C. Zhang, F. Li, Y. Leng, Effect of Pb^{2+} on the production of hydroxyl radical during solid-state fermentation of straw with Phanerochaete chrysosporium, Biochem. Eng. J. 84 (2014) 9-15.

[60] A.A. Burbano, D.D. Dionysiou, M.T. Suidan, T.L. Richardson, Oxidation kinetics and effect of pH on the degradation of MTBE with Fenton reagent, Water Res. 39 (2005) 107-118.

[61] A. Kudo, K. Ueda, H. Kato, I. Mikami, Photocatalytic O_2 evolution under visible light irradiation on $BiVO_4$ in aqueous $AgNO_3$ solution, Catal. Lett. 53 (1998) 229-230.

[62] Y. Lin, D. Li, J. Hu, G. Xiao, J. Wang, W. Li, X. Fu, Highly Efficient Photocatalytic Degradation of Organic Pollutants by PANI-Modified TiO_2 Composite, J. Phys. Chem. C 116 (2012) 5764-5772.

[63] P.S. Rao, E. Hayon, Experimental determination of the redox potential of the superoxide radical $\bullet O^{2-}$, Biochem Biophys Res Commun 51 (1973) 468-473.

[64] X. Pan, Y.-J. Xu, Defect-Mediated Growth of Noble-Metal (Ag, Pt, and Pd) Nanoparticles on TiO_2 with Oxygen Vacancies for Photocatalytic Redox Reactions under Visible Light, J.Phys. Chem. C 117 (2013) 17996-18005.

[65] N.K. Eswar, S.A. Singh, G. Madras, Photoconductive network structured copper oxide for simultaneous photoelectrocatalytic degradation of antibiotic (tetracycline) and bacteria (E. coli), Chem. Eng. J. 332 (2018) 757-774.

[66] K. Li, Y. Zhao, M.J. Janik, C. Song, X. Guo, Facile preparation of magnetic mesoporous Fe_3O_4/C/Cu composites as high performance Fenton-like catalysts, Appl. Surf. Sci. 396 (2016) 1383-1392.

[67] Y. Zhang, J. He, R. Shi, P. Yang, Preparation and photo Fenton-like activities of high crystalline CuO fibers, Appl. Surf. Sci. 422 (2017).

[68] H. Zhao, L. Qian, X. Guan, D. Wu, G. Zhao, Continuous bulk FeCuC aerogel with ultradispersed metal nanoparticles: an efficient 3D heterogeneous electro-Fenton cathode over a wide range of pH 3–9, Environ. Sci. Technol. 50 (2016) 5225-5233.

[69] C. Guo, J. Xu, S. Wang, Y. Zhang, Y. He, X. Li, Photodegradation of sulfamethazine in an aqueous solution by a bismuth molybdate photocatalyst, Catal. Sci. Technol. 3 (2013) 1603-1611.

[70] A. Fabiańska, A. Białkbielińska, P. Stepnowski, S. Stolte, E.M. Siedlecka, Electrochemical degradation of sulfonamides at BDD electrode: kinetics, reaction pathway and eco-toxicity evaluation, J. Hazard. Mater. 280 (2014) 579-587.

[71] X. Gong, D. Huang, Y. Liu, Z. Peng, G. Zeng, P. Xu, M. Cheng, R. Wang, J. Wan, Remediation of contaminated soils by biotechnology with nanomaterials: bio-behavior, applications, and perspectives, Crit. Rev. Biotechnol. 38 (2017) 1-14.

[72] D. Huang, X. Wang, C. Zhang, G. Zeng, Z. Peng, J. Zhou, M. Cheng, R. Wang, Z. Hu, X. Qin, Sorptive removal of ionizable antibiotic sulfamethazine from aqueous solution by graphene oxide-coated biochar nanocomposites: Influencing factors and mechanism, Chemosphere 186 (2017) 414-421.

[73] M. Pérez-Moya, M. Graells, G. Castells, J. Amigó, E. Ortega, G. Buhigas, L.M. Pérez, H.D. Mansilla, Characterization of the degradation performance of the sulfamethazine antibiotic by photo-Fenton process, Water Res. 44 (2010) 2533-2540.

[74] J. Jung, Y. Kim, J. Kim, D.-H. Jeong, K. Choi, Environmental levels of ultraviolet light

potentiate the toxicity of sulfonamide antibiotics in Daphnia magna, Ecotoxicology 17 (2008) 37-45.

[75] D. Mansour, F. Fourcade, S. Huguet, I. Soutrel, N. Bellakhal, M. Dachraoui, D. Hauchard, A. Amrane, Improvement of the activated sludge treatment by its combination with electro Fenton for the mineralization of sulfamethazine, Int. Biodeterior. Biodegrad. 88 (2014) 29-36.

[76] A. Ledjeri, I. Yahiaoui, H. Kadji, F. Aissani-Benissad, A. Amrane, F. Fourcade, Combination of the Electro/Fe^{3+}/peroxydisulfate (PDS) process with activated sludge culture for the degradation of sulfamethazine, Environ. Toxicol. Pharmacol. 53 (2017) 34-39.

[77] D. Mansour, F. Fourcade, I. Soutrel, D. Hauchard, N. Bellakhal, A. Amrane, Relevance of a combined process coupling electro-Fenton and biological treatment for the remediation of sulfamethazine solutions – Application to an industrial pharmaceutical effluent, Comptes Rendus Chimie 18 (2015) 39-44.

[78] D. Huang, W. Xue, G. Zeng, J. Wan, G. Chen, C. Huang, C. Zhang, M. Cheng, P. Xu, Immobilization of Cd in river sediments by sodium alginate modified nanoscale zero-valent iron: Impact on enzyme activities and microbial community diversity, Water Res. 106 (2016) 15-25.

[79] X. Gong, D. Huang, Y. Liu, G. Zeng, R. Wang, J. Wan, C. Zhang, M. Cheng, X. Qin, W. Xue, Stabilized nanoscale zero-valent iron mediated cadmium accumulation and oxidative damage of Boehmeria nivea (L.) Gaudich cultivated in cadmium contaminated sediments, Environ. Sci. Technol. 51 (2017) 11308–11316.

[80] E.G. Garrido-Ramírez, J.F. Marco, N. Escalona, M.S. Ureta-Zañartu, Preparation and characterization of bimetallic Fe–Cu allophane nanoclays and their activity in the phenol oxidation by heterogeneous electro-Fenton reaction, Micropor. Mesopor. Mat. 225 (2016) 303-311.

[81] H. Lv, H. Zhao, T. Cao, L. Qian, Y. Wang, G. Zhao, Efficient degradation of high concentration azo-dye wastewater by heterogeneous Fenton process with iron-based metal-organic framework, J. Mol. Catal. A: Chem. 400 (2015) 81-89.

[82] W. Wang, P. Xu, M. Chen, G. Zeng, C. Zhang, C. Zhou, Y. Yang, D. Huang, C. Lai, M. Cheng, L. Hu, W. Xiong, H. Guo, M. Zhou, Alkali Metal-Assisted Synthesis of Graphite Carbon Nitride with Tunable Band-Gap for Enhanced Visible-Light-Driven Photocatalytic Performance, ACS Sustain. Chem. Eng. 6 (2018) 15503-15516.

[83] T.A. Vu, G.H. Le, C.D. Dao, L.Q. Dang, K.T. Nguyen, P.T. Dang, H.T. Tran, Q.T. Duong, T.V. Nguyen, G.D. Lee, Isomorphous substitution of Cr by Fe in MIL-101 framework and its application as a novel heterogeneous photo-Fenton catalyst for reactive dye degradation, RSC Adv. 4 (2014) 41185-41194.

Figure captions:

Fig. 1. XRD patterns of the prepared catalysts.

Fig. 2. SEM images of Cu-Fe PBA (A) and CuFeO (B), SEM-EDS elemental mapping images of CuFeO (C-H), TEM images of CuFeO (I-K), and the corresponding FFT-filtered TEM pattern images recorded from the selected area FFT pattern (L).

Fig. 3. FT-IR patterns (A) and XPS spectra (B) of the prepared catalysts.

Fig. 4. The high resolution XPS of Cu 2p (A, B) and Fe 2p (C, D) of the prepared catalysts.

Fig. 5. Removal efficiency of SMZ (A) and kinetic curves (B) in different reaction systems; effect of solution pH (C) and H_2O_2 concentrations (D) on SMZ degradation in the photo-Fenton system. Reaction conditions: SMZ concentration = 500 mg/L; catalyst loading = 500 mg/L; pH=6 (expect C); H_2O_2 concentration = 60 mM (expect D); T = 20 °C.

Fig. 6. (A) DMPO spin-trapping ESR spectra recorded from different Fenton-like systems. Reaction conditions: catalyst loading = 500 mg/L; DMPO concentration = 50 mM; pH=6; T = 20 °C. (B) Effect of radical scavengers on SMZ degradation. Reaction conditions: SMZ concentration = 500 mg/L; catalyst loading = 500 mg/L; pH=6; T = 20 °C.

Fig. 7. High resolution XPS spectra of Cu $2p_{3/2}$ (A, B) and Fe $2p_{3/2}$ (C, D) in CuFeO nanospheres before and after photo-Fenton reaction.

Fig. 8. Proposed photo-Fenton reaction mechanism over the cubic lattice structure of CuFeO.

Fig. 9. LC spectra of SMZ degradation intermediates detected in the CuFeO/H_2O_2/ Vis system (A), and the proposed degradation pathways of SMZ the photo-Fenton system (B).

Fig. 10. (A) Reusability test of CuFeO for SMZ removal. Reaction conditions: SMZ concentration = 500 mg/L; catalyst loading = 500 mg/L; pH=6; T = 20 °C. (B) XRD patterns, (C) FT-IR and (D) XPS spectra (C) of CuFeO before and after reaction.

Prussian blue analogue derived magnetic Cu-Fe oxide as a recyclable photo-Fenton catalyst for the efficient removal of sulfamethazine at near neutral pH values

Min Cheng [a,b,1], Yang Liu [a,b,1], Danlian Huang [a,b,1], Cui Lai [a,b,1], Guangming Zeng [a,b,*], Jinhui Huang [a,b,*], Zhifeng Liu [a,b], Chen Zhang [a,b], Chengyun Zhou [a,b], Lei Qin [a,b], Weiping Xiong [a,b], Huan Yi [a,b], Yang Yang [a,b]

a. College of Environmental Science and Engineering, Hunan University, Changsha, Hunan 410082, China

b. Key Laboratory of Environmental Biology and Pollution Control (Hunan University), Ministry of Education, Changsha, Hunan 410082, China

1 These authors contribute equally to this article.

* Corresponding author at: College of Environmental Science and Engineering, Hunan University, Changsha, Hunan 410082, China.
Tel.: +86–731– 88822754; fax: +86–731–88823701.
E-mail address: zgming@hnu.edu.cn (G.M. Zeng), huangjinhui@hnu.edu.cn (J.H.Huang).

Abstract

The presence of antibiotics in aquatic environments has attracted global concern. Heterogeneous photo-Fenton process is an attractive yet challenging method for antibiotics degradation, especially when such a process can be operated at neutral pH values. In this work, a new magnetic Cu-Fe oxide (CuFeO) was developed as the heterogeneous photo-Fenton catalyst through a facile two-step method. The obtained CuFeO particles were found to be more efficient to activate H_2O_2 into radicals (•OH and •O_2^-) than Cu-Fe Prussian blue analogue (Cu-Fe PBA, the precursor) at near neutral conditions. The removal rate of sulfamethazine (SMZ) in CuFeO/H_2O_2/Vis system was much higher than those in CuO/H_2O_2/Vis and Fe_3O_4/H_2O_2/Vis systems. It was observed that nearly complete removal of SMZ from ultrapure water, river water and tap water can be achieved in 30 min in CuFeO/H_2O_2/Vis system. The influence of different process parameters on the SMZ degradation efficiency was then examined and the catalytic stability of CuFeO was also tested. The SMZ degradation intermediates during the process were analyzed and the degradation pathway was proposed based on LC–MS results. The mechanisms for H_2O_2 activation were studied by X-ray photoelectron spectrum analysis, radical scavenging and electron spin-trapping experiments. It is suggested that the synergistic effect among photo-induced electrons, Cu and Fe in CuFeO exhibits excellent performance in the catalytic activation of H_2O_2. This work is expected to provide useful information for the design and synthesis of bimetallic oxide for heterogeneous photo-Fenton reactions.

Keywords: Advanced oxidation process; Photo-Fenton; Wastewater; Antibiotics; Metal−organic frameworks; Degradation

1. Introduction

Water pollution is one of the most serious environmental problems in the world. Huge amounts of organic pollutants, such as dyes, pesticides and antibiotics, are released daily into natural water channels [1-3]. Many of these contaminants are able to cause damages to living organisms including human being, which has gained increasing concerns in recent years [4-7]. This problem has been exacerbated by the fact that the vast majority of organic contaminants are resistance to microbial attack and show high stability under sunlight irradiation [8-11]. As a result, some persistent organic contaminants have been frequently detected in lakes, rivers and groundwater all over the world [12-14]. Therefore, searching for effective approaches for the removal of organic contaminants from the polluted water is important and necessary.

As a typical advanced oxidation process (AOP), Fenton process has gained wide spread acceptance for efficient degradation of recalcitrant organic contaminants [15-19]. As shown in eqs. 1, Fenton reaction causes the decomposition of hydrogen peroxide (H_2O_2) and the generation of highly reactive hydroxyl radicals (•OH) [20], which are able to degrade most organic contaminants. More importantly, Fe^{3+} can be reduced to Fe^{2+} by H_2O_2 via Fenton-like reaction (eqs. 2) [21], which enables the continuous generation of •OH. However, the traditional Fenton process generally requires to be operated under acidic pH conditions and may also suffer from the loss of catalyst, which limit its practical applications. The heterogeneous Fenton-like processes using solid catalyst can overcome these drawbacks [22-24], but many of them still suffer from the problem of low utilization rate of H_2O_2 and long reaction time. Therefore, the development of new types of Fenton-like catalysts is still urgently needed.

$$Fe^{2+} + H_2O_2 \rightarrow Fe^{3+} + HO^- + \bullet OH \quad (1)$$

$$Fe^{3+} + H_2O_2 \leftrightarrows Fe^{2+} + H^+ + \bullet OOH \quad (2)$$

Metal−organic frameworks (MOFs) are an emerging class of porous materials assembled from organic ligands and metal ions (or clusters) [25]. The synthesis of MOFs has attracted tremendous attention in the recent years due to the possibility to obtain various numbers of porous materials that could be of great interest for applications in a number of fields such as separation [26], catalysis [27], storage [28], and sensing [29]. The occurrence of MOFs also brings a great deal of opportunities for the development of new heterogeneous Fenton-like catalysts with excellent characteristic features, such as large surface area and uniform pore sizes [27-29]. This large surface could provide abundant active sites, and the high porosity is very useful to expose the active sites completely to reactant(s) [27]. Several iron-containing MOFs, for example, MIL-53(Fe), MIL-68(Fe), MIL-100(Fe) and Prussian blue analogues (PBAs), were found to be effective for the activation of H_2O_2 [1, 30].

The combination of photo-energies (ultraviolet light/visible light) can largely enhance the efficiency of MOFs catalyzed Fenton-like process, which is current active area of interest for this technology [1]. In 2015, Li et al. [31] have developed two Fe-Co PBAs, $Fe[Co(CN)_6]\bullet 2H_2O$ and $Fe_3[Co(CN)_6]_2\bullet 12H_2O$, as excellent photo-Fenton catalysts. In this report, the removal efficiency of Rhodamine B (RhB, 12 mg/L) by Fe^{II}-Co PBA/H_2O_2 in 30 min reached 93%. In a recent study, the MIL-53(Fe)/H_2O_2/Vis system exhibited significantly higher efficiency for the degradation of organic contaminants than TiO_2/Vis, Fe(II)/H_2O_2 or MIL-53 (Fe)/H_2O_2 system [32]. It was suggested that two mechanisms could be responsible for the excellent catalytic performance of MOFs catalysts in the photo-Fenton system. Firstly,

iron sites on the surface of catalyst can catalyze the decomposition of H_2O_2 to generate •OH through Fenton-like reaction. Secondly, H_2O_2 as an efficient scavenger could capture the photo-induced electrons (e^-) in the catalyst to form •OH [1].

The bimetallic catalyst, Cu-Fe oxide has gained particular attention in the Fenton chemistry, not only because of its good catalytic performance but also copper is not regarded as a potential carcinogen [33]. Recently, some researchers have studied the feasibility of using MOFs to obtain porous nanostructured oxides. The pioneering works showed that the original morphology of the precursor can be almost retained after the thermal treatment, while the catalytic performance can be largely improved [34-36]. To our knowledge, however, no study on the preparation of Cu-Fe oxide from Cu-Fe PBAs and its application for Fenton-like reactions has been reported. Therefore, in this current study, a facile two-step strategy was developed to synthesize porous Cu-Fe oxide (CuFeO) by heating the Cu-Fe PBAs. The morphology and chemicals structures of the prepared catalysts before and after the Fenton process were thoroughly characterized by various techniques. Sulfamethazine (SMZ), one of the most commonly used antibiotics, was used as the model organic pollutant due to its adverse effects on living being and frequent occurrence in natural water environment [37, 38]. The catalytic properties of the prepared catalysts was evaluated by activation of H_2O_2 under the visible light irradiation ($\lambda > 420$ nm).

The main objective of this study was to construct a new MOFs-derived photo-Fenton catalyst for the efficient removal of organic pollutants. The catalytic performance of the CuFeO was studied in details and the involved reactive species were also investigated. More importantly, the synergistic effect among photo-induced e^-, Cu and Fe in CuFeO was

explored in order to understand the catalytic mechanism. Additionally, the possible degradation pathways of SMZ in this photo-Fenton system were proposed based on the identified intermediates during the degradation process and the stability and reusability of the catalyst were also evaluated. This work is expected to help to develop new types of MOFs derived photo-Fenton catalyst and give a deeper insight into the mechanisms of heterogeneous photo-Fenton process.

2. Experimental section

2.1. Chemicals and Reagents.

Sulfamethazine ($C_{14}H_{20}ClNO_2$, standard grade) was purchased from Sigma-Aldrich Company (Missouri, USA). The analytical grade cupric chloride tetrahydrate ($CuCl_2 \cdot 4H_2O$, analytical grade), potassium hexacyanoferrate (III) ($K_3[Fe(CN)_6]$ and polyvinylpyrrolidone (PVP) were obtained from Sinopharm Chemical Reagent Corp (China).

2.2. Synthesis of Cu-Fe PBAs and CuFeO

The Cu-Fe PBAs were synthesized according to a reported method with some modification [31]. In brief, 2 g of PVP was first dissolved in 100 mL $CuCl_2 \cdot 4H_2O$ (50 mM) solution. A certain amount (50 mL, 100 mL or 200 mL) of $K_3[Fe(CN)_6]$ (50 mM) solution was then dropwise added into the aforementioned solution. The mixed solution was then stirred for 30 min, the obtained precipitate was collected via centrifugation, and finally the Cu-Fe PBAs can be obtained by the subsequent washing and drying procedures. To prepare the CuFeO, the obtained Cu-Fe PBAs was heated to 550 °C with a temperate ramp of 3.6 °C min^{-1} and kept at the same temperature for 2 h in air.

2.3. Characterization

The morphology of Cu-Fe PBA and CuFeO was examined by scanning electron microscopy (FEI Quanta 400) and FEI Tecnai G2F20 transmission electron microscopy (TEM). Energy dispersive X-ray spectroscopy (EDS) of the prepared catalysts was obtained using an EDAX Genesis X-ray spectrometer. The size distribution of the prepared catalysts was measured with the dynamic light scattering (DLS) method. The prepared catalysts were fully dispersed in water with the help of ultrasound radiation. The measurement was carried out using a DynaPro Dynamic Light Scatterer (Malvern Instruments). The Brunauer–Emmett–Teller (BET) specific surface area, the Barrett–Joyner–Halenda (BJH) pore volume and pore size of the catalyst were measured using the Micromeritics ASAP 2010 analyzer. The crystal structure of the Cu-Fe PBAs and CuFeO was studied using a D/max-2500 X-ray diffractometer. X-ray photoelectron spectrum (XPS) recorded on the Axis Ultra spectrometer were fitted using XPSPEAK41 software. Fourier transform infrared spectroscopy (FT-IR) spectra were obtained by BIO RAD FTS-600 spectrometer. The thermogravimetric (TG) analysis was conducted on a Setaram Setsys 16/18 thermo-analyzer. The magnetic properties of the prepared catalysts were investigated with a MPMS (SQUID) XL vibration sample magnetometer (VSM) at room temperature. The electron spin resonance (ESR) measurement carried out with a Bruker ER200-SRC spectrometer.

2.4. Photo-Fenton reaction

The photo-Fenton reaction was performed in 250 mL reactors containing 100 mL of 50 mg L^{-1} SMZ solution under the visible-light (λ > 420 nm) irradiation with a 300 W Xe lamp. All the experiments were performed in triplicate. In a typical test, 50 mg of catalyst was added to 100 mL of SMZ solution (50 mg/L) and stirred for 30 min to establish the

adsorption−desorption equilibrium. After that, a certain amount of H_2O_2 solution (30 %, w/w) was then added to trigger the Fenton-like reaction. At the same time, the reactor was exposed to the 300 W Xe lamp. In the recyclability test, the CuFeO catalyst at the end of each run could be separated simply with a magnet. In a typical procedure, the catalysts were fixed at the bottom of flask by a magnet, and then the solution was carefully drawn out of the reactor. The catalyst was washed with ultrapure water for 3 times. After that, the magnet was removed, and the reactor was placed in the oven (60 °C) to remove the residual water.

2.5. Analytical methods

The concentration of SMZ during the process was determined by high performance liquid chromatography (HPLC, Agilent 1200 series) according to a published method [37]. The SMZ degradation kinetic was fitted by the pseudo first-order model (eqs. 3).

$$\mathrm{Ln}\,(C_t / C_0) = -kt \quad (3)$$

Where C_t is the SMZ concentration at a certain reaction time (t) and C_0 is the initial SMZ concentration.

In addition, the mineralization of SMZ in the photo-Fenton-like system was evaluated with a TOC-5000A model analyzer. The degradation intermediates were determined by the Agilent 1290/6460 high-performance liquid chromatography mass spectrometry (LC-MS) system. The detailed description of the operation condition of LC-MS was provided in Supplementary Material. The toxic effect of SMZ and the degradation intermediates during the process was evaluated by traditional bacterial growth. *Escherichia coli* (*E. coli*) was selected as a model bacterium for testing. In a typical test, 0.5 mL of bacterial stock solution (3.0×10^7 CFU mL^{-1}) was added to 49.5 mL of sterile solution that containing 48.5 mL of

ultrapure water and 1 mL of SMZ solution (1 mL of ultrapure water or 1 mL of reaction solution sampled at different time points during the photo-Fenton treatment). The mixed solution was kept in an incubator (37 ℃) for 1 h, then diluted and spread on Eosin Methylene Blue Agar plate. After that, the plate was allowed to incubate at 37 ℃ for 24 h. The viable cell density of each sample was measured by standard plate count method. The concentration of leached metals in the solution was determined by a DR 2800 spectrophotometer (Hach, USA) using the standard methods.

3. Results and discussion

3.1. Characterization of Cu-Fe PBA and CuFeO

Fig. 1 shows the XRD patterns of the 3 obtained Cu-Fe PBAs with different initial ratios of Cu/Fe. The results revealed that Cu/Fe(1:2) PBA, Cu/Fe(1:1) PBA and Cu/Fe(2:1) PBA have almost the same XRD patterns. That is to say, the ratio of Fe/Cu had no obvious influence on the final product. All the characteristic diffraction peaks (2θ; 17.61º, 24.91º, 35.62º, 39.96º, 43.93º, 51.24º, 54.47º and 57.91º) could be assigned to $Cu_3[Fe(CN)_6]_2$ (JCPDS No. 86-0514). No other impurity diffraction peaks were detected in these samples, indicating the high purity of the products. The as-prepared Cu-Fe PBA could be transformed into CuFeO after heating in air at 550 ºC. As indicated in TG analysis (Fig. S1), the weight loss of Cu-Fe PBA took place in 3 different stages, and the total weight loss rate was about 26%, 3% or 30%, respectively. The weight loss in the first stage (below 150 ºC) and second stage (150-280 ºC) were due to the removal of the crystalline and coordinated water, respectively. The weight loss over 280 ºC was caused by the decomposition of C-N ligands [35]. In this stage, the organic ligands can be oxidized into gases (CO_2, NO_x, etc.) and the

Cu-Fe PBAs were decomposed into CuFeO. Consequently, the thermal treatment led to a significant change in the XRD patterns. In XRD patterns of CuFeO (derived from Cu/Fe(2:1) PBA), two distinct diffraction peaks at 2θ values of 35.56º and 38.75º (Fig. 1) were assigned to the (311) and (111) crystal plane of Fe_3O_4 (JCPDS No. 88-0315) and CuO (JCPDS No. 48-1548), respectively.

The morphology and microstructure of Cu-Fe PBA and CuFeO were investigated by SEM and TEM technologies. As shown in Fig. 2A, Cu-Fe PBA was comprised of many tiny particles, which is likely due to the formation of compactly arranged $Cu_3[Fe(CN)_6]_2 \bullet nH_2O$. It can be observed that SEM image of CuFeO (Fig. 2B) is very similar to that of Cu-Fe PBAs, indicating no significant change occurred in the morphology of Cu-Fe PBAs during the heat treatment. EDS analysis indicated that Cu-Fe PBA mainly consists of N, C, Fe, Cu and O (Fig. S2B). After the thermal treatment, these elements are still detected (Fig. S2D), but the signal strength of N and C decreased very obviously. This is in consisted with the elemental mapping images, which show C and N were almost completely removed from Cu-Fe PBA. In addition, the element mapping clearly illustrates the homogeneous distribution of Fe, Cu and O species in the CuFeO particles (Fig. 2C-2H). TEM images (Fig. 2I and J) confirmed the uniform structures of CuFeO. Fig. 2K and 2L show the HR-TEM image and FFT-filtered TEM pattern images of CuFeO, the lattice spacings of 0.29 nm and 0.25 nm were correspond well to the (2 2 0) plane Fe_3O_4 (JCPDS No. 88-0315) and (1 1 -1) plane of CuO (JCPDS No. 48-1548), respectively.

DLS analysis showed that the average size of Cu-Fe PBA and CuFeO (dispersed in water) was 225.8 and 240.0 nm, respectively (Fig. S3). The average size of CuFeO is very

closed to that of Cu-Fe PBA, suggesting the thermal treatment did not significantly change the morphology of Cu-Fe PBA, which is in consistent with the results obtained from SEM analysis. The BET surface area and BJH pore volume of CuFeO particles are 178.35 m^2/g and 0.6993 cm^3/g, respectively, which are much higher than those of the reported Cu-Fe bimetallic catalysts [33, 39, 40]. As shown in Fig. S4, the BET isotherm of CuFeO particles belongs to type IV with H3 type hysteresis loops, indicating that CuFeO particles were mesoporous. The inset of Fig. S4 is the BJH pore size distribution plots of CuFeO particles. According to the BJH analysis, the pore size of the CuFeO catalyst was determined to be 17.47 nm. The high specific surface area and porous structure of the catalysts may facilitate the catalytic performance.

The FTIR spectra of the as-synthesized Cu-Fe PBA and CuFeO were shown in Fig. 3A. As can be seen in Fig. 3A, the two peaks detected at 1651 cm^{-1} (H-O-H bending mode) and 3440 cm^{-1} (O-H stretching mode) demonstrated the presence of water molecules in the structure of Cu-Fe PBA [31], which is in good agreement with the TG analysis (Fig. S1). The absorption band at 2102 cm^{-1} is assignable to the C-N stretching vibration of PBA [41]. As compared with Cu-Fe PBA, the number of characteristic peaks in CuFeO is much less. Noticeably, the characteristic peaks of C-N stretching vibration (2102 cm^{-1}) completely disappeared from the spectrum of Cu-Fe PBA after the heating treatment. The strong band emerged at 570 cm^{-1} in CuFeO pattern is the characteristic peak of the Fe-O stretching vibration from Fe_3O_4 [42].

The surface chemical composition and electronic state of Cu-Fe PBA and CuFeO were determined by the XPS. As revealed in Fig. 3B, five elements: Cu, Fe, O, N, and C were

detected in the XPS survey spectrum of Cu-Fe PBA. For CuFeO, the enhanced signal of Cu, Fe and O were observed in the survey spectrum, while no significant signal of N and C were detected. The changes observed in the high resolution XPS of Cu 2p (Fig. 4A and 4B) confirmed that the CuO was truly produced in CuFeO. The two peaks located at 933.6 eV and 953.4 eV are belonging to Cu $2p_{3/2}$ and Cu $2p_{1/2}$ of CuO, respectively. CuO is also known to possess characteristic high-intensity shake-up satellites [43]. Previous studies have demonstrated the satellites are usually located at a higher binding energy than the main Cu $2p_{3/2}$ and Cu $2p_{1/2}$ peaks by about 9 eV [44], which are in good agreement with our result. The observed peak located at 962.1 eV is the satellite peak for the Cu $2p_{1/2}$, and the peaks at 943.5 eV and 941.1 eV are the signals for the presence of satellite peaks of Cu $2p_{3/2}$. In the high resolution XPS of Fe $2p_{3/2}$ of Cu-Fe PBA (Fig. 4C), the binding energy of Fe $2p_{3/2}$ at 708.3 eV could be corresponded to Fe(III). The high resolution XPS of Fe in CuFeO (Fig. 4D) is quite similar to that of Fe_3O_4 [45]. The Fe $2p_{3/2}$ spectrum (Fig. 4D) of CuFeO can be split into three peaks with binding energies at 712.6 eV, 711.0 and 709.9, which could be assigned to tetrahedral Fe(III), octahedral Fe(III) and octahedral Fe(II), respectively [46, 47]. Overall the XPS results coincided well with the XRD, SEM, TEM and FT-IR analysis.

According to the above analysis, we speculated that the synthesized CuFeO should be a kind of magnetic material due to the existence of Fe_3O_4. To verify this speculation, the magnetic property of the prepared catalysts was thus studied. Fig. S5 presents the magnetic hysteresis curves for Cu-Fe PBA, CuFeO and the used-CuFeO. These curves display the evolution of magnetization (*M*) as a function of applied field (*H*). As indicated in Fig. S5, no magnetism was found in Cu-Fe PBA, while CuFeO exhibited obvious magnetism. Moreover,

CuFeO could maintain its original magnetism even after 5 degradation cycles. The saturation magnetization value (*M*s) of CuFeO was measured to be 14.18 emu g^{-1}, which is about 25% of that of pure magnetic Fe_3O_4 under the same conditions. Generally, catalysts with high *M*s values means that they can be easily separated from the solution by magnet. In this work, CuFeO particles could be collected simply with a magnet in 10 s as shown in the inset picture of Fig. S5. This enhances the technical and economic feasibility because it allows the convenient separation and recycling of catalyst by applying an external magnetic field.

3.2. Catalytic performance of CuFeO

The adsorption of SMZ by Cu-Fe PBAs and CuFeO was studied in the first step. As revealed in Fig. S6, adsorption of SMZ by Cu-Fe PBAs and CuFeO achieved adsorption equilibrium in 30 min. We also found that both Cu-Fe PBAs and CuFeO exhibited similar and negligible SMZ adsorption capacity (about 1% of SMZ was removed by adsorption). Then, the degradation behaviors of SMZ were studied by different Fenton-like processes to evaluate the catalytic performance of CuFeO (Fig. 5A). On the one side, the photo-Fenton performance of CuFeO was investigated under different reaction conditions. It was found that neither CuFeO/Vis nor CuFeO/H_2O_2 could effectively degrade SMZ, while CuFeO/H_2O_2/Vis can almost completely remove SMZ in 30 min, suggesting both H_2O_2 and light irradiation are essential for the efficient catalytic reaction. On the other side, the photo-Fenton performance of CuFeO/H_2O_2/Vis was compared with those of other photo-Fenton system. As displayed in Fig. 5A, H_2O_2/Vis could hardly degrade any SMZ, which is in well accordance with the previous studies [31, 35]. The SMZ degradation efficacy of CuFeO/H_2O_2/Vis was significantly higher than that of Cu-Fe PBA/H_2O_2/Vis, and much higher than the sum of

CuO/H_2O_2/Vis and Fe_3O_4/H_2O_2/Vis. In this work, 95.42% of SMZ was removed after 30 min in $CuFeO/H_2O_2$/Vis system. The degradation efficiency of SMZ in this process is higher than those of many reported AOPs, including photo-Fenton process [48], electro-Fenton process [18, 49], photocatalytic processes [50, 51], and peroxymonosulfate/ persulfate-based oxidation [52, 53]. Besides, these results are consistent with the results of TOC analysis (Fig. S7). The results showed that the concentration of TOC decreased continuously during the photo-Fenton process in the $CuFeO/H_2O_2$/Vis system, and about 50% of TOC can be removed after 30 minutes' treatment, suggesting that CuFeO has high potential for the real applications. This excellent photo-Fenton activity of CuFeO is likely because CuFeO has porous structure with abundant metals (Fe and Cu) sites. In this study, the SMZ degradation kinetics can be well described by the first order kinetics as displayed in Fig. 5B. The apparent rate constant (k) of CuFeO system was 0.09961 min^{-1}, which is much higher than that of CuO (0.01332 min^{-1}), Fe_3O_4 (0.00534 min^{-1}), or CuO-Fe PBA (0.04328 min^{-1}) system for the SMZ degradation under the same conditions.

It is well known that pH of the solution plays an important role in the Fenton/Fenton-like reactions [8, 54, 55]. Therefore, the effect of solution pH on the removal of SMZ by $CuFeO/H_2O_2$/Vis was examined. As shown in Fig. 5C, the removal efficiency of SMZ increased markedly from 71.3% to 98.1% in 30 min as pH decreased from 10.0 to 4.0, which indicated that lower pH favored the degradation of SMZ in the $CuFeO/H_2O_2$/Vis system. Two mechanisms can be responsible for this phenomenon. Firstly, better efficiency at lower pH values can be due to the higher leaching of iron and copper ions as the pH decreases, which facilitates the faster homogeneous photo-Fenton reaction [56]. Secondly,

H_2O_2 is less stable at higher pH conditions and tend to decompose into H_2O [57]. From another point of view, at least 70% of SMZ can be degraded in 30 min in the tested pH range (4.0 to 10.0). In particularly, we found that 95.42% of SMZ was removed after 30 minutes' treatment at a near neutral pH (pH=6.0). Traditional homogeneous Fenton process generally needs to be operated at acidic pH conditions, which hinder the industrial application of the technology because the pollutant solutions usually have near neutral pH values [23]. In this regard, the CuFeO/H_2O_2/Vis system showed a remarkable advantage for the practical applications due to the broader working environment.

In addition, the degradation of SMZ at different H_2O_2 concentrations (20 to 100 mM) was studied. The experimental results (Fig. 5D) showed the removal efficiency of SMZ increased significantly along with the increase of H_2O_2 concentration from 20 to 60 mM, indicating that H_2O_2 concentrations were significantly related to the degradation of SMZ. The important roles that H_2O_2 plays in this photo-Fenton process were discussed later in the mechanism section. However, the increase in degradation rate of SMZ became insignificant when H_2O_2 concentration increased from 60 to 80 mM, and even started to decline when H_2O_2 concentration further increased to 100 mM. This may possibly result from the scavenging of •OH by excessive H_2O_2 (eqs. 4 and 5). For an excessive H_2O_2 loading, H_2O_2 can react with •OH to generate hydroperoxyl radicals (•OOH) and superoxide anions ($•O_2^-$) [58]. Compared with •OH, $•O_2^-$ and •OOH have much lower oxidation potentials, and thus led to lower SMZ degradation efficiency [48, 59, 60].

$$•OH + H_2O_2 \rightarrow H_2O + •OOH \quad (4)$$

$$•OOH \leftrightarrow •O_2^- + H^+ \quad (5)$$

3.3. Identification of the dominant radicals

To identify the radical generation, the ESR/DMPO experiments were performed. As seen from Fig. 6A, no signal of DMPO-•O_2^- was detected in the dark, while the light was on, the characteristic signals of DMPO-•O_2^- with an intensity ratio of 1:1:1:1 could be observed, indicating the generation of •O_2^- during the photo-Fenton process. In the dark, a weak ESR signal assigned to DMPO-•OH (with an intensity ratio of 1:2:2:1) was obtained, confirming the low catalytic performance of CuFeO for decomposing H_2O_2. In the photo-Fenton process, much stronger signal of DMPO-•OH could be detected (Fig. 6A). And the peaks intensity of •OH enhanced with the irradiation from 5 min to 10 min, suggesting •OH played an important role in the enhancement of photocatalytic performance.

In order to elucidate the activation mechanism in depth, the involved active species during the photo-Fenton process were identified by the photoinduced electron (e^-) and holes (h^+) and free radicals trapping experiments. As indicated in Fig. 6B, the addition of silver nitrate ($AgNO_3$) [61], as a scavenger for photoinduced e^- dramatically suppressed the photo-Fenton reaction. A more distinct inhibition phenomenon was observed when the scavenger of tert-butyl alcohol (TBA) for •OH was added to the reaction system [62]. The removal rate of SMZ decreased from 96.72% to 17.13% in the presence of 20 mM of TBA, which suggested that •OH played a crucial role in the catalytic degradation processes. When 1.4-benzoquinone (BQ) for superoxide radical (•O_2^-) is added [63], the degradation rate of SMZ displayed a slight decrease, indicating that •O_2^- played a minor role in SMZ degradation. The introduction of ethylenediamintetraacetic acid disodium (EDTA-2Na) as a

scavenger for h^+ has small influence on the degradation of SMZ [64], suggesting that photoinduced h^+ is not involved in SMZ degradation.

3.4. Mechanisms study

The XPS spectra of the CuFeO before and after the degradation process were also used to explore the H_2O_2 activation mechanism. As can be seen, Cu 2p spectrum of fresh CuFeO (Fig. 7A) displayed a single peak with binding energy at 933.6 eV, which is assigned to Cu (II) [44]. After the catalytic reaction, a new peak belongs to Cu (I) appeared at 735.2 eV in the deconvoluted Cu $2p_{3/2}$ spectrum (Fig. 7B), suggesting that Cu_2O was generated on the surface of CuFeO [65]. As for Fe, three peaks at 709.9, 711.0, and 712.6 eV [46] can be found in the deconvoluted Fe $2p_{3/2}$ spectra before and after the catalytic reaction, however, about 13% of the total Fe was transformed from octahedral Fe(II) (709.9 eV) to octahedral Fe(III) (711.0 eV) (Fig. 7C and 7D). The collective results indicated that both Cu species and Fe species take part in the catalytic reaction.

Fe_3O_4 and CuO are two widely studied heterogeneous Fenton-like catalyst, they can activate H_2O_2 to produce active radicals via eqs. 6-9 [42, 44]. Specifically, Fe^{II} (or Cu^{I}) can catalyze H_2O_2 decomposition to produce •OH, and then Cu and Fe at higher valence states were reduced by H_2O_2 to complete the redox cycle (eqs. 6-9), which ensure the catalytic reactions work continuously. However, the reaction rate of Cu^{II} and H_2O_2 (eqs. 9), Fe^{III} and H_2O_2 (eqs. 6) are both very slow and would thus slow the regeneration of Cu^{I} and Fe^{II}, which is mainly responsible for the relatively low SMZ degradation rate in CuO/H_2O_2 and Fe_3O_4/H_2O_2 system. Under the light radiation, the Fe_3O_4 and CuO can be excited and produce the holes (h^+) and electron (e^-) (eqs. 10 and 11) [66]. It was known that the h^+ could react

with H_2O to generate •OH (eqs. 12) or directly oxidize pollutants (eqs. 13) [67]. However, based on the results obtained from trapping experiments (Fig. 6B), the above reactions must play a minor role in the degradation of SMZ. This can explain the relative low SMZ degradation efficiency in CuFeO/Vis system. As seen from Fig. 6B, the photo-induced e^- plays an important role in SMZ degradation. This is because e^- could not only react with H_2O_2 to produce active •OH (eqs. 14), but also can cause an in–situ recycling of copper species ($Cu^{II} \rightarrow Cu^{I}$) and iron species ($Fe^{III} \rightarrow Fe^{II}$) through eqs. 15 and 16 [68], respectively. In addition, the reduction of Fe^{III} by Cu^{I} is thermodynamically favorable (eqs. 17) according to the standard reduction potentials of the Fe and Cu (eqs. 15 and 16) [68]. These processes facilitate the continuous cycle of Fe^{III}/Fe^{II} and Cu^{II}/Cu^{I} in CuFeO/H_2O_2/Vis system. Overall, the collective results indicated that the photo-induced e^- did significantly contribute to the improvement of •OH generation. On the basis of the above discussion, a reasonable schematic mechanism for enhancing •OH generation in CuFeO/H_2O_2 photo-Fenton process was illustrated in Fig. 8. In this system, high yield of •OH can be continuously generated by photo-induced e^- and surface copper species and iron species. And then the formed radicals (•OH mainly) reacted with SMZ, leading to the degradation intermediates and final mineralization products.

$$\equiv Fe^{II} + H_2O_2 \rightarrow \equiv Fe^{III} + \bullet OH + OH^- \quad (6)$$

$$\equiv Fe^{III} + H_2O_2 \rightarrow \equiv Fe^{II} + \bullet OOH + H^+ \quad (7)$$

$$\equiv Cu^{I} + H_2O_2 \rightarrow \equiv Cu^{II} + \bullet OH + OH^- \quad (8)$$

$$\equiv Cu^{II} + H_2O_2 \rightarrow \equiv Cu^{I} + \bullet OOH + H^+ \quad (9)$$

$$CuO + h\nu \rightarrow CuO\ (e^- + h^+) \quad (10)$$

$Fe_3O_4 + hv \rightarrow Fe_3O_4\ (e^- + h^+)$ (11)

$H_2O + h^+ \rightarrow \bullet OH + H^+$ (12)

$h^+ + \text{pollutant} \rightarrow \text{degradation products}$ (13)

$H_2O_2 + e^- \rightarrow \bullet OH + OH^-$ (14)

$\equiv Cu^{II} + e^- \rightarrow \equiv Cu^{I} \quad E_0 = 0.16\ V$ (15)

$\equiv Fe^{III} + e^- \rightarrow \equiv Fe^{II} \quad E_0 = 0.77\ V$ (16)

$\equiv Fe^{III} + Cu^{I} \rightarrow \equiv Fe^{II} + \equiv Cu^{II}$ (17)

3.5. Degradation intermediates of SMZ and the toxicity assessment

To fully understand the degradation process of SMZ in CuFeO/H_2O_2/Vis system, LC-MS analysis was further performed to identify the degradation intermediates of SMZ. The LC patterns displayed in Fig. 9A showed the intensity of SMZ peaks (3.48 min) decreased quickly during the photo-Fenton process. Meanwhile, another distinct peak emerged at 0.756 min, indicating that SMZ was decomposed into intermediates gradually. In this work, 3 main degradation intermediates were identified by LC-MS analysis, which included 2-amino-4,6-dimethylpyrimidine (A, *m/z* 124), 4-aminophenol (B, *m/z* 110), and 2-amino-4,6-dimethylpyrimidin-5-ol (C, *m/z* 140) (Fig. S8). Further, it was found that A and B were the dominant products during the degradation process. On the basis of the above results and the results published previously [23, 69], a possible degradation pathway of SMZ in the CuFeO/H_2O_2/Vis system was proposed in Fig. 9B. First, the attack of active species resulted in the cleavage of S-N bond in SMZ, forming two aromatic intermediates respectively with aniline ring and pyrimidine, which was also observed in an electrochemical degradation system [70]. Then, C-N bond on the aniline residue of SMZ was cleaved to form

B, and meanwhile, the hydroxylation of the pyrimidine residue of SMZ led to the formation of C. Finally, B and C could be further decomposed to inorganic species (H_2O, CO_2, etc.).

The results showed that SMZ in this CuFeO/H_2O_2/Vis system can be degraded into different intermediates in a very short time (within 30 min). However, this does not guarantee the toxicity abatement of the resulting wastewater since the intermediates can be more toxic than the starting pollutants in some cases [71, 72]. Therefore, the antimicrobial activity of the treated solutions was studied. Preliminary tests suggested that the growth of *E. coli* can be inhibited by SMZ solution and the intermediates solutions as compared to the blank (sterile water). The E. coli growth was lower in the photo-Fenton treated samples than in the initial SMZ solution (Fig. S9). The results suggested that the intermediates have higher capacity for inhibiting *E. coli* growth than that of the parent SMZ. Similar results have been reported elsewhere [18, 73, 74], for example, Perez-Moya et al. [73] reported that the toxicity of an SMZ solution increases during its degradation by means of photo-Fenton reactions. It was suggested that some degradation intermediates, such as cyclic/aromatic compounds and quinone derivatives, are toxic towards the bacteria even at very low concentration [18]. Barhoumi et al. [18] found that the toxicity of the solution can be reduced by prolonging the time of Fenton process. In this work, we also found that the decrease of toxicity at 60 min (Fig. S9). This is probably due to the further degradation of toxic intermediates by $^{\bullet}OH$. It is well-known that $^{\bullet}OH$ can mineralize most kinds of organic pollutants to carbon dioxide (CO_2), water (H_2O) and inorganics. On the other hand, there are also reports showing that the biodegradability of SMZ degradation intermediates (produced during the Fenton/Fenton-like process) was higher than that of SMZ [75-77], suggesting a combined Fenton and biological

treatment may be suitable for the depleting toxicity of SMZ solution. Taken together, the results suggest the toxicity of the treated SMZ solution needs to be considered carefully in the practical cases.

3.6. The recyclability and chemical stability of CuFeO

From the view of long-term practical applications, the recyclability of the synthesized catalysts is an important issue that should be considered. The result displayed in Fig. 10A demonstrates the as-synthetized CuFeO exhibited good recyclability. The slight decline in catalytic activity after five-cycle runs is likely due to the blockage of active sites by degradation intermediates [31, 35].

The stability of the MOFs-derived catalysts is another key issue to be considered. Firstly, it is important to know whether the CuFeO catalyst could maintain its initial structures during the oxidation process. In the experiment, we studied the XRD patterns, FTIR spectra and XPS patterns of CuFeO before and after the reaction. Results showed both the XRD patterns (Fig. 10B), FTIR spectra (Fig. 10C), and full XPS spectra (Fig. 10D) of CuFeO before and after photo-Fenton process were almost the same, suggesting that the crystal structure of CuFeO was very stable during the oxidation process. Secondly, the leaching metal ions from CuFeO particles were studied. In this work, the concentrations of Cu and Fe in the solution increased quickly during the first 10 min, but a slight decrease was observed from 20 min to 30min (Fig. S10). The concentrations of Cu and Fe in the solution at the end of the process were 2.10 and 1.31 mg/L, respectively. The relatively low metal leaching suggests CuFeO could be used as highly active and stable heterogeneous catalysts for the heterogeneous photo-Fenton process [78-83].

The removal efficiency of SMZ by CuFeO/H_2O_2/Vis system was also investigated using different types of water, which include ultrapure water, tap water (supplied by Changsha Running-water Company), municipal wastewater (obtained from Changsha GuoZhen sewage treatment plant, China) and river water (taken from Xiangjiang River). The results showed near complete removal of SMZ can be obtained in ultrapure water, river water and tap water, while about 84% of SMZ was removed in municipal wastewater (Fig. S11). The relatively lower removal of SMZ for wastewater is likely due to the blockage of light and competition of •OH by the abundant organic matters in municipal wastewater. Over all, it can be concluded that CuFeO is a promising photo-Fenton catalyst for the practical application. Besides, the versatility of this CuFeO/H_2O_2/Vis system is also enhanced by the fact the catalyst can be easily separated from the solution by a magnetic field, which enables the reuse of the catalyst.

4. Conclusions

In this study, the magnetic Cu-Fe oxide (CuFeO) was synthesized via a facile strategy by heating Cu-Fe PBA. The as-synthesized CuFeO exhibited high catalytic activity at a wide pH range. 95.42% of SMZ was removed after 30 minutes' photo-Fenton treatment at a near neutral pH (pH=6.0). Through ESR/DMPO and radical scavenger experiments, both •OH and •O_2^- were proved to be involved and the former played a more critical role in the degradation of SMZ. Based on the LC–MS analysis, the SMZ degradation intermediates were identified and the possible degradation pathway was proposed. CuFeO was shown to be stable and reusable even after a five-cycle test. In addition to the relatively low metal leaching and magnetic properties of CuFeO, the synthesized catalyst has a promising potential for the

treatment of organic wastewater. Furthermore, our findings may expand the further development of other Cu-Fe bimetallic heterogeneous Fenton-like catalysts for the degradation of organic pollutants by activation of H_2O_2.

Acknowledgements

This study was financially supported by the Program for the National Natural Science Foundation of China (51879101, 51579098, 51779090, 51709101, 51521006, 51809090, 51278176, 51378190), the National Program for Support of Top-Notch Young Professionals of China (2014), the Program for Changjiang Scholars and Innovative Research Team in University (IRT-13R17), the Program for New Century Excellent Talents in University (NCET-13-0186), Hunan Provincial Science and Technology Plan Project (2016RS3026, 2017SK2243), and the Fundamental Research Funds for the Central Universities (531109200027, 531107051080, 531107050978, 531107051205).

References

[1] M. Cheng, C. Lai, Y. Liu, G. Zeng, D. Huang, C. Zhang, L. Qin, L. Hu, C. Zhou, W. Xiong, Metal-organic frameworks for highly efficient heterogeneous Fenton-like catalysis, Coord. Chem. Rev. 368 (2018) 80-92.

[2] M. Cheng, G. Zeng, D. Huang, C. Lai, Y. Liu, C. Zhang, R. Wang, L. Qin, W. Xue, B. Song, S. Ye, H. Yi, High adsorption of methylene blue by salicylic acid–methanol modified steel converter slag and evaluation of its mechanism, J. Colloid Interface Sci. 515 (2018) 232-239.

[3] M. Cheng, G. Zeng, D. Huang, C. Lai, Z. Wei, N. Li, P. Xu, C. Zhang, Y. Zhu, X. He, Combined biological removal of methylene blue from aqueous solutions using rice straw

and Phanerochaete chrysosporium, Appl. Microbiol. Biotechnol. 99 (2015) 5247-5256.

[4] M. Cheng, G. Zeng, D. Huang, C. Yang, C. Lai, C. Zhang, Y. Liu, Advantages and challenges of Tween 80 surfactant-enhanced technologies for the remediation of soils contaminated with hydrophobic organic compounds, Chem. Eng. J. 314 (2017) 98-113.

[5] M. Cheng, G. Zeng, D. Huang, C. Yang, C. Lai, C. Zhang, Y. Liu, Tween 80 surfactant-enhanced bioremediation: toward a solution to the soil contamination by hydrophobic organic compounds, Crit. Rev. Biotechnol. 38 (2018) 17-30.

[6] Y. Liu, G. Zeng, H. Zhong, Z. Wang, Z. Liu, M. Cheng, G. Liu, X. Yang, S. Liu, Effect of rhamnolipid solubilization on hexadecane bioavailability: enhancement or reduction?, J. Hazard. Mater. 322 (2017) 394-401.

[7] O. Sacco, V. Vaiano, C. Han, D. Sannino, D.D. Dionysiou, Photocatalytic removal of atrazine using N-doped TiO2 supported on phosphors, Appl. Catal. B Environ. 164 (2015) 462-474.

[8] E. Brillas, I. Sirés, M.A. Oturan, Electro-Fenton process and related electrochemical technologies based on Fenton's reaction chemistry, Chem. Rev. 109 (2009) 6570-6631.

[9] H. Yi, D. Huang, L. Qin, G. Zeng, C. Lai, M. Cheng, S. Ye, B. Song, X. Ren, X. Guo, Selective prepared carbon nanomaterials for advanced photocatalytic application in environmental pollutant treatment and hydrogen production, Appl. Catal. B Environ. 239 (2018) 408-424.

[10] S. Wacławek, H.V. Lutze, K. Grübel, V.V. Padil, M. Černík, D.D. Dionysiou, Chemistry of persulfates in water and wastewater treatment: A review, Chem. Eng. J. 330 (2017) 44-62.

[11] J. Lalley, C. Han, X. Li, D.D. Dionysiou, M.N. Nadagouda, Phosphate adsorption using modified iron oxide-based sorbents in lake water: Kinetics, equilibrium, and column tests, Chem. Eng. J. 284 (2016) 1386-1396.

[12] X. Zhou, C. Lai, D. Huang, G. Zeng, L. Chen, L. Qin, P. Xu, M. Cheng, C. Huang, C. Zhang, Preparation of water-compatible molecularly imprinted thiol-functionalized activated titanium dioxide: Selective adsorption and efficient photodegradation of 2, 4-dinitrophenol in aqueous solution, J. Hazard. Mater. 346 (2018) 113.

[13] C. Lai, M.M. Wang, G.M. Zeng, Y.G. Liu, D.L. Huang, C. Zhang, R.Z. Wang, P. Xu, M. Cheng, C. Huang, Synthesis of surface molecular imprinted TiO_2/graphene photocatalyst and its highly efficient photocatalytic degradation of target pollutant under visible light irradiation, Appl. Surf. Sci. 390 (2016) 368-376.

[14] L. Qin, G. Zeng, C. Lai, D. Huang, P. Xu, C. Zhang, M. Cheng, X. Liu, S. Liu, B. Li, H. Yi, “Gold rush” in modern science: Fabrication strategies and typical advanced applications of gold nanoparticles in sensing, Coord. Chem. Rev. 359 (2018) 1-31.

[15] D. Huang, C. Hu, G. Zeng, M. Cheng, P. Xu, X. Gong, R. Wang, W. Xue, Combination of Fenton processes and biotreatment for wastewater treatment and soil remediation, Sci. Total Environ. 574 (2017) 1599-1610.

[16] C. Hu, D. Huang, G. Zeng, M. Cheng, X. Gong, R. Wang, W. Xue, Z. Hu, Y. Liu, The combination of Fenton process and Phanerochaete chrysosporium for the removal of bisphenol A in river sediments: Mechanism related to extracellular enzyme, organic acid and iron, Chem. Eng. J. 338 (2018) 432-439.

[17] B. Li, C. Lai, G. Zeng, L. Qin, H. Yi, D. Huang, C. Zhou, X. Liu, M. Cheng, P. Xu, C.

Zhang, F. Huang, S. Liu, Facile Hydrothermal Synthesis of Z-Scheme $Bi_2Fe_4O_9/Bi_2WO_6$ Heterojunction Photocatalyst with Enhanced Visible Light Photocatalytic Activity, ACS Appl. Mater. Interfaces 10 (2018) 18824-18836.

[18] N. Barhoumi, N. Oturan, H. Olvera-Vargas, E. Brillas, A. Gadri, S. Ammar, M.A. Oturan, Pyrite as a sustainable catalyst in electro-Fenton process for improving oxidation of sulfamethazine. Kinetics, mechanism and toxicity assessment, Water Res. 94 (2016) 52-61.

[19] S. Ammar, M.A. Oturan, L. Labiadh, A. Guersalli, R. Abdelhedi, N. Oturan, E. Brillas, Degradation of tyrosol by a novel electro-Fenton process using pyrite as heterogeneous source of iron catalyst, Water Res. 74 (2015) 77-87.

[20] F. Haber, J. Weiss, The catalytic decomposition of hydrogen peroxide by iron salts, in: Proceedings of the Royal Society of London A: Mathematical, Physical and Engineering Sciences, The Royal Society, 1934, pp. 332-351.

[21] C. Walling, A. Goosen, Mechanism of the ferric ion catalyzed decomposition of hydrogen peroxide. Effect of organic substrates, JACS 95 (1973) 2987-2991.

[22] M. Cheng, G. Zeng, D. Huang, C. Lai, Y. Liu, P. Xu, C. Zhang, J. Wan, L. Hu, W. Xiong, C. Zhou, Salicylic acid–methanol modified steel converter slag as heterogeneous Fenton-like catalyst for enhanced degradation of alachlor, Chem. Eng. J. 327 (2017) 686-693.

[23] M. Cheng, G. Zeng, D. Huang, C. Lai, Y. Liu, C. Zhang, J. Wan, L. Hu, C. Zhou, W. Xiong, Efficient degradation of sulfamethazine in simulated and real wastewater at slightly basic pH values using Co-SAM-SCS/H_2O_2 Fenton-like system, Water Res. 138

(2018) 7-18.

[24] M. Cheng, G. Zeng, D. Huang, C. Lai, P. Xu, C. Zhang, Y. Liu, J. Wan, X. Gong, Y. Zhu, Degradation of atrazine by a novel Fenton-like process and assessment the influence on the treated soil, J. Hazard. Mater. 312 (2016) 184-191.

[25] S.S. Han, J.L. Mendoza-Cortes, W.A. Goddard, III, Recent advances on simulation and theory of hydrogen storage in metal-organic frameworks and covalent organic frameworks, Chem. Soc. Rev. 38 (2009) 1460-1476.

[26] W. Xiong, G. Zeng, Z. Yang, Y. Zhou, C. Zhang, M. Cheng, Y. Liu, L. Hu, J. Wan, C. Zhou, R. Xu, X. Li, Adsorption of tetracycline antibiotics from aqueous solutions on nanocomposite multi-walled carbon nanotube functionalized MIL-53(Fe) as new adsorbent, Sci. Total Environ. 627 (2018) 235-244.

[27] Q. Yang, Q. Xu, H.L. Jiang, Metal-organic frameworks meet metal nanoparticles: synergistic effect for enhanced catalysis, Chem. Soc. Rev. 46 (2017) 4774.

[28] L.J. Murray, M. Dinca, J.R. Long, Hydrogen storage in metal-organic frameworks, Chem. Soc. Rev. 38 (2009) 1294-1314.

[29] Y. Bai, Y. Dou, L.-H. Xie, W. Rutledge, J.-R. Li, H.-C. Zhou, Zr-based metal–organic frameworks: design, synthesis, structure, and applications, Chem. Soc. Rev. 45 (2016) 2327-2367.

[30] C. Zhou, C. Lai, D. Huang, G. Zeng, C. Zhang, M. Cheng, L. Hu, J. Wan, W. Xiong, M. Wen, X. Wen, L. Qin, Highly porous carbon nitride by supramolecular preassembly of monomers for photocatalytic removal of sulfamethazine under visible light driven, Appl. Catal. B Environ. 220 (2018) 202-210.

[31] X. Li, J. Liu, A.I. Rykov, H. Han, C. Jin, X. Liu, J. Wang, Excellent photo-Fenton catalysts of Fe–Co Prussian blue analogues and their reaction mechanism study, Appl. Catal. B Environ. 179 (2015) 196-205.

[32] Y. Gao, G. Yu, K. Liu, S. Deng, B. Wang, J. Huang, Y. Wang, Integrated adsorption and visible-light photodegradation of aqueous clofibric acid and carbamazepine by a Fe-based metal-organic framework, Chem. Eng. J. 330 (2017) 157-165.

[33] Y. Lei, C.-S. Chen, Y.-J. Tu, Y.-H. Huang, H. Zhang, Heterogeneous degradation of organic pollutants by persulfate activated by CuO-Fe_3O_4: mechanism, stability, and effects of pH and bicarbonate ions, Environ. Sci. Technol. 49 (2015) 6838-6845.

[34] L. Hu, Q. Chen, Hollow/porous nanostructures derived from nanoscale metal-organic frameworks towards high performance anodes for lithium-ion batteries, Nanoscale 6 (2014) 1236-1251.

[35] X. Li, Z. Wang, B. Zhang, A.I. Rykov, M.A. Ahmed, J. Wang, $FexCo_{3-x}O_4$ nanocages derived from nanoscale metal–organic frameworks for removal of bisphenol A by activation of peroxymonosulfate, Appl. Catal. B Environ. 181 (2016) 788-799.

[36] G.X. Huang, C.Y. Wang, C.W. Yang, P.C. Guo, H.Q. Yu, Degradation of Bisphenol A by Peroxymonosulfate Catalytically Activated with $Mn_{1.8}Fe_{1.2}O_4$ Nanospheres: Synergism between Mn and Fe, Environ. Sci. Technol. (2017) 12611-12618.

[37] C. Zhang, C. Lai, G. Zeng, D. Huang, C. Yang, Y. Wang, Y. Zhou, M. Cheng, Efficacy of carbonaceous nanocomposites for sorbing ionizable antibiotic sulfamethazine from aqueous solution, Water Res. 95 (2016) 103-112.

[38] W. Xue, D. Huang, G. Zeng, J. Wan, C. Zhang, R. Xu, M. Cheng, R. Deng, Nanoscale

zero-valent iron coated with rhamnolipid as an effective stabilizer for immobilization of Cd and Pb in river sediments, J. Hazard. Mater. 341 (2017) 381.

[39] H.T. Dang, T.K. Le, Precursor chain length dependence of polymeric precursor method for the preparation of magnetic Fenton-like $CuFe_2O_4$-based catalysts, J. Sol-Gel Sci. Technol. 80 (2016) 160-167.

[40] F. Qi, W. Chu, B. Xu, Comparison of phenacetin degradation in aqueous solutions by catalytic ozonation with $CuFe_2O_4$ and its precursor: Surface properties, intermediates and reaction mechanisms, Chem. Eng. J. 284 (2016) 28-36.

[41] J.B. Ayers, W.H. Waggoner, Synthesis and properties of two series of heavy metal hexacyanoferrates, J. lnorg. Nucl. Chem. 33 (1971) 721-733.

[42] M. Wang, G. Fang, P. Liu, D. Zhou, C. Ma, D. Zhang, J. Zhan, Fe_3O_4@β-CD nanocomposite as heterogeneous Fenton-like catalyst for enhanced degradation of 4-chlorophenol (4-CP), Appl. Catal. B Environ. 188 (2016) 113-122.

[43] M. Okada, L. Vattuone, K. Moritani, L. Savio, Y. Teraoka, T. Kasai, M. Rocca, X-ray photoemission study of the temperature-dependent CuO formation on Cu(410) using an energetic O_2 molecular beam, PhRvB 75 (2007) 233413.

[44] S. Dolai, R. Dey, S. Das, S. Hussain, R. Bhar, A.K. Pal, Cupric oxide (CuO) thin films prepared by reactive d.c. magnetron sputtering technique for photovoltaic application, J. Alloys Compd. 724 (2017) 456-464.

[45] G.-X. Huang, C.-Y. Wang, C.-W. Yang, P.-C. Guo, H.-Q. Yu, Degradation of Bisphenol A by Peroxymonosulfate Catalytically Activated with Mn1.8Fe1.2O4 Nanospheres: Synergism between Mn and Fe, Environ. Sci. Technol. 51 (2017) 12611-12618.

[46] D. Wilson, M.A. Langell, XPS analysis of oleylamine/oleic acid capped Fe_3O_4 nanoparticles as a function of temperature, Appl. Surf. Sci. 303 (2014) 6-13.

[47] A. Petran, T. Radu, B. Culic, R. Turcu, Tailoring the properties of magnetite nanoparticles clusters by coating with double inorganic layers, Appl. Surf. Sci. 390 (2016) 1-6.

[48] J. Gao, S. Wu, Y. Han, F. Tan, Y. Shi, M. Liu, X. Li, 3D mesoporous $CuFe_2O_4$ as a catalyst for photo-Fenton removal of sulfonamide antibiotics at near neutral pH, J. Colloid Interface Sci. 524 (2018) 409-416.

[49] A. Ledjeri, I. Yahiaoui, H. Kadji, F. Aissani-Benissad, A. Amrane, F. Fourcade, Combination of the Electro/Fe^{3+}/peroxydisulfate (PDS) process with activated sludge culture for the degradation of sulfamethazine, Environ. Toxicol. Pharmacol. 53 (2017) 34-39.

[50] C. Zhou, C. Lai, P. Xu, G. Zeng, D. Huang, C. Zhang, M. Cheng, L. Hu, J. Wan, Y. Liu, W. Xiong, Y. Deng, M. Wen, In Situ Grown Agl/$Bi_{12}O_{17}C_{l2}$ Heterojunction Photocatalysts for Visible Light Degradation of Sulfamethazine: Efficiency, Pathway, and Mechanism, ACS Sustain. Chem. Eng. 6 (2018) 4174-4184.

[51] N. Wang, X. Li, Y. Yang, T. Guo, X. Zhuang, S. Ji, T. Zhang, Y. Shang, Z. Zhou, Enhanced photocatalytic degradation of sulfamethazine by Bi-doped TiO_2 nano-composites supported by powdered activated carbon under visible light irradiation, Sep. Purif. Technol. 211 (2018) 673-683.

[52] Y. Feng, J. Liu, D. Wu, Z. Zhou, Y. Deng, T. Zhang, K. Shih, Efficient degradation of sulfamethazine with $CuCo_2O_4$ spinel nanocatalysts for peroxymonosulfate activation,

Chem. Eng. J. 280 (2015) 514-524.

[53] Y. Fan, Y. Ji, D. Kong, J. Lu, Q. Zhou, Kinetic and mechanistic investigations of the degradation of sulfamethazine in heat-activated persulfate oxidation process, J. Hazard. Mater. 300 (2015) 39-47.

[54] B. Shao, Z. Liu, G. Zeng, Z. Wu, Y. Liu, M. Cheng, M. Chen, Y. Liu, W. Zhang, H. Feng, Nitrogen-Doped Hollow Mesoporous Carbon Spheres Modified g-C_3N_4/Bi_2O_3 Direct Dual Semiconductor Photocatalytic System with Enhanced Antibiotics Degradation under Visible Light, ACS Sustain. Chem. Eng. 6 (2018) 16424–16436.

[55] B. Shao, Z. Liu, G. Zeng, Y. Liu, X. Yang, C. Zhou, M. Chen, Y. Liu, Y. Jiang, M. Yan, Immobilization of laccase on hollow mesoporous carbon nanospheres: Noteworthy immobilization, excellent stability and efficacious for antibiotic contaminants removal, J. Hazard. Mater. 362 (2019) 318-326.

[56] M. Cheng, G. Zeng, D. Huang, C. Lai, P. Xu, C. Zhang, Y. Liu, Hydroxyl radicals based advanced oxidation processes (AOPs) for remediation of soils contaminated with organic compounds: A review, Chem. Eng. J. 284 (2016) 582-598.

[57] L. Szpyrkowicz, C. Juzzolino, S.N. Kaul, A Comparative study on oxidation of disperse dyes by electrochemical process, ozone, hypochlorite and fenton reagent, Water Res. 35 (2001) 2129-2136.

[58] W. Li, Y. Wang, A. Irini, Effect of pH and H_2O_2 dosage on catechol oxidation in nano-Fe_3O_4 catalyzing UV–Fenton and identification of reactive oxygen species, Chem. Eng. J. 244 (2014) 1-8.

[59] M. Cheng, G. Zeng, D. Huang, L. Liu, M. Zhao, C. Lai, C. Huang, Z. Wei, N. Li, P. Xu,

C. Zhang, F. Li, Y. Leng, Effect of Pb^{2+} on the production of hydroxyl radical during solid-state fermentation of straw with Phanerochaete chrysosporium, Biochem. Eng. J. 84 (2014) 9-15.

[60] A.A. Burbano, D.D. Dionysiou, M.T. Suidan, T.L. Richardson, Oxidation kinetics and effect of pH on the degradation of MTBE with Fenton reagent, Water Res. 39 (2005) 107-118.

[61] A. Kudo, K. Ueda, H. Kato, I. Mikami, Photocatalytic O_2 evolution under visible light irradiation on $BiVO_4$ in aqueous $AgNO_3$ solution, Catal. Lett. 53 (1998) 229-230.

[62] Y. Lin, D. Li, J. Hu, G. Xiao, J. Wang, W. Li, X. Fu, Highly Efficient Photocatalytic Degradation of Organic Pollutants by PANI-Modified TiO_2 Composite, J. Phys. Chem. C 116 (2012) 5764-5772.

[63] P.S. Rao, E. Hayon, Experimental determination of the redox potential of the superoxide radical $\bullet O^{2-}$, Biochem Biophys Res Commun 51 (1973) 468-473.

[64] X. Pan, Y.-J. Xu, Defect-Mediated Growth of Noble-Metal (Ag, Pt, and Pd) Nanoparticles on TiO_2 with Oxygen Vacancies for Photocatalytic Redox Reactions under Visible Light, J.Phys. Chem. C 117 (2013) 17996-18005.

[65] N.K. Eswar, S.A. Singh, G. Madras, Photoconductive network structured copper oxide for simultaneous photoelectrocatalytic degradation of antibiotic (tetracycline) and bacteria (E. coli), Chem. Eng. J. 332 (2018) 757-774.

[66] K. Li, Y. Zhao, M.J. Janik, C. Song, X. Guo, Facile preparation of magnetic mesoporous Fe_3O_4/C/Cu composites as high performance Fenton-like catalysts, Appl. Surf. Sci. 396 (2016) 1383-1392.

[67] Y. Zhang, J. He, R. Shi, P. Yang, Preparation and photo Fenton-like activities of high crystalline CuO fibers, Appl. Surf. Sci. 422 (2017).

[68] H. Zhao, L. Qian, X. Guan, D. Wu, G. Zhao, Continuous bulk FeCuC aerogel with ultradispersed metal nanoparticles: an efficient 3D heterogeneous electro-Fenton cathode over a wide range of pH 3–9, Environ. Sci. Technol. 50 (2016) 5225-5233.

[69] C. Guo, J. Xu, S. Wang, Y. Zhang, Y. He, X. Li, Photodegradation of sulfamethazine in an aqueous solution by a bismuth molybdate photocatalyst, Catal. Sci. Technol. 3 (2013) 1603-1611.

[70] A. Fabiańska, A. Białkbielińska, P. Stepnowski, S. Stolte, E.M. Siedlecka, Electrochemical degradation of sulfonamides at BDD electrode: kinetics, reaction pathway and eco-toxicity evaluation, J. Hazard. Mater. 280 (2014) 579-587.

[71] X. Gong, D. Huang, Y. Liu, Z. Peng, G. Zeng, P. Xu, M. Cheng, R. Wang, J. Wan, Remediation of contaminated soils by biotechnology with nanomaterials: bio-behavior, applications, and perspectives, Crit. Rev. Biotechnol. 38 (2017) 1-14.

[72] D. Huang, X. Wang, C. Zhang, G. Zeng, Z. Peng, J. Zhou, M. Cheng, R. Wang, Z. Hu, X. Qin, Sorptive removal of ionizable antibiotic sulfamethazine from aqueous solution by graphene oxide-coated biochar nanocomposites: Influencing factors and mechanism, Chemosphere 186 (2017) 414-421.

[73] M. Pérez-Moya, M. Graells, G. Castells, J. Amigó, E. Ortega, G. Buhigas, L.M. Pérez, H.D. Mansilla, Characterization of the degradation performance of the sulfamethazine antibiotic by photo-Fenton process, Water Res. 44 (2010) 2533-2540.

[74] J. Jung, Y. Kim, J. Kim, D.-H. Jeong, K. Choi, Environmental levels of ultraviolet light

potentiate the toxicity of sulfonamide antibiotics in Daphnia magna, Ecotoxicology 17 (2008) 37-45.

[75] D. Mansour, F. Fourcade, S. Huguet, I. Soutrel, N. Bellakhal, M. Dachraoui, D. Hauchard, A. Amrane, Improvement of the activated sludge treatment by its combination with electro Fenton for the mineralization of sulfamethazine, Int. Biodeterior. Biodegrad. 88 (2014) 29-36.

[76] A. Ledjeri, I. Yahiaoui, H. Kadji, F. Aissani-Benissad, A. Amrane, F. Fourcade, Combination of the Electro/Fe^{3+}/peroxydisulfate (PDS) process with activated sludge culture for the degradation of sulfamethazine, Environ. Toxicol. Pharmacol. 53 (2017) 34-39.

[77] D. Mansour, F. Fourcade, I. Soutrel, D. Hauchard, N. Bellakhal, A. Amrane, Relevance of a combined process coupling electro-Fenton and biological treatment for the remediation of sulfamethazine solutions – Application to an industrial pharmaceutical effluent, Comptes Rendus Chimie 18 (2015) 39-44.

[78] D. Huang, W. Xue, G. Zeng, J. Wan, G. Chen, C. Huang, C. Zhang, M. Cheng, P. Xu, Immobilization of Cd in river sediments by sodium alginate modified nanoscale zero-valent iron: Impact on enzyme activities and microbial community diversity, Water Res. 106 (2016) 15-25.

[79] X. Gong, D. Huang, Y. Liu, G. Zeng, R. Wang, J. Wan, C. Zhang, M. Cheng, X. Qin, W. Xue, Stabilized nanoscale zero-valent iron mediated cadmium accumulation and oxidative damage of Boehmeria nivea (L.) Gaudich cultivated in cadmium contaminated sediments, Environ. Sci. Technol. 51 (2017) 11308–11316.

[80] E.G. Garrido-Ramírez, J.F. Marco, N. Escalona, M.S. Ureta-Zañartu, Preparation and characterization of bimetallic Fe–Cu allophane nanoclays and their activity in the phenol oxidation by heterogeneous electro-Fenton reaction, Micropor. Mesopor. Mat. 225 (2016) 303-311.

[81] H. Lv, H. Zhao, T. Cao, L. Qian, Y. Wang, G. Zhao, Efficient degradation of high concentration azo-dye wastewater by heterogeneous Fenton process with iron-based metal-organic framework, J. Mol. Catal. A: Chem. 400 (2015) 81-89.

[82] W. Wang, P. Xu, M. Chen, G. Zeng, C. Zhang, C. Zhou, Y. Yang, D. Huang, C. Lai, M. Cheng, L. Hu, W. Xiong, H. Guo, M. Zhou, Alkali Metal-Assisted Synthesis of Graphite Carbon Nitride with Tunable Band-Gap for Enhanced Visible-Light-Driven Photocatalytic Performance, ACS Sustain. Chem. Eng. 6 (2018) 15503-15516.

[83] T.A. Vu, G.H. Le, C.D. Dao, L.Q. Dang, K.T. Nguyen, P.T. Dang, H.T. Tran, Q.T. Duong, T.V. Nguyen, G.D. Lee, Isomorphous substitution of Cr by Fe in MIL-101 framework and its application as a novel heterogeneous photo-Fenton catalyst for reactive dye degradation, RSC Adv. 4 (2014) 41185-41194.

Figure captions:

Fig. 1. XRD patterns of the prepared catalysts.

Fig. 2. SEM images of Cu-Fe PBA (A) and CuFeO (B), SEM-EDS elemental mapping images of CuFeO (C-H), TEM images of CuFeO (I-K), and the corresponding FFT-filtered TEM pattern images recorded from the selected area FFT pattern (L).

Fig. 3. FT-IR patterns (A) and XPS spectra (B) of the prepared catalysts.

Fig. 4. The high resolution XPS of Cu 2p (A, B) and Fe 2p (C, D) of the prepared catalysts.

Fig. 5. Removal efficiency of SMZ (A) and kinetic curves (B) in different reaction systems; effect of solution pH (C) and H_2O_2 concentrations (D) on SMZ degradation in the photo-Fenton system. Reaction conditions: SMZ concentration = 500 mg/L; catalyst loading = 500 mg/L; pH=6 (expect C); H_2O_2 concentration = 60 mM (expect D); T = 20 °C.

Fig. 6. (A) DMPO spin-trapping ESR spectra recorded from different Fenton-like systems. Reaction conditions: catalyst loading = 500 mg/L; DMPO concentration = 50 mM; pH=6; T = 20 °C. (B) Effect of radical scavengers on SMZ degradation. Reaction conditions: SMZ concentration = 500 mg/L; catalyst loading = 500 mg/L; pH=6; T = 20 °C.

Fig. 7. High resolution XPS spectra of Cu $2p_{3/2}$ (A, B) and Fe $2p_{3/2}$ (C, D) in CuFeO nanospheres before and after photo-Fenton reaction.

Fig. 8. Proposed photo-Fenton reaction mechanism over the cubic lattice structure of CuFeO.

Fig. 9. LC spectra of SMZ degradation intermediates detected in the CuFeO/H_2O_2/ Vis system (A), and the proposed degradation pathways of SMZ the photo-Fenton system (B).

Fig. 10. (A) Reusability test of CuFeO for SMZ removal. Reaction conditions: SMZ concentration = 500 mg/L; catalyst loading = 500 mg/L; pH=6; T = 20 °C. (B) XRD patterns, (C) FT-IR and (D) XPS spectra (C) of CuFeO before and after reaction.

Figure

Fig. 1

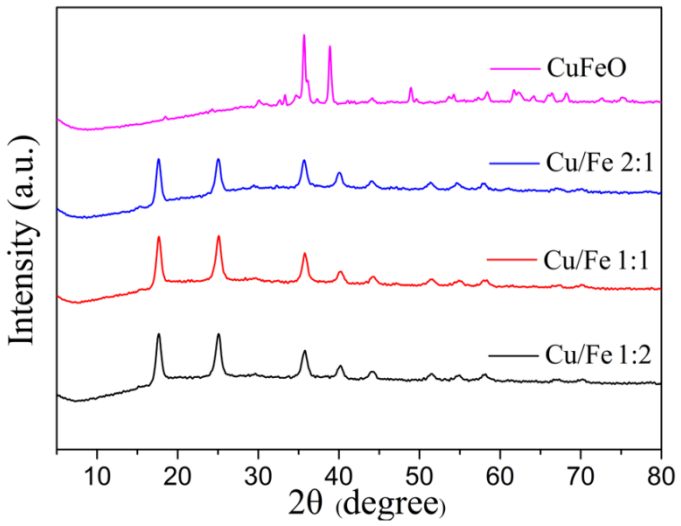

Figure

Fig. 2

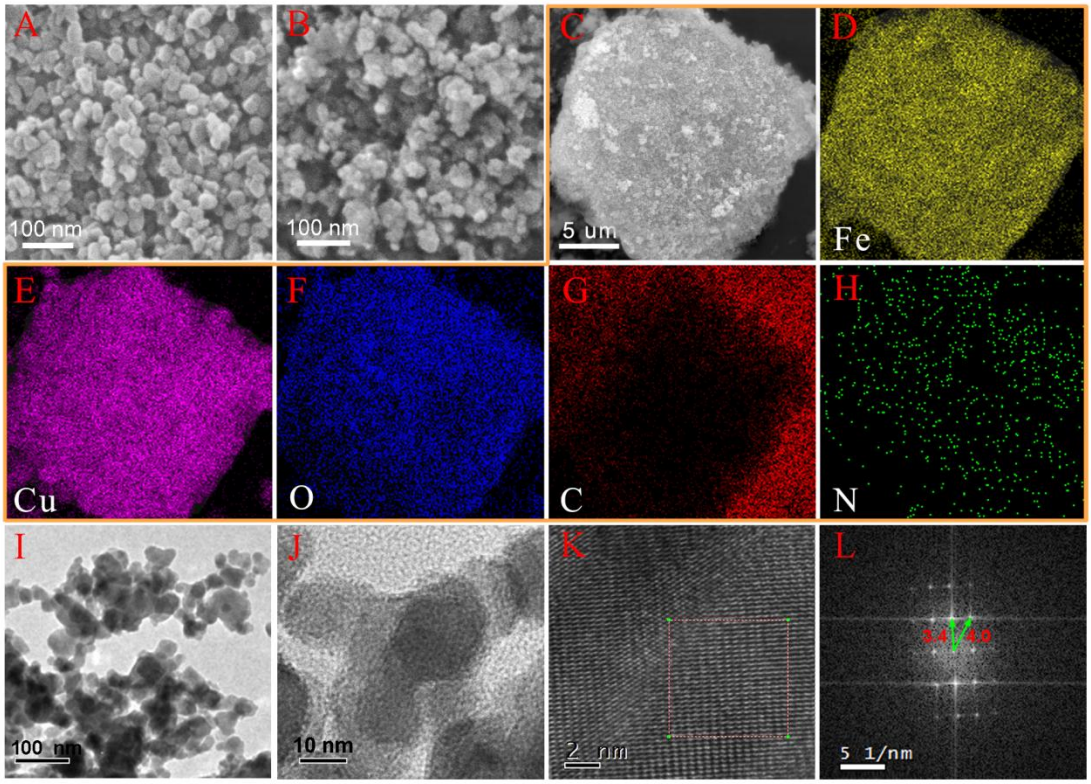

Figure

Fig. 3

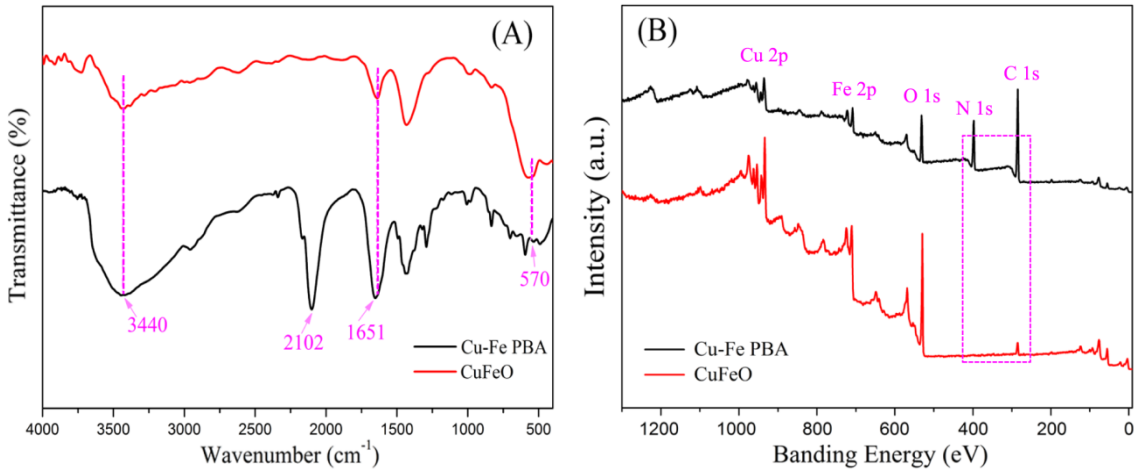

Figure

Fig. 4

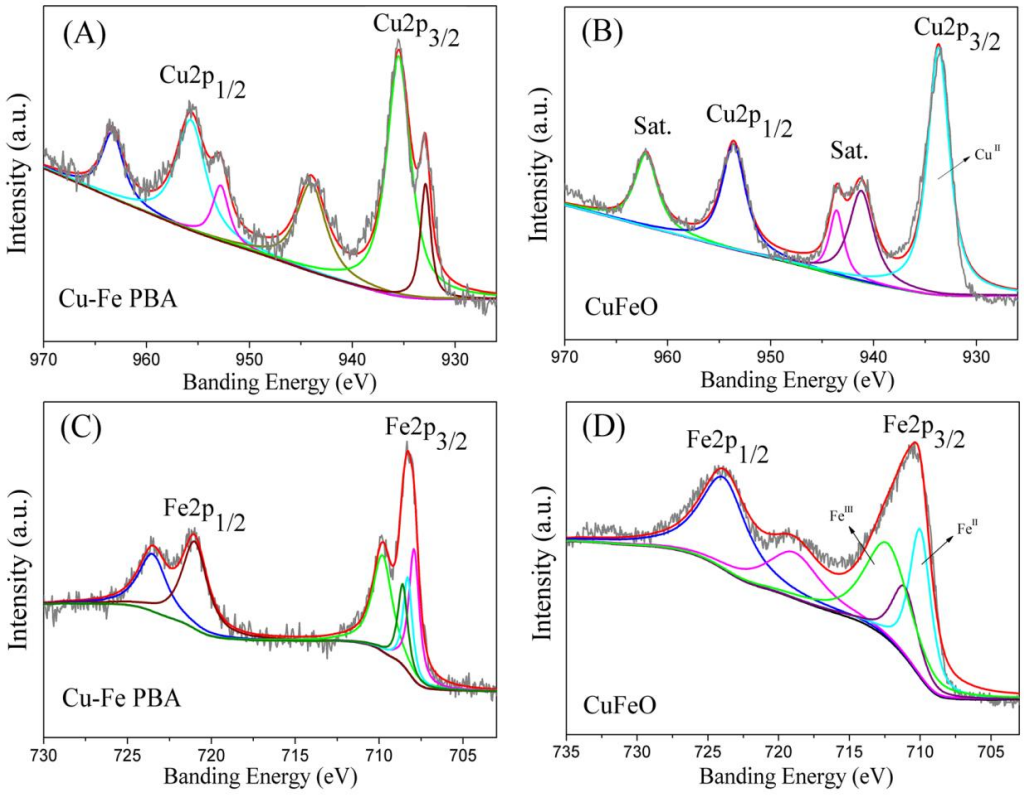

Figure

Fig. 5

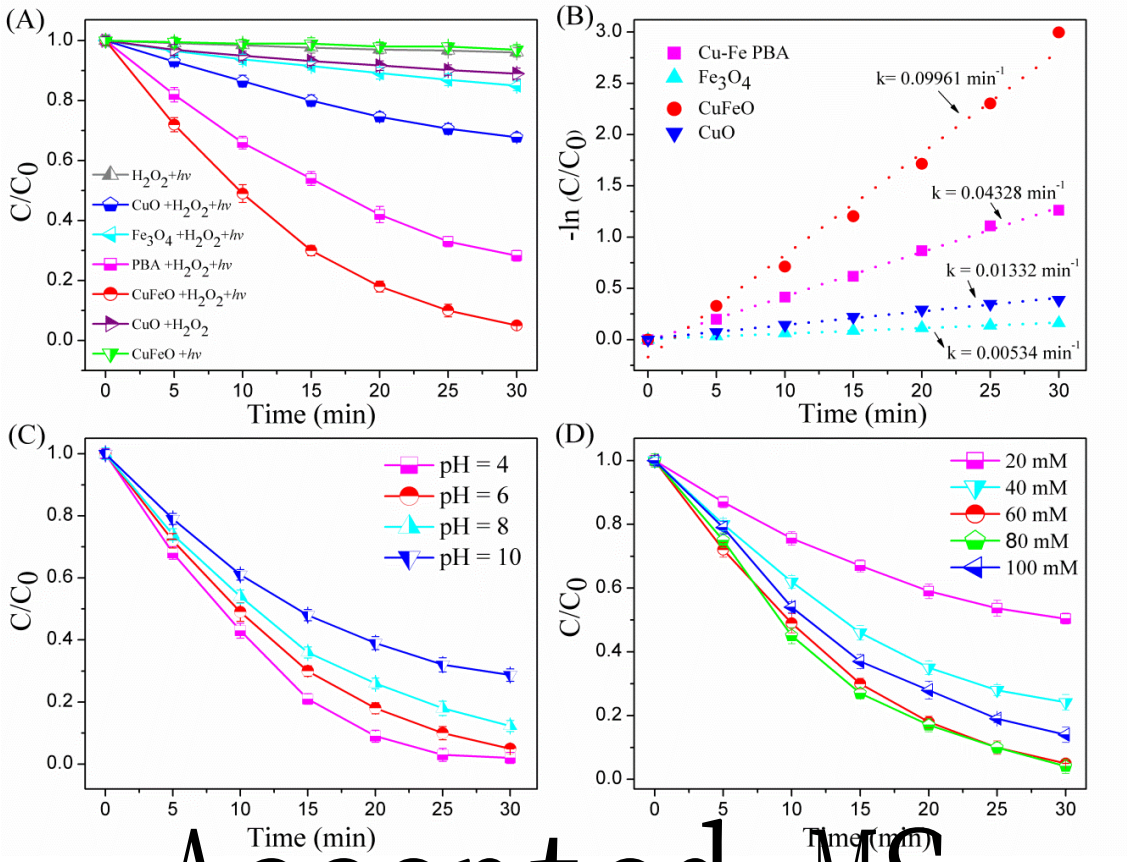

Figure

Fig. 6

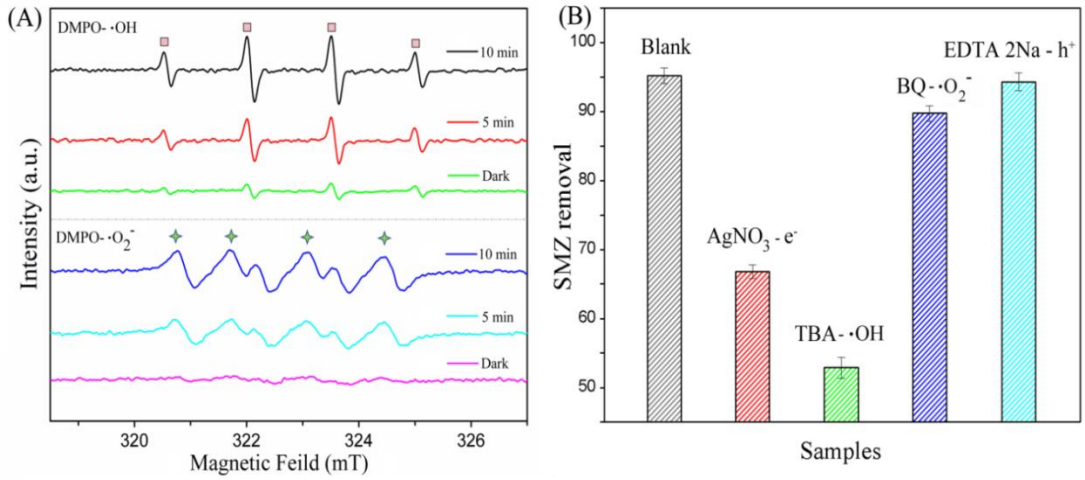

Accepted MS

Figure

Fig. 7

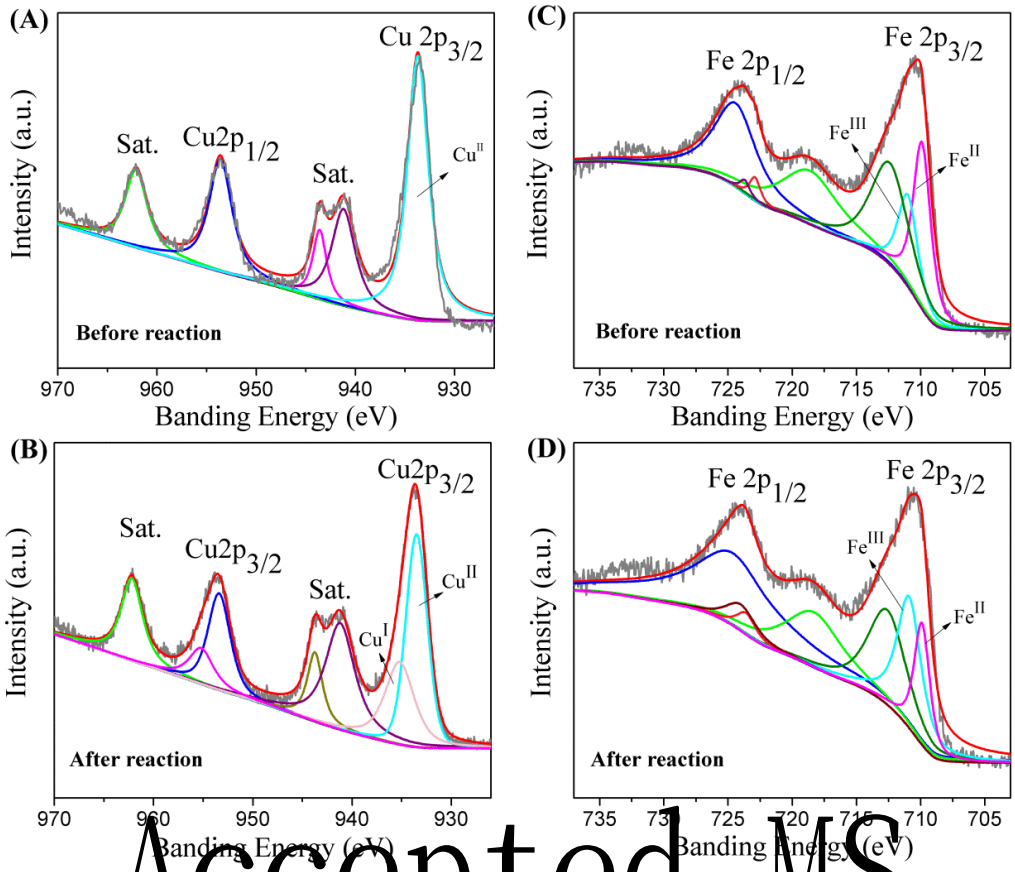

Figure

Fig. 8

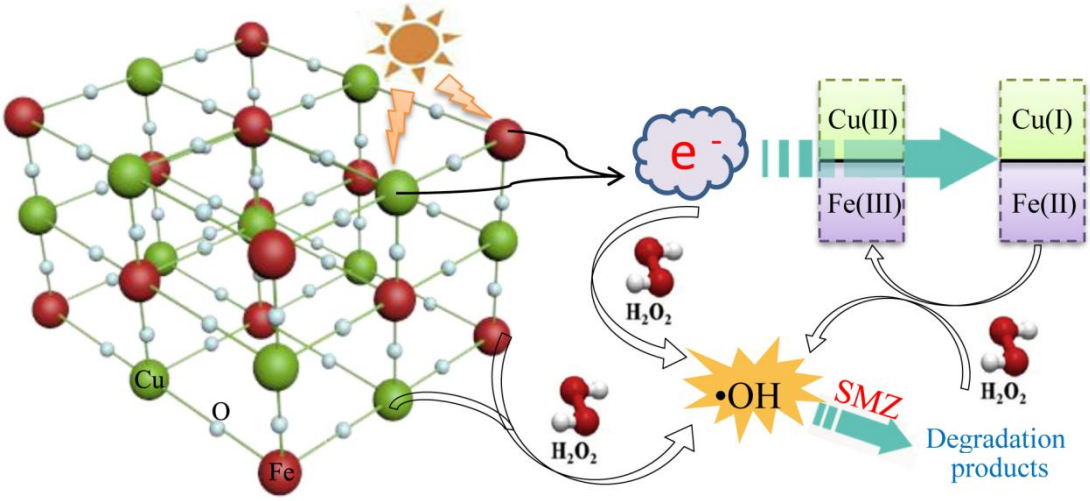

Accepted MS

Figure

Fig. 9

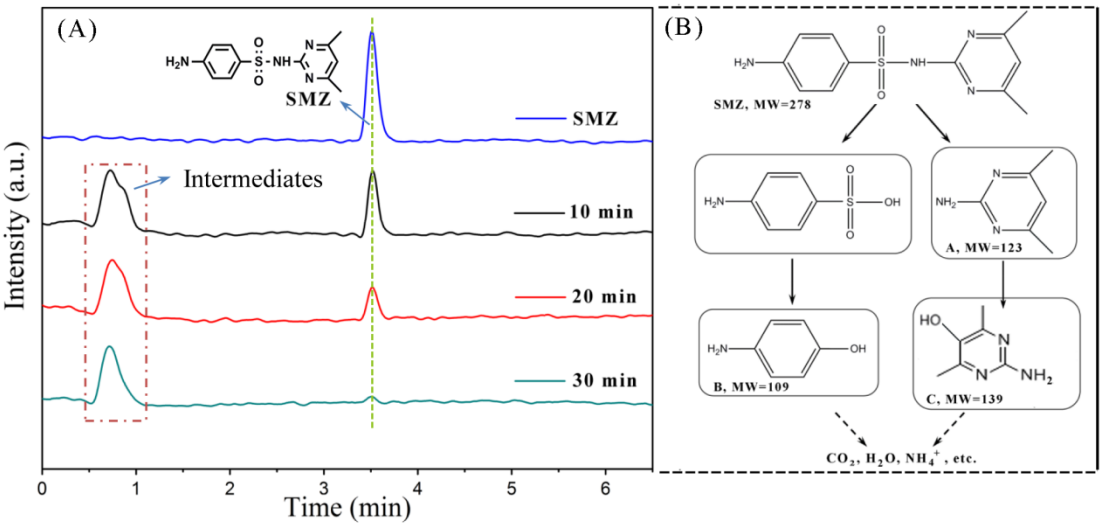

Figure

Fig. 10

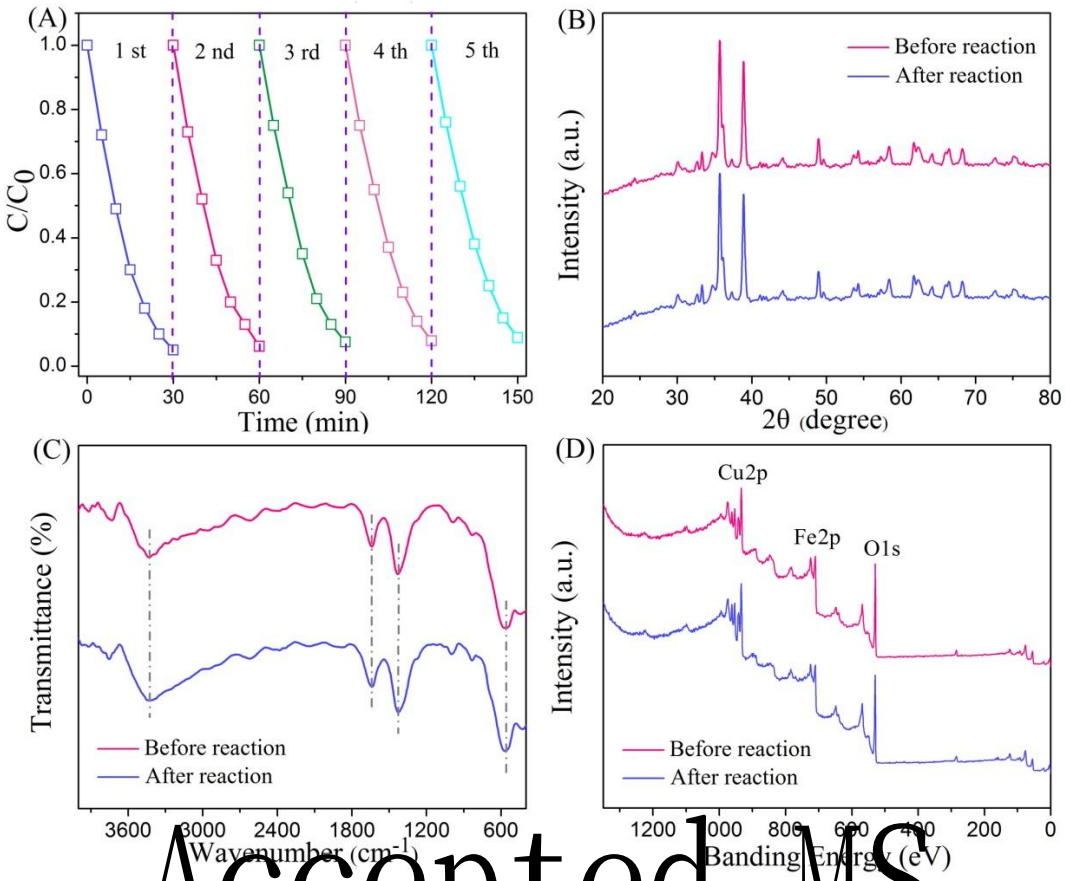

Accepted MS